Towards understanding the mechanism of cohesin loading

Sarah E. Dixon
Trinity College

Department of Biochemistry
University of Oxford

Thesis submitted for the degree of
Doctor of Philosophy
Trinity Term 2013

To my parents

Acknowledgements

This work was generously funded by the Medical Research Council.

It is a pleasure to thank the many individuals that helped me at various times during my DPhil. Foremost, my thanks go to Kim Nasmyth, who allowed me to undertake my research project under his supervision and Maria Demidova, whose results strongly influenced the path my research followed. In addition, I wish to thank our ChIP-sequencing collaborators in Japan, Katsuhiko Shirahige and Yuki Katou, whose results are presented in Fig. II-17, Fig. II-19 and Appendices I and II.

I am grateful to have been surrounded by many excellent scientists during my time in Oxford, many of whom have become dear friends and without whom this DPhil would have been much more difficult to complete. In particular, I wish to thank Chris Chan and Frédéric Beckouët for their helpful guidance on countless occasions, and Frédéric Beckouët, Raquel Oliveira, Ana-Maria Farcas, Johanna Scheinost and Christian Eichinger for their critical reading of parts (in some cases the entirety) of this thesis.

Finally, I wish to thank everybody with whom I've shared a pint, or a tea (or sometimes a pint of tea) over the past four years for having lightened my spirits along the way. The motivation and moral support provided by my fellow students, particularly William Upcher and Sonya Hanson, and the encouragement of my non-scientist friends, particularly Lucy Sorell, Jane Smithson and Rosy Rickett, have been invaluable. Most of all, I am heavily indebted to my family for their unconditional love and support.

Abstract

When a cell divides into two, it is imperative that each resultant daughter receives a full complement of chromosomes; DNA is ultimately responsible for all cellular processes. Cohesion between sister chromatids from the moment of their generation in S phase is central to ensuring the fidelity of chromosome segregation. Smc1 and Smc3 proteins interact with each other *via* their hinges and with a bridging kleisin subunit *via* their heads to form the cohesin ring. It is cohesin, through entrapment of sister chromatid within its ring, that confers sister chromatid cohesion. The process of cohesin's loading onto DNA is poorly understood. While it is thought to depend on ATP hydrolysis, opening of the ring at one of its three interfaces, and the as yet undefined action of the kollerin complex, comprising Scc2 and Scc4 proteins, the sequence of events as they occur are yet to be defined.

A recent screen for suppressors of a thermosensitive *scc4* allele in budding yeast revealed a mutation within Smc1's hinge that could bypass the kollerin subunit. Here, the Smc1 suppressor mutation is investigated. Through targeted mutagenesis, the Smc1D588Y mutant identified in the screen and two additional point mutants, Smc1D588F and Smc1D588W, are herein proven able to bypass Scc4 function completely. Thus we provide the strongest evidence to date to suggest that cohesin's hinge is a critical factor in its loading. Biochemical evidence shows that isolated Smc1 hinge mutants are defective in their binding to Smc3 hinges. This, together with the genetic link made between the hinge and loading complex, suggests that hinge opening might be a requisite for loading.

Through mutagenesis of Scc2 and Scc4 we show that the N-terminus of each protein is responsible for their dimerisation. Furthermore, the N-terminus of Scc2 confers no function other than in its binding to Scc4. Finally, we show that Scc4 is required for the enrichment of both Scc2 and cohesin at centromeres, but not at arm loci. Our results are therefore indicative of there being two different pathways of cohesin loading.

Contents

Acknowledgements i

Abstract ii

List of abbreviations vi

Chapter I: Introduction 1

THE CELL 1

The fundamental unit of life 1

A precisely controlled cycle 2

Mitotic entry: preparing DNA for division 4

Mitotic exit: the dissolution of sister chromatid cohesion 8

STRUCTURAL MAINTENANCE OF CHROMOSOMES PROTEINS 9

An evolutionarily conserved family of ATPases 9

SMC protein structure 11

THE COHESIN COMPLEX 16

A tripartite ring-shaped molecule 16

The topological embrace 18

THE COHESIN CYCLE 20

Cohesin loading 20

Sites of cohesin loading and residence 25

Cohesion establishment and maintenance 28

Removal of cohesin from chromosomes 29

COHESINOPATHIES 31

Thesis objective 35

Chapter II: A mutation in Smc1 overcomes the requirement for Scc4 and weakens the hinge interface 37

INTRODUCTION 37

RESULTS 42

A mutation within Smc1 bypasses the requirement for Scc4 42

Smc1's D588 is a highly conserved residue within cohesin's hinge interface 45

Scc2 is not upregulated in the absence of Scc4 47

Uncharged aromatic residue substitutions in Smc1 at position 588 can bypass the requirement for Scc4 49

smc3(K652Y) is unable to bypass the requirement for Scc4 51

Suppressor mutations in Smc1 hinge weaken the interaction between Smc1 and Smc3 54

Hinge mutations predicted to weaken Smc1/Smc3 interaction are not able to bypass Scc4 56

The ability of smc1(D588Y/W/F) to bypass Scc4 cannot be reversed by complementary mutations in Smc3 60

smc1(D588Y) mutation does not facilitate an interaction between kollerin and cohesin 61

smc1(D588Y) rescues Smc3 acetylation defect of cells in which Scc4 is inactivated 62

Defects in sister chromatid cohesion are observed in the absence of Scc4 63

Defects in mitotic chromosome segregation are observed in the absence of Scc4 65

Cohesin's pericentromeric chromatin enrichment is aberrant in the absence of Scc4 68

Scc2 is not enriched at centromeric chromatin in the absence of Scc4 71

smc1(D588Y) scc4Δ confers a meiotic defect 73

DISCUSSION 75

Chapter III: Biochemical studies of kollerin **89**

INTRODUCTION 89

RESULTS 92

Putative kinase in Scc2 is not essential for cell viability 92

Kollerin is a heterodimeric complex 93

Mutation of Scc4's moderately well-conserved Y40 confers the thermosensitive phenotype of scc4-4 95

Scc4Y40 mutants are defective in Scc2 binding 97

N-terminally truncated Scc2 is unable to bind Scc4 98

N-terminally truncated Scc2 is unable to support yeast growth 99

Growth of cells expressing N-terminally truncated Scc2 is restored by scc4Δ suppressor mutation smc1(D588Y) 100

DISCUSSION 102
Chapter VI: Summary and future directions 109
SUMMARY 109
FUTURE DIRECTIONS 110
How is the hinge opened and how is it locked? 110
At what point(s) is hinge opening required? 112
Chapter V: Materials and methods 115
Yeast strains and growth conditions 115
Fluorescence-activated cell sorting 115
Yeast transformation 116
Genomic integration 117
Yeast genomic DNA preparation 118
Tetrad dissection 119
Preparation of denatured yeast cell extracts 119
Preparation of native yeast cell extracts 120
Quantitation of protein concentration in crude extracts 121
Immunoprecipitation 121
Protein gel electrophoresis, gel staining and Western blotting 122
Site-directed mutagenesis 123
Overlapping PCR 124
Protein purification 125
In vitro hinge binding assay 126
Chromosome loss assay 127
GFP dots assay 127
Live cell imaging 128
Multiple sequence alignment 128
Homology modelling 130
List of strains 130
References 134
APPENDIX I: *ChIP-sequencing of SCC1-PK*$_6$ **146**
APPENDIX II: *ChIP-sequencing of SCC2-PK*$_3$ **148**

List of abbreviations

°C	degrees Celcius
2XTY	2 times tryptone yeast extract
5-FOA	5-Fluoroorotic Acid
Å	Ångströms
ADE (*ade*)	Adenine-requiring
APC/C	Anaphase-promoting complex or cyclosome
ATP	Adenosine-5'-triphosphate
B. subtilis	*Bacillus subtilis*
BiFC	Bimolecular fluorescence complementation
bp	base pair
BPA	*para*-benzoyl-L-phenylalanine
BSA	Bovine serum albumin
Bub	Budding uninhibited by benzimidazole
C- (terminal)	Carboxy-
CDC (Cdc)	Cell Division Cycle
Cdh	Cdc20 homologue
CDK	Cyclin dependent kinase
CdLS	Cornelia de Lange Syndrome
CEN	Centromere
CFIII	Chromosome fragment *CEN3.L URA3 SUP11*
ChIP	Chromatin immunoprecipitation
Chk	Checkpoint kinase
Chl	Chromosome loss
co-IP	co-immunoprecipitation
CTCF	CCCTC- binding factor
CTF (Ctf)	Chromosome transmission fidelity
d	days

DBF (Dbf)	Dumbbell former
ddH_2O	Double-distilled water
DDK	Dbf4-dependent kinase
DNA	Deoxyribonucleic acid
dNTPs	Deoxyribonucleotide triphosphate
DTT	Dithiothreitol
E. coli	*Escherichia coli*
ECO (Eco, *eco*)	Establishment of cohesion
EDTA	Ethylenediaminetetraacetic acid
EMCCD	Electron multiplying charge-coupled device
FACS	Fluorescence-activated cell sorting
Fig.	Figure
FKBP12	FK506 binding protein 12
FRAP	Fluorescence recovery after photobleaching
FRB	FKBP-rapamycin binding domain of mTOR
FRET	Förster resonance energy transfer
g	Gravitational force
G_1 (phase)	Gap 1
G_2 (phase)	Gap 2
G_2/M (phase)	Gap 2/Mitosis
GFP	Green Fluorescent Protein
h	hours
H (1, 2A, 2B, 3, 4)	Histone
HA	hemagglutinin
HEAT	Huntingtin, Elongation factor 3, Protein Phosphatase 2A, TOR1
HEPES	4-(2-hydroxyethyl)-1-piperazineethanesulfonic acid
HRP	Horseradish peroxidase
IP	immunoprecipitation
kb	kilobases
kDa	kiloDaltons

kpsi	thousand pounds per square inch
LEU (*leu*)	Leucine requiring
M	Molar
M (phase)	Mitosis
M. musculus	*Mus musculus*
Mad	Mitotic-arrest deficient
MAU (MAU)	Maternal-effect uncoordinated
MBP	Maltose Binding Protein
MCC	Mitotic checkpoint complex
min	minutes
MIS, Mis	Minichromosome instability
mL	millilitres
mM	millimolar
mRNA	Messenger ribonucleic acid
MTW (Mtw)	Mis twelve-like
MukB	Mukaku[1] B
myc	myelocytomatosis
N- (terminal)	amino-
N.A.	Numerical aperture
N/A	not applicable
NaCl	sodium chloride
NBD	Nucleotide Binding Domain
ng	Nanograms
NH (group)	amine
NIPBL (NIPBL)	Nipped-B-like
nM	nanomolar
nm	nanometre
NTP	Nucleotide triphosphate
OD	Optical density
OD_{600}	Optical density at 600 nanometres

1 From Japanese, 無核 (*mukaku*, "anucleate")

p (-value)	probability
PAGE	Polyacrylamide gel electrophoresis
PBS	Phosphate-buffered saline
PBST	PBS + 0.05 % TWEEN® 20
PCNA	Proliferating Cell Nuclear Antigen
PCR	Polymerase Chain Reaction
Pds	Precocious dissociation of sisters
PEG	poly(ethylene glycol)
pGAL	Galactose-inducible promoter
PK	small epitope on the P/V proteins of the paramyxovirus simian virus 5
Pkh	Protein kinase B-activating kinase homologue
PMSF	phenylmethylsulfonyl fluoride
pre-RC	pre-replication complex
PVDF	Polyvinylidene fluoride
RAD (Rad)	Radiation sensitive
RBS	Roberts Syndrome
RFP	Red Fluorescent Protein
rpm	revolutions per minute
S (phase)	Synthesis
S. cerevisiae	*Saccharomyces cerevisiae*
S. pombe	*Schizosaccharomyces pombe*
SAC	Spindle-assembly checkpoint
SCC (Scc, *scc*)	Sister Chromatid Cohesion
ScpA	Segregation and condensation protein A
SDS	Sodium dodecyl sulfate
sec	seconds
SMC (SMC, Smc, *smc*)	Structural Maintenance of Chromosomes (previously Stability of minichromosomes)
SUMO	Small ubiquitin-like modifier
SUP	Suppressor

T. maritima	*Thermatoga maritima*
TCA	Trichloroacetic acid
TE	Tris EDTA
tetO	Tetracycline operator
TetR	Tetracycline repressor
TEV	Tobacco Etch Virus
TPR	Tetratricopeptide repeat
tRNA	Transfer ribonucleic acid
TRP (*trp*)	Tryptophan requiring
URA (*ura*)	Uracil requiring
UV	ultraviolet
v/v	volume/volume
w/v	mass/volume
WB	Western blot
YEP	Yeast Extract Peptone
YPD	Yeast Extract Peptone Dextrose
µg	micrograms
µL	microlitres
µM	micromolar
Φ	hydrophobic residue

Chapter I

Introduction

Introduction

THE CELL

The fundamental unit of life

Upon observing razorfish clams emerging, fully formed, from their burrows on sandy shores, and flies apparently hatching from dewdrops on the leaves of trees, Aristotle naturally concluded that these animals had been formed by the mystical phenomenon of spontaneous generation (Aristotle, 343BC). Whilst it remains to this day a seemingly impossible task to define the essence of life itself, over the centuries it has become patently obvious to us that the ancient Greek polymath was erroneous in his claim because all organisms arise by descent from genetically similar parents.

It was with the advent of the light microscope in the 17th century that the complexity of living things began to be uncovered. The English physicist Robert Hooke was the first to use this invention to describe the intricate nature of biological structures. His exquisite illustrations of cork tissue showed that it was composed of box-like building blocks or "cells" [2] (Hooke, 1665). Almost two centuries passed before Schwann and Schleiden's cell theory proposed that these very building blocks were in fact the fundamental unit of life – they are "the basis of all tissues" (Schwann & Schleiden, 1847). It was not long after this that Rudolf Virchow's concise formulation, "*omnis cellula e cellula*"[3],

2 So-called for their resemblance to the small, austere rooms inhabited by monks.

3 Translated "every cell from a cell".

conclusively rejected the theory of Aristotelian abiogenesis in favour of the principle that all cells arise from the division of pre-existing cells (Virchow, 1860). Cell division is therefore not just one of the most extraordinary events occurring in all biological systems, it is also fundamental to the continuation of life. Consequently, it is unsurprising that the mechanisms governing this phenomenon are incredibly precisely controlled.

A precisely controlled cycle

The division of one cell into two is a complex operation, but one that can be divided into four distinct phases (Fig I-1). A series of molecular switches is responsible for ensuring the timely and sequential progression from one to the next. The switches are composed of two classes of protein: cyclins and their dependent kinases. The activity of cyclin-dependent kinases (CDKs) depends on their association with different cyclins, and changes in cyclin levels during the cell cycle lead to corresponding oscillations in the activity of CDKs. Activated Cdk-cyclin complexes, through phosphorylation of their substrates, initiate the cascade of events that must occur before progression to the next phase of the cycle (Morgan, 1997). The combination of both positive and double negative feedback loops in the intricate biochemical circuit introduces 'bistability' to the system. This ensures that, when all conditions are satisfied for the cell's progression to the next phase of the cycle, there is no intermediate state; the transition occurs in a committed and unidirectional manner (Novak *et al.*, 2007).

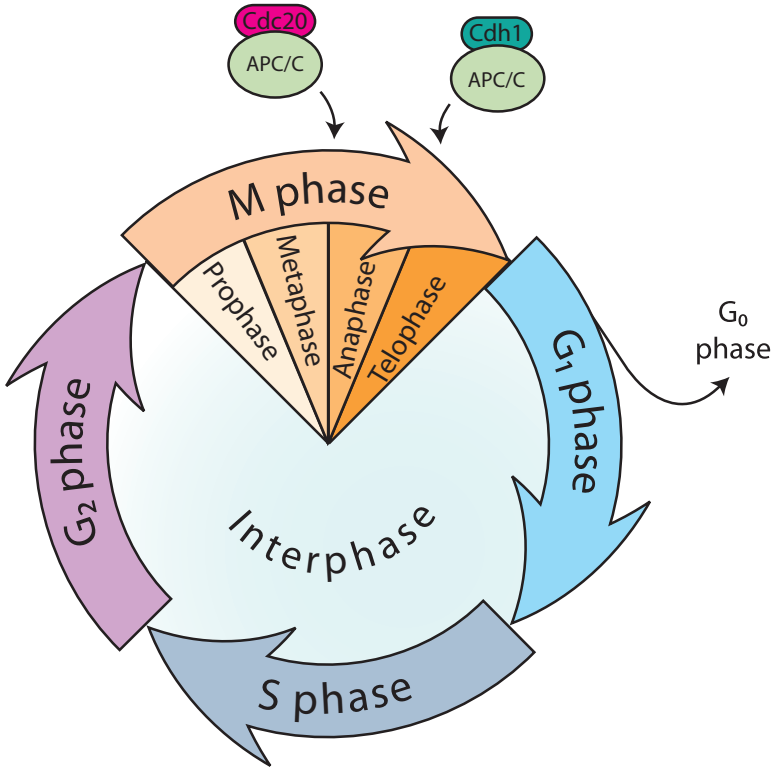

Figure I-1. The cell cycle.
The cell cycle may be split into four broad stages. In G_1 a cell either leaves the cell cycle to a quiescent G_0 phase, or grows and readies itself for S phase, during which its entire genome is replicated. In G_2 phase the cell continues to grow, repairs DNA damage caused by replication, and prepares for the final stage, mitosis. Mitosis can further be split into four stages: prophase, metaphase, anaphase and telophase. APC^{Cdc20} is kept inactive until the metaphase-to-anaphase transition. Its activation triggers anaphase through targeting proteins for destruction, including securin and M cyclin. Following anaphase, Cdh1 replaces Cdc20 as the activator of APC and the newly formed APC^{Cdh1} promotes mitotic exit.

A cell begins its cyclical journey in the first gap (G_1) phase, during which it grows prior to making the commitment to enter synthesis (S) phase, whereupon its entire genome is replicated. Cells in G_1 phase do not have to proceed to S phase; if the conditions for cell cycle progression are not met, they may exit the cycle and assume a quiescent state: G_0. Next, cells enter the second gap (G_2) phase. This is a stage in which the completion of replication is verified prior to the commitment to enter the final and most striking step

of the cycle: mitotic (M) phase[4] (Morgan, 2007). Denoting the stage at which replicated genetic material must be equally apportioned into two equal shares, M phase is a complex and highly ordered affair. This is reflected in the fact that, while G_1, S and G_2 phases are collectively termed interphase, M phase itself is further subdivided into four distinct phases: prophase, metaphase, anaphase and telophase (Fig. I-1).

Mitotic entry: preparing DNA for division

The transition into M phase is promoted by an increase in the cellular concentration of mitotic cyclin (M cyclin). Its binding to CDK induces chromosome condensation and assembly of the mitotic spindle (Morgan, 2007). Until entry to M phase, the DNA molecules that constitute a cell's genome form what appears to be a disorganised and tangled web contained within its nucleus. Since it is of paramount importance that the chromosomes are equally distributed when the time comes to divide, these long string-like molecules undergo gross structural changes during prophase; the genome is entirely reorganised such that each chromosome, consisting of two sister chromatids, is visibly distinguishable as a discrete rod-like structure (Sumner, 1991).

Multiple levels of protein-mediated DNA compaction are required to generate such condensed structures. It is estimated that the linear DNA of the eukaryotic genome undergoes up to 10,000-fold compaction to form mitotic

4 From Greek, μίτος (*mitos*, "thread"), referring to the appearance of chromosomes during this phase.

chromosomes (Cooper, 2000). The basic repeating unit of DNA consists of the DNA double helix wound around nucleosomes into an 11 nm-wide fibre, in a manner resembling 'beads on a string' (Carlson *et al.*, 1975; Oudet *et al.*, 1975). Nucleosomes comprise two of each of the positively charged histone proteins H2A, H2B, H3 and H4 joined together to form a histone octamer, to which negatively charged DNA can bind tightly. Histone H1 is present on the DNA linking these repeating units and is thought to have a role in further condensing chromatin into a 30 nm-wide fibre (Thoma *et al.*, 1979; Ohsumi *et al.*, 1993). Although this form of DNA has been observed using electron microscopy (Marsden & Laemmli, 1979; Olins & Olins, 2003), its existence *in vivo* is uncertain (Maeshima *et al.*, 2010; Grigoryev & Woodcock, 2012; Nishino *et al.*, 2012).

Condensation of chromatin during mitosis is further mediated by the condensin complex, whose activation is directly dependent on its phosphorylation by M cyclin-Cdk (Hirano, 2005). Condensin belongs to a family of protein complexes that contain Structural Maintenance of Chromosomes (SMC) proteins, which will be discussed in more detail later. The additional level of condensation conferred by condensin is essential; cells that have compromised condensin function commonly experience difficulty in segregating DNA (Saka *et al.*, 1994; Strunnikov *et al.*, 1995; Bhat *et al.*, 1996).

Far from being a disorderly, knotted mess, upon chromosome condensation it becomes clear that each chromatid has in fact been physically linked with its homologous partner since S phase. The connections are conferred

partly by the intertwining, or catenation, of DNA that is an inherent result of its replication (Sundin & Varshavsky, 1981, DiNardo *et al.*, 1984). It is, however, the proteinaceous links of another member of the SMC protein-containing complexes, cohesin, that impart the most significant portion (Michaelis *et al.*, 1997; Guacci *et al.*, 1997; Farcas *et al.*, 2011). Even more apparent, come the alignment of sisters in a planar fashion during metaphase, is how the physical relationship that has been maintained between them since their synthesis is integral to assuring the fidelity of mitosis.

The metaphase alignment of sister chromatids relies on the mitotic spindle, the assembly of which is dependent on the activity of M cyclin-Cdk complexes following the breakdown of the nuclear envelope (Nigg, 2001). Nuclear envelope breakdown is an aspect of mitosis not shared by yeasts, which undergo 'closed' mitosis within an intact nuclear membrane (Morgan, 2007). Microtubules emanating from the two spindle-pole bodies on opposite sides of the cell attach to pairs of chromatids *via* the large multi-subunit protein complexes that assemble at their centromeres, called kinetochores. The spindle assembly checkpoint (SAC) is a molecular switch that will not allow progression to the next stage of the cycle until all sister kinetochores have made amphitelic attachments; that is connections to opposing microtubules (Fig. I-2a). Having made such attachments, chromosomes are able to be drawn to the centre of the spindle and are said to be bi-oriented. It is this cohesion-dependent bi-orientation that ensures the fidelity of chromosome segregation.

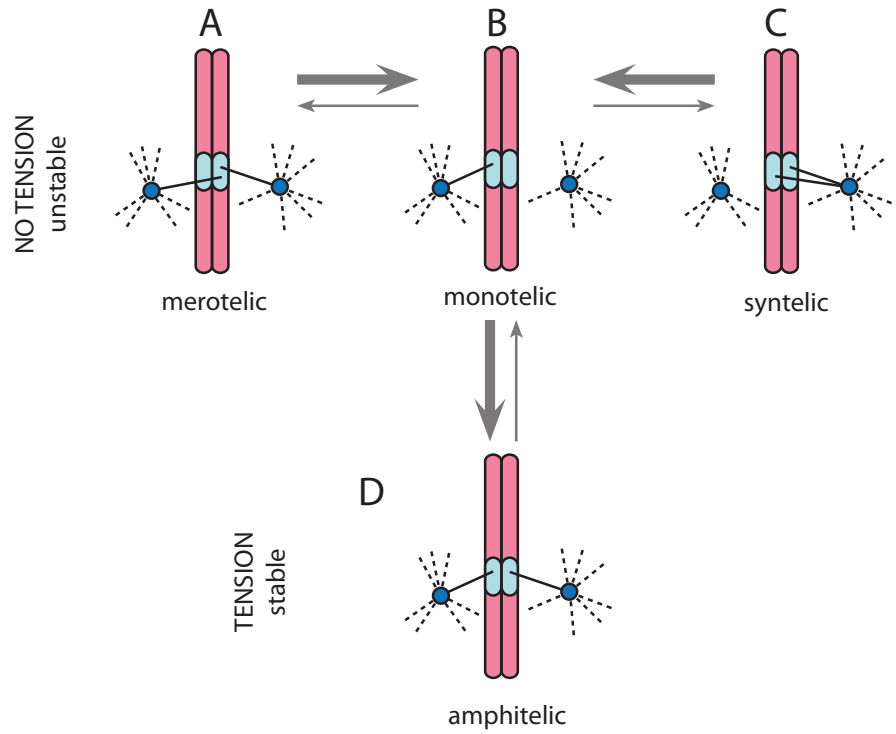

Figure I-2. Example kinetochore-microtubule attachments.
A-C Incorrect kinetochore-microtubule attachments. **A** Merotelic attachment of one kinetochore to two opposing spindle microtubules. **B** Monotelic attachment of only one kinetochore of a pair to spindle microtubules. **C** Syntelic attachment of two kinetochores to the spindle microtubules emanating from the same pole. Each case results in a lack of tension and is therefore unstable. Error correction leads to **D** amphitelic attachment of both kinetochores to opposing spindle microtubules. This correct attachment leads to tension and is therefore stable.

The pulling forces of the spindle generate tension across the kinetochore. Tension directly stabilises amphitelic attachments (Akiyoshi *et al.*, 2010). In the event of incorrect kinetochore-microtubule attachments, such as only one kinetochore from a pair of sister chromatids making attachments with microtubules (monotelic attachment), or one or both kinetochores from a pair of sister chromatids becoming attached to microtubules emanating from the same pole (syntelic attachment), tension across the kinetochore is absent (Fig. I-2). The kinetochore-associated kinase Aurora B destabilises these, thus promoting error-correction (Liu *et al.*, 2009). Once the highly dynamic

microtubules of the spindle act to draw all bi-oriented chromosomes to the centre, thus forming the metaphase plate, the cell is ready to enter anaphase.

Mitotic exit: the dissolution of sister chromatid cohesion

Premature loss of sister chromatid cohesion can have disastrous consequences: incorrect chromosome segregation leads to abnormal chromosome number, or aneuploidy. In single-celled organisms this is normally lethal, whereas in metazoans aneuploidy is closely associated with cancer and developmental disease. Thus only when all sister chromatids achieve a state of bi-orientation is the SAC satisfied and loss of sister chromatid cohesion permitted through activation of the master regulator of anaphase, the anaphase-promoting complex or cyclosome (APC/C).

Until bi-orientation, APC/C and its activator Cdc20 (APC^{Cdc20}) are kept inactive by a mitotic checkpoint complex (MCC) consisting of Mad2, Mad3 and Bub3 (Sudakin *et al.*, 2001). APC/C is an E3 ubiquitin ligase whose M cyclin-Cdk-mediated activation leads to the polyubiquitination of target proteins, thus marking them for degradation by the proteasome. Two major targets of APC^{Cdc20} are securin and M cyclin itself (Musacchio & Salmon, 2007). Destruction of the former leads to the rapid and synchronous loss of sister chromatid cohesion, while destruction of the latter ensures a committed exit from mitosis.

Securin interacts with and inhibits the thiol protease separase, which is further kept inactive by inhibitory phosphorylation by M cyclin-Cdk

(Stemmann *et al.*, 2001). Thus the activation of APC^{Cdc20} has a dual effect in activating separase, both through removing securin and preventing any further inhibitory phosphorylation from occurring. Separase is now free to cut the cohesive ties between sister chromatids. Through proteolytic cleavage of the cohesin complex by separase (Uhlmann *et al.*, 1999; 2000), sister chromatids may finally disengage from their long and tight embrace and be guided by the mitotic spindle to opposite poles of the cell.

Telophase follows nuclear division. At this point, each half of the cell contains an identical set of single chromosomes and the end of mitosis is imminent. Caused by the negative feedback loop generated by APC^{Cdc20}-mediated destruction of M cyclin-Cdk, Cdh1 replaces Cdc20 as the activator of APC/C (Visintin *et al.*, 1997; Peters, 2002). The newly formed APC^{Cdh1} complex promotes disassembly of the spindle and reassembly of the nuclear envelope. The final step is cytokinesis; that is constriction around the spindle mid-zone leading to fission of the cell into two.

STRUCTURAL MAINTENANCE OF CHROMOSOMES PROTEINS

An evolutionarily conserved family of ATPases

The molecules of DNA that constitute a cell's genome are enormous relative to the cell itself. Evidently it is of paramount importance that these molecules are organised in an orderly fashion. A eukaryotic cell achieves this partly through packaging chromosomes as chromatin, as discussed previously.

However, the challenges faced during the duplication and partitioning of genetic material are common to all species, including those lacking nucleosomes. An additional family of proteins, present in both prokaryotes and eukaryotes, is on hand to confront these challenges.

The proteins of the Structural Maintenance of Chromosomes (SMC) family exist throughout evolution from bacteria to humans (Cobbe & Heck, 2004). Proteins of this family are defined by their characteristic modular structure and ATPase activity. They perform fundamental roles in chromosome organisation: prokaryotic SMCs usually perform a key function in partitioning genetic material during binary fission, while SMC proteins in eukaryotes have been implicated in diverse processes such as modulating chromatin architecture, facilitating DNA repair, modulating gene expression, regulating X chromosome dosage compensation and ensuring the faithful segregation of sister chromatids during cell division (Jessberger, 2002).

Six *SMC* genes are present in eukaryotes, their products forming three SMC heterodimer-containing complexes: cohesin, containing Smc1 and Smc3; condensin, containing Smc2 and Smc4; and the as yet unnamed Smc5/Smc6 complex. Prokaryotes normally possess one SMC-encoding gene whose product homodimerises. Although certain bacteria, including *E. coli*, possess no canonical SMC protein, the structurally related orthologue MukB performs an equivalent role during replication and cell division (Niki *et al.*, 1992; Melby *et al.*, 1998; Sherratt, 2003). In addition to this, another SMC-like protein, Rad50, functions in the DNA double-strand break repair pathway and is conserved

from bacteriophages to mammals (Cromie *et al.*, 2001). The ancient ancestry of these distantly related proteins and their prevalence throughout all species highlights the fundamental roles, common to all fields of life, that they play in maintaining and organising genomes.

SMC protein structure

The first group to consider the sequence of the translated *SMC1* gene product from *S. cerevisiae* identified a 1225-amino acid protein with several distinct predicted domains (Strunnikov *et al.*, 1993). There were two putative globular domains at the N- and C-termini that flanked two central α-helical stretches with a high probability of forming a coiled coil. This characteristic modular architecture, bearing similarity both to electron micrographs of *E. coli*'s homodimer-forming MukB protein reported by Niki *et al.* (1992) and to the structure of yeast Rad50 predicted by Alani *et al.* (1989), was taken to define the novel SMC family of proteins (Fig. I-3A).

The large globular heads residing at the two extremes of SMC proteins invariably contain highly conserved motifs associated with ATP-binding cassettes (ABCs); for this reason, they are termed nucleotide-binding domains (NBDs). The N-terminal globular domain possesses the GXXXXGK(T/S)[5] Walker A motif (Walker *et al.*, 1982). This common nucleotide-binding motif functions through hydrogen bond interaction between the essential lysine residue and the nucleotide's β- and γ-phosphates. The C-terminal globular

5 Where X denotes any amino acid.

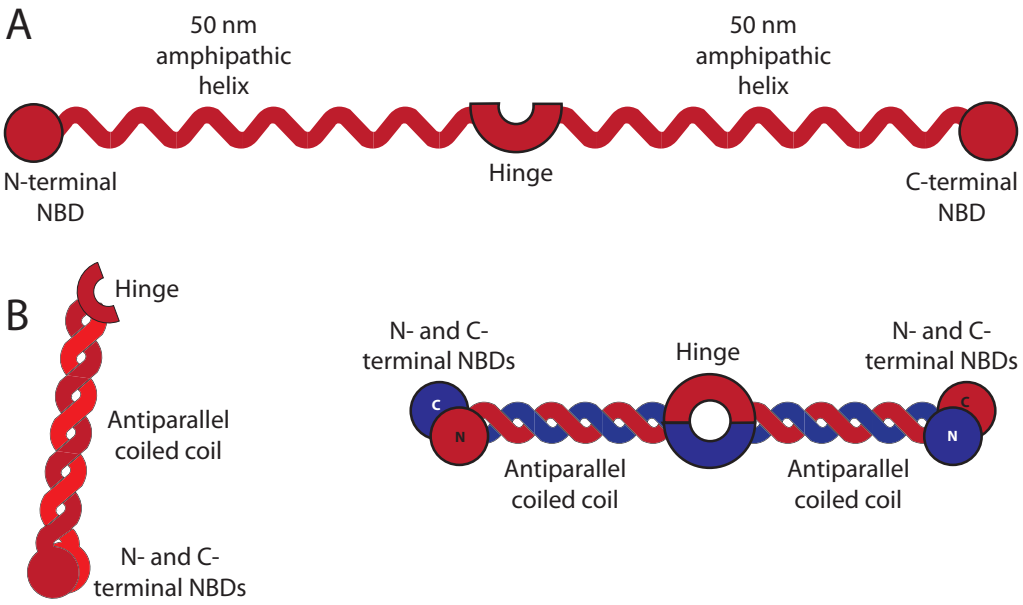

Figure I-3. Structure and folding of SMC proteins.
A Schematic diagram of an unfolded SMC protein. At the N- and C-termini are NBDs and in the centre is a hinge. The heads and hinges are separated by two 50 nm stretches of amphipathic helix.
B Diagram depicting the ways in which an SMC protein might form an active ABC-like ATPase, either by folding at its central hinge domain to form an intramolecular coiled coil thus bringing the NBDs at the N- and C-termini together (left panel), or by interaction of two SMC proteins in an anti-parallel manner (right panel).

domain contributes the Walker B consensus sequence ΦΦΦΦDE[6], providing the ATPase active site glutamate residue and further stabilising nucleotide binding through co-ordination of a Mg^{2+} ion (Gaudet & Wiley, 2001; Verdon *et al.*, 2003).

Having been identified on the basis of sequence homologies, it was unclear whether or not the SMC protein formed a functional ABC-like ATPase; neither Walker motif alone is capable of binding ATP, and these motifs are present on domains separated by two long amphipathic α-helices. To form a functional ATPase would mean either that SMC proteins must dimerise such that the N-terminal Walker A motif from one SMC lies adjacent to the

6 Where Φ denotes a hydrophobic amino acid.

C-terminal Walker B motif from the other, and *vice versa*, i.e. forming an intermolecular antiparallel coiled coil, or that the entire molecule must fold back on itself to bring the two heads into close proximity by forming an intramolecular antiparallel coiled-coil (Fig. I-3B). It was both through electron microscopy following fusion of the rod-shaped fibronectin protein to Smc3's N- and C-termini, and through solving the crystal structure of the Smc1 and Smc3 central 'hinge' domains that the latter model was conclusively shown to be correct (Haering *et al.*, 2002) and is now known to be true of all SMC and SMC-like proteins (Melby et al., 1998; Hirano, 2006).

The final requirement in forming an active ATPase is interaction between the ABC signature motif (LSGG[Q/E]) and ATP. Like with related ATPases, such as Rad50 and ABC transporters (Hopfner *et al.*, 2000; Smith *et al.*, 2002), structural studies of the SMC heads have shown that this is dependent upon dimerisation of two molecules, such that the ATP bound in the active site of one NBD contacts the signature motif of a complementary NBD, and *vice versa* (Arumugam *et al.*, 2003). Thus, each SMC dimer is capable of binding two ATP molecules.

In addition to ATP-dependent dimerisation at the NBD heads, SMC molecules interact *via* the hinge domains that are formed from the amino acids in the middle of the molecule that separate the two amphiphatic α-helices (Haering *et al.*, 2002). Unlike the contact made at the other end of the coiled coil, the dimerisation that takes place between the hinges is independent of nucleotide binding. As such, purified SMC dimers are often seen to form

V-shaped molecules according to electron microscopy, with closed hinges and open heads (Melby *et al.*, 1998; Anderson *et al.*, 2002; Haering *et al.*, 2002).

The crystal structures of SMC hinges from various species have revealed several striking features that are remarkably well conserved throughout evolution. However, this dimerisation interface is where SMC dimers differ from their distantly related counterparts Rad50 and MukB. While Rad50 dimerises *via* a zinc hook CXXC motif, in which a Zn^{2+} ion is chelated between two cysteine residues from each monomer (Hopfner *et al.*, 2002), MukB's hinge domain is less structurally divergent than SMC hinges, despite having little sequence similarity. It is, however, missing the central pore that is a conserved characteristic of the homodimeric SMC from *T. maritima* through to the mouse cohesin and condensin hinge heterodimers (Haering *et al.*, 2002; Griese *et al.*, 2010; Ku *et al.*, 2010; Li *et al.*, 2010; Kurze *et al.*, 2011; Fig. I-4).

The interaction between two SMC hinges is one of twofold rotational pseudosymmetry. The high level of conservation between members of this family of proteins means that, even in a heterodimeric complex, the points of contact above the pore are almost identical to those below it. Nevertheless, there is sufficient sequence diversity within the family to ensure that each SMC monomer is only able to interact with its partner. Cohesin's Smc3 hinge, for example, is unable to interact with condensin's Smc4 hinge (Griese *et al.*, 2010).

A final feature of the hinge dimerisation domain is that the central pore is invariably positively charged. Even in *H. salinarum*, an archaeon whose

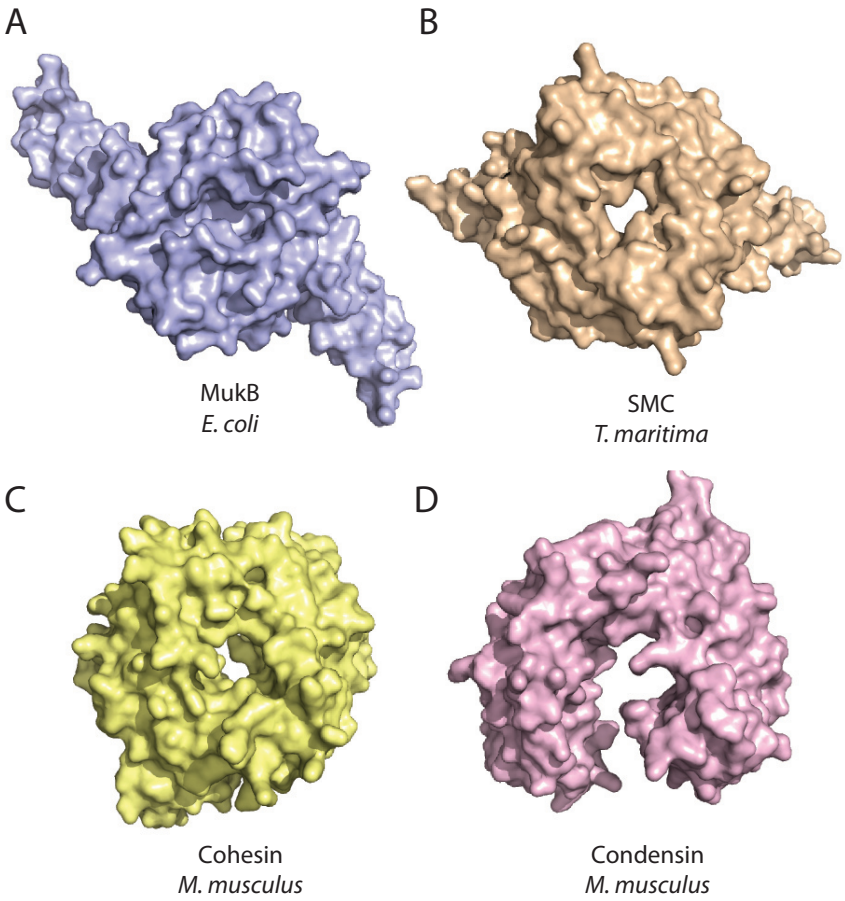

Figure 1-4. Spatially aligned crystal structures of SMC hinges from various organisms. **A** *E. coli*'s MukB homodimer, although highly divergent in primary sequence, exhibits remarkable structural homology to **B** the SMC hinge homodimer of *T. maritima*, and the SMC hinge heterodimers of **C** cohesin and **D** condensin from *M. musculus*. Note that MukB is lacking the central pore that is present in the SMCs from *T. maritima* and *M. musculus*, and that condensin's hinge is in an open conformation, which is postulated to be an intermediate in hinge dimer assembly (PDB identifiers: 2WMM, Ku *et al.*, 2010; 1GXL, Haering *et al.*, 2002; 2WD5, Kurze *et al.*, 2011; 3L51, Griese *et al.*, 2010).

high-salt habitat has resulted in its expression of abnormally acidic proteins, this positive charge remains. In addition, neutralising this positive charge in yeast cohesin hinges renders the complex unable to stably associate with DNA (Kurze *et al.*, 2011). Might the positive charge serve a role in mediating the interaction of SMC protein-containing complexes with negatively charged DNA? Certainly, isolated cohesin and condensin hinge domains display the ability to interact with DNA *in vitro* (Chiu *et al.*, 2004; Griese *et al.*, 2010). The

effect of pore charge neutralising mutations on this interaction, however, has thus far not been investigated.

The SMC family is defined by its structural attributes. The prevalence of such homologous protein architecture throughout evolution is indicative of the way in which each protein is constructed being fundamental to its role in maintaining the genome. However, the roles of each SMC protein-containing complex are diverse and highly specialised, and as such, the higher order complexes that they form, and the accessory subunits that regulate them play equally as important roles in SMC protein function.

THE COHESIN COMPLEX

A tripartite ring-shaped molecule

While all complexes containing SMC proteins contribute essential roles to maintaining the genomes of the organisms in which they are found, the focus from now will be with cohesin, the complex that is tasked primarily with ensuring the fidelity of sister chromatid segregation during mitosis and meiosis. The structural similarities between cohesin and the other SMC complexes do not end here however; in addition to ATP-dependent dimerisation of the head domains, all SMC dimers are bridged by a protein of the kleisin[7] family to form a ring-shaped trimer (Schleiffer *et al.*, 2003). In the case of cohesin, it is the α-kleisin (known as Rad21, Rec8, Mcd1 and Scc1 across various organisms but referred to as Scc1 herein) that has this duty.

7 From Greek, κλείσιμο (*kleísimo*, "closure") for its role in closing the ring.

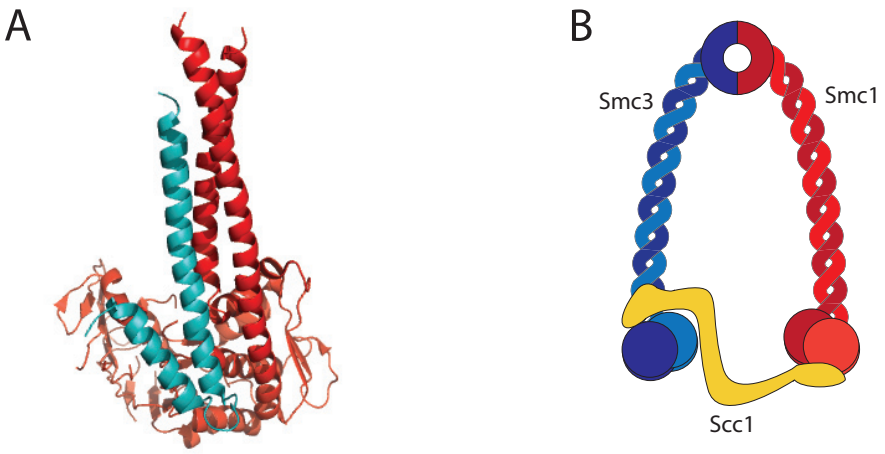

Figure 1-5. Asymmetric contacts between SMC proteins and kleisin subunit.
A Crystal structure of *B. subtilis* SMC-kleisin interface showing that contact is made between the SMC coiled coil (red) and an N-terminal extension from the kleisin (teal) (PDB identifier 3ZGX; Bürmann *et al.*, 2013). This is in contrast to the kleisin's C-terminal contact, which interacts with the SMC head.
B Schematic diagram of the proposed conformation of the cohesin complex showing Scc1 to make asymmetric contacts with the SMC proteins.

A globular winged-helix motif at the C-terminus of Scc1 interacts with the NBD of Smc1 and, no doubt due in large part to the homology between Smc1 and Smc3 head domains in addition to corroborating biochemical data, it has long been assumed that Scc1's N-terminus makes a similar contact with Smc3 (Gruber *et al.*, 2003; Haering *et al.*, 2004). However, attempts to crystallise Scc1's N-terminus in complex with Smc3's NBD have thus far not been successful. Indeed, in light of the recently published crystal structure of *B. subtilis* SMC head making asymmetrical contacts with its bridging kleisin (ScpA) despite its being a homodimer (Bürmann *et al.*, 2013), it is seeming increasingly likely that the assumptions that have been made of cohesin are incorrect and that Scc1 in fact may interact with Smc3's coiled coil (Fig. I-5).

The topological embrace

A protein's structure often holds the key to understanding the mechanism by which it acts. In the case of cohesin, its role in holding sister chromatids together and the fact that it is estimated to form a ring immediately bring to mind a model whereby two sister chromatids are entrapped within one cohesin ring (Fig. I-6a). With a predicted diameter of approximately 40 nm (Haering *et al.*, 2002), the ring should comfortably accommodate two 11 nm chromatin fibres. Consistent with this notion, proteolytic cleavage of cohesin is sufficient to destroy the connection between the sister DNAs with which it interacts, both *in vivo* and *in vitro* (Uhlmann *et al.*, 1999; 2000; Gruber *et al.*, 2003; Ivanov & Nasmyth, 2005; Oliveira *et al.*, 2010; Tachibana-Konwalski *et al.*, 2010). In addition, linearisation of a circular minichromosome is able to release the cohesin molecules that were previously bound (Ivanov & Nasmyth, 2005). Whereas the results of the former experiments may still be explained by physical models, such as one whereby cohesin molecules acts as a tether between sister DNAs, the results of Ivanov and Nasmyth (2005) imply that cohesin may simply slide off the minichromosome, which would not be the case should a physical contact be made between cohesin and DNA.

The above evidence argues strongly in favour of a topological rather than physical model of cohesion, and is corroborated by a similar experiment performed with condensin (Cuylen *et al.*, 2011), perhaps suggesting a mechanism of DNA entrapment common to all SMC complexes. It does not, however, eliminate all alternatives to the simple ring model. Several models

exist whereby multiple rings cooperate to build sister chromatid cohesion. Notable examples, depicted in Figure I-6, are the 'handcuff' model, in which a cohesin molecule entraps a single chromatin fibre and interacts physically with a cohesin molecule entrapping its sister, and models involving cohesin molecules that interlink themselves as well as DNA, or those that oligomerise to form large rings of higher order.

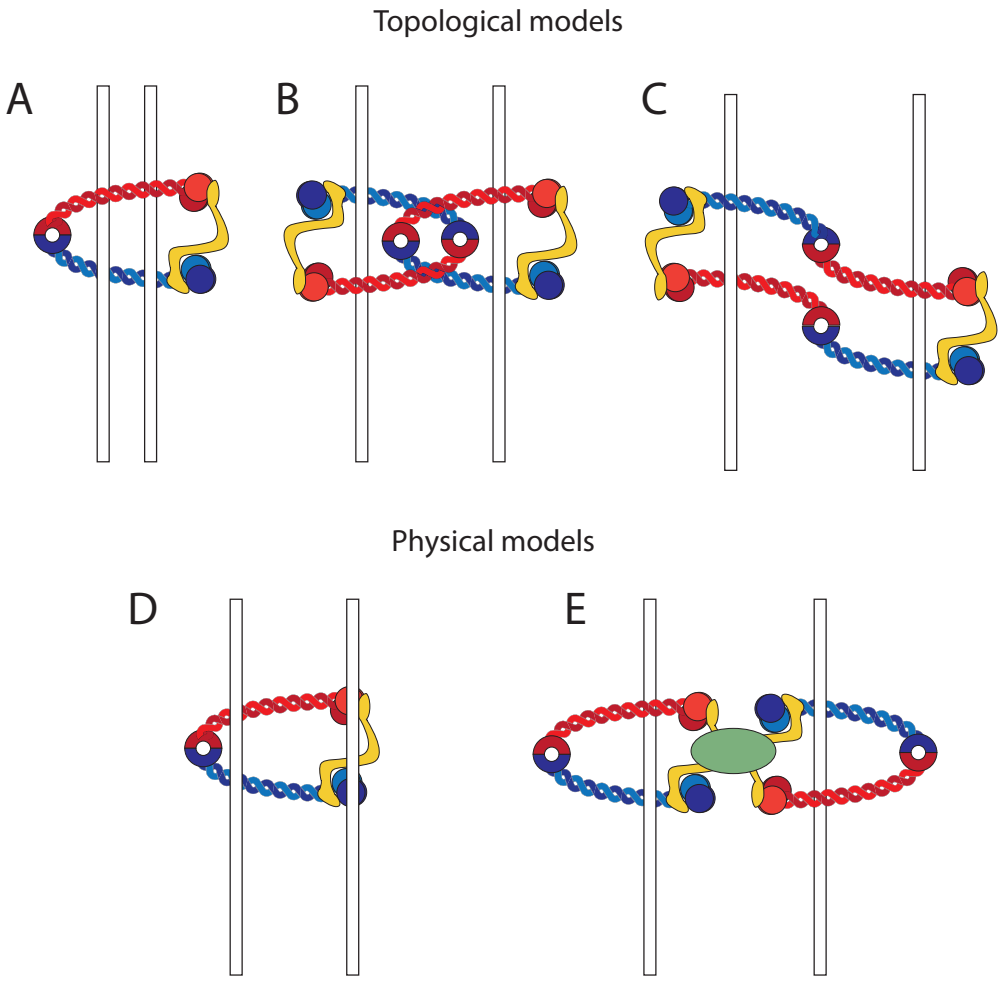

Figure I-6. Models for sister chromatid cohesion.
A The ring model, involving topological entrapment of two sister chromatids within one ring.
B A handcuff model, whereby each sister is topologically entrapped within a cohesin ring and two rings interact topologically with each other.
C A dimeric ring model, in which two cohesin molecules multimerise to entrap sisters within a large ring.
D Simple physical contact between cohesin and DNA holds sisters together.
E A variant handcuff model in which each sister is topologically entrapped within a cohesin ring and two rings are connected by a physical bridge.

The strongest evidence to date that cohesin entraps sister DNAs within one ring comes from Haering *et al.* (2008). Their experiment made use of a modified cohesin ring in which Smc3 and Scc1 were expressed as a fusion protein and both the Smc1/Smc3 hinge and the Scc1/Smc1 head interfaces were engineered to contain cysteine residues that could react *in vitro* with a thiol-reactive crosslinker; thus the trimeric ring could be covalently closed at all three interfaces. Upon purifying dimeric circular minichromosomes linked by cohesin, and inducing covalent bond formation at the two target interfaces, it was found that dimers persisted in denaturing conditions. In addition, this convincing rebuttal of physical 'handcuff'-like models provided further evidence to support the single ring hypothesis. By performing the experiment with extracts from cells that express two types of Smc3-Scc1 fusion protein, one able to be cleaved by Tobacco Etch Virus (TEV) protease, and one unable, half the dimeric minichromosomes were resistant to TEV-mediated cleavage. One would expect a lower percentage of TEV resistance should double or multimeric rings be responsible for holding sisters together, thus the result is in favour of a single ring entrapment model.

THE COHESIN CYCLE

Cohesin loading

Cohesin's topological embrace of DNA provides a fathomable mechanism by which sister chromatids may be ensured to remain in their partnered state

until the moment arises to separate them. It does, however, raise the question of how the ring is able to trap sister DNAs inside itself. Disregarding the seemingly implausible model that would involve DNA being transiently broken to allow cohesin to slide onto it before then being repaired, one option would be that the separate subunits that constitute cohesin congregate at DNA and assemble as a ring-shaped complex *de novo* around it. While this model would easily explain the way in which two sister chromatids end up inside the ring, it only raises more questions as to how this process is controlled such that it occurs only in the vicinity of DNA and, indeed, that it traps only replicated sisters within it. The more likely scenario, supported by several lines of evidence, is that cohesin's first association with DNA is as a pre-formed ring. Particularly, both electron micrographic and biochemical data indicate that soluble cohesin assumes an annular conformation even in the absence of DNA (Anderson *et al.*, 2002; Gruber *et al.*, 2003). In addition, it appears that these rings first associate with single chromatids prior to their replication. In most eukaryotes, due to the presence of an intact population of cohesin following anaphase (discussed later) this can occur as early as telophase (Losada *et al.*, 1998; Sumara *et al.*, 2000; Gerlich *et al.*, 2006); in yeast, cohesin's loading is limited temporally by the synthesis of both Scc1 and securin, which occurs in G_1 phase (Guacci *et al.*, 1997; Michaelis *et al.*, 1997; Uhlmann *et al.*, 1999). While it remains unclear whether or not the cohesin that associates with chromatin prior to DNA replication does so topologically, to end up in a situation whereby the ring embraces both sisters would logically require transient dissociation of at least one of its three junctions.

The task of defining the so-called 'DNA entry gate' was taken on by Gruber *et al.*, (2006). Expressing Smc3-Scc1 or Scc1-Smc1 as fusion proteins in yeast in the absence of their wild type counterparts resulted in functional cohesin rings, implying that neither interface between SMC protein heads and α-kleisin acts as a sole entry gate. While the hinges of Smc1 and Smc3 cannot be fused in the same manner owing to their being in the middle of the protein, replacing these domains with substitute dimerisation domains belonging to p14 and MP1, respectively, prevents cohesin loading entirely. Furthermore, by introducing the rapamycin-dependent dimerisation domains FRB and FKBP12 into a flexible loop of the wild type hinges, the researchers found that addition of rapamycin prevented sister chromatid cohesion only when added when added to cells before S phase. Its addition after S phase had no effect on cohesion. While these experiments certainly provide conclusive evidence that the hinge plays a crucial role further to Smc1/Smc3 dimerisation, and are consistent with the hypothesis that the hinge is DNA's gate into the ring, definitive confirmation that this is the case is still lacking. In the case of *B. subtilis* SMC proteins, the hinge domain appears to facilitate physical interaction between cohesin and DNA. In fact, DNA binding to the hinge itself may be involved in stimulating ATPase activity (Hirano & Hirano, 2002; 2006).

Although the cohesin ring is formed of a trimer of Smc1, Smc3 and Scc1 proteins, an additional protein, namely Scc3, is a stably bound and integral member of the cohesin holocomplex. It interacts with the ring *via* the C-terminus of Scc1 (Haering *et al.*, 2002). While there is no evidence to suggest

that Scc3 plays a role in the loading *per se*, in its abesnce cohesin is unable to associate with DNA (Hu *et al.*, 2011). It has been suggested that Scc3 might form a proteinaceous link between two cohesin molecules in the previously discussed 'handcuff'-like model of sister chromatid cohesion (Zhang *et al.*, 2008b). However, the fact that all four cohesin subunits exist on chromosomes in 1:1:1:1 stoichiometry is inconsistent with this notion (Chan *et al.*, 2012).

For its association with DNA, the cohesin holocomplex depends on the evolutionarily conserved kollerin[8] complex, comprising Scc2 and Scc4 proteins (Furuya *et al.*, 1998; Ciosk *et al.*, 2000; Gillespie & Hirano, 2004; Takahashi *et al.*, 2004; Watrin *et al.*, 2006; Seitan *et al.*, 2006; Bernard *et al.*, 2006). Remarkably, this DNA recruitment appears to be mutual, at least at centromeres; kollerin fails to accumulate at centromeres prior to Scc1's transcription or in the absence of complete cohesin rings (Fernius *et al.*, 2013).

Kollerin is less well studied, both structurally and functionally, than other essential contributors to cohesin-mediated cohesin. In fact, its Scc2 subunit was first identified in *S. pombe*, where it was thought to impart sister chromatid cohesion in a cohesin independent manner (Furuya *et al.*, 1998). However, despite being essential during G_1/S phase for cohesion until the metaphase/anaphase transition, both Scc2 and Scc4 are dispensible following replication, since inactivating either subunit in G_2 phase does not result in a loss of cohesion (Ciosk *et al.*, 2000; Bernard *et al.*, 2006). This has finally led to the understanding that it is *via* cohesin that the complex functions.

8 From Greek, κολλάω (*kollao*, "to glue"), for its role in attaching cohesin to chromosomes.

Kollerin's large subunit Scc2 (approximately 170 kDa in *S. cerevisiae*) is predicted to consist mainly of α-helical HEAT (Huntingtin, Elongation factor 3, Protein Phosphatase 2A, TOR1) repeat motifs (Andrade & Bork, 1995; Neuwald & Hirano, 2000; Panizza *et al.*, 2000). The smaller subunit Scc4 (approximately 70 kDa in *S. cerevisiae*) is predicted to be composed of a different class of α-helical fold, namely the tetratricopeptide repeat (TPR) motif (Watrin *et al.*, 2006). It is proposed that the two subunits interact *via* their respective N-termini (Seitan *et al.*, 2006; Takahashi *et al.*, 2008; Braunholz *et al.*, 2012), the specific functions of the rest of the proteins, however, remain elusive. These two highly repetitive folds are typical of proteins involved in mediating protein-protein interactions (Andrade & Bork, 1995; Blatch & Lässle, 1999; D'Andrea & Regan, 2003), and as such kollerin may act as a platform at sites of cohesin loading, onto which mutliple factors assemble, thus facilitating the process. Correspondingly, despite not forming a strong or stoichiometric interaction with cohesin, data acquired from both mass spectrometry following kollerin purification, and immunoprecipitation of either cohesin or kollerin, indicate that a weak and/or transient interaction between the two complexes may take place (Tóth *et al.*, 1999; Arumugam *et al.*, 2003).

Aside from its role in cohesin loading, kollerin's Scc2 subunit has been implicated in the chromatin association of the other eukaryotic SMC protein complexes, namely condensin and the Smc5/Smc6 complex (Lindroos *et al.*, 2006; D'Ambrosio *et al.*, 2008), which may be indicative of a common mechanism for loading of all three complexes.

A final requirement for the stable association of cohesin with DNA is ATP binding and hydrolysis at the NBD heads of both Smc1 and Smc3 (Arumugam *et al.*, 2003; Weitzer *et al.*, 2003).

Sites of cohesin loading and residence

A distinct profile of cohesin's binding to DNA in budding yeast has been widely reported using chromatin immunoprecipitation techniques (Blat & Kleckner, 1999; Megee *et al.*, 1999; Tanaka *et al.*, 1999; Laloraya *et al.*, 2000). Cohesin is predominantly enriched in a domain of approximately 20-50 kb surrounding the centromere and also associates with discrete intergenic regions spaced at approximately 11 kb intervals between convergent genes (Glynn *et al.*, 2004; Lengronne *et al.*, 2004; Lindroos *et al.*, 2006). While these arm loci of cohesin enrichment are reportedly A-T-rch (Blat & Kleckner, 1999), no reports to date have revealed nucleotide sequence element specificity of either cohesin or kollerin. Instead, there appear to be a number of protein factors located on DNA itself that are essential for both complexes to localise to chromatin. One such factor, identified in *X. laevis* egg extracts, is the pre-replication complex (pre-RC), which assembles on DNA prior to the initiation of replication during the process of replication licensing (Gillespie & Hirano, 2004; Takahashi *et al.*, 2004). In fact, kollerin co-immunoprecipitates with the pre-RC associated activator of replication Cdc7-Drf1 (Dbf4-dependent kinase, DDK) which acts through phosphorylating the Mcm2-7 helicase component of pre-RCs (Takahashi *et al.*, 2008). Importantly, this implicates

cohesin and its loader at sites of replication at which it is imperative that cohesion establishment occurs.

In budding yeast, cohesin's centromeric enrichment is dependent on approximately 125 bp of underlying DNA sequence. Insertion of this short sequence into a small minichromosome of around 5 kb length permits its cohesion-mediated bi-orientation and faithful transmission (Megee & Koshland, 1999). Removal of the core centromere sequence from a yeast chromosome greatly reduces cohesin's association at the locus, while placing it at an ectopic arm locus causes centromere-like cohesin enrichment (Weber *et al.*, 2004). Specifically, outer kinetochore proteins of the Ctf19 complex (e.g. Ctf19, Mcm21, Iml3 and Chl4) have been shown to be essential for the localisation of this population of cohesin (Eckert *et al.*, 2007; Fernius & Marston, 2009; Ng *et al.*, 2009). More recently, a link has in fact been drawn between DDK and the Ctf19 complex. DDK is recruited to kinetochores in telophase/G_1 phase, whereupon it facilitates both replication initiation and cohesin loading. In the absence of Ctf19 or Chl4 proteins, the centromeric recruitment of DDK is severely reduced, having concordant deleterious effects on the enrichment of both Scc2 at the centromere and cohesin at the pericentromere (Natsume *et al.*, 2013).

Cohesin's distribution in fission yeast is largely similar to that in budding yeast (Lengronne *et al.*, 2004). However, pericentromeric cohesin accumulation and the mediation of sister chromatid cohesion is dependent on Swi6, a heterochromatin protein 1 (HP1)-like factor that interacts with

heterochromatic regions around the centromere (Nonaka *et al.*, 2002). Interestingly, Swi6 has also been shown to interact with DDK (Bailis *et al.*, 2003; Hayashi *et al.*, 2009). Together these results strongly indicate that DDK is a key factor in determining sites of kollerin and cohesin recruitment both at centromeric and arm loci. While it is currently unclear whether this occurs directly or indirectly *via* the replication initiation proteins that it targets, the mechanism may be common to all species.

As briefly mentioned, kollerin and cohesin do not appear to colocalise according to both live cell imaging and chromatin immunoprecipitation. How then is the cohesin loading complex able to facilitate cohesin loading? Using cohesin mutants that are defective in ATP hydrolysis and are thereby trapped in an intermediate step in the loading reaction, Hu *et al.* (2011) have shown that, at this intermediate step, kollerin and cohesin in fact do colocalise at core centromeres and highly transcribed genes. Whereas cohesion is mediated by cohesin that is stably bound to chromosomes (Gerlich *et al.*, 2006; Yeh *et al.*, 2008), ATP binding-defective cohesin fails to localise to DNA at all, and ATP hydrolysis-defective cohesin rapidly dissociates from it (Arumugam *et al.*, 2003; Weitzer *et al.*, 2003; Hu *et al.*, 2011). Thus ATP hydrolysis is essential for cohesion establishment. It is proposed that the energy produced by this reaction may be transmitted to opening the hinge interface (Hu *et al.*, 2011).

Following cohesion establishment, kollerin is dispensible (Ciosk *et al.*, 2000; Lengronne *et al.*, 2006) and the distribution of cohesin is no longer dictated by that of kollerin. Consistent with topological models of entrapment,

the ring appears able to translocate from its sites of loading at centromeres and highly transcribed genes to its pericentromeric and intragenic chromosomal addresses, respectively (Lengronne *et al.*, 2004; Hu *et al.*, 2011).

Cohesion establishment and maintenance

As previously discussed, cohesin is able to associate with DNA from telophase onwards. However the establishment of sister chromatid cohesion is temporally confined to the time during S phase that DNA replication occurs (Uhlmann & Nasmyth, 1998; Lengronne *et al.*, 2006). Cohesion subunits expressed after DNA replication (in G_2/M), while able to localise to DNA, are unable to form cohesive structures on it (Ström *et al.*, 2004; Ström & Sjögren, 2005; Lengronne *et al.*, 2006). In accordance with this, studies into the residence time of cohesin on DNA have revealed two populations: an unstable state corresponding to association during G_1, and a stable state following DNA replication (Gerlich *et al.*, 2006).

An essential factor involved in transforming unstably bound cohesin into a stably bound complex is the evolutionarily conserved acetyl transferase Eco1. Several studies have shown that two conserved adjacent lysines in the N-terminal head domain of Smc3 are its essential targets (Rolef Ben-Shahar *et al.*, 2008; Ünal *et al.*, 2008; Zhang *et al.*, 2008a; Rowland *et al.*, 2009). These lysine residues become acetylated only from the time of DNA replication, and are deacetylated followign the loss of cohesion at anaphase (Beckouët *et al.*, 2010; Borges *et al.*, 2010). The temporal regulation of Smc3 acetylation thus

precisely reflects the transition between unstable and stable populations of cohesin reported by Gerlich *et al.* (2006). The way in which Eco1 is coupled to transcription is suggested to be through its physical interaction with proliferating cell nuclear antigen (PCNA), a component of active replication forks (Moldovan *et al.*, 2006).

Less well understood is the contribution of the small ubiquitin-like modifier (SUMO) to cohesion establishment. SUMOylation occurs on lysine residues of several cohesin subunits and has recently been suggested to play as important a role as Smc3 acetylation in cohesion, since rings with abolished SUMOylation cause cohesion defects, but without affecting Smc3's acetylation (Almedawar *et al.*, 2012). The mechanism by which this modification stabilises cohesin's DNA association, however, remains to be elucidated.

Removal of cohesin from chromosomes

It was briefly mentioned earlier that sister chromatid cohesion is rapidly lost at the metaphase-to-anaphase transition upon activation of APC^{Cdc20}. The subsequent destruction of securin activates the protease separase, which cleaves its cohesin substrate twice in its Scc1 subunit, immediately and irreversibly opening the ring and leading to the instant dissolution of the connection between sisters (Uhlmann *et al.*, 1999; 2000; Musacchio & Salmon, 2007).

In mammalian cells an alternative pathway of cohesin removal exists, operating in prophase prior to APC^{Cdc20} activation (Losada *et al.*, 1998). This

pathway does not depend on cleavage by separase, but instead, just as in cohesin loading, predicts that one of the three interfaces must dissociate to release the entrapped DNA. The prophase pathway depends on Wapl (Gandhi *et al.*, 2006; Kueng *et al.*, 2006), a cohesin-associated protein. By removing cohesin in a cleavage-independent manner, an intact soluble pool of cohesin exists following metaphase for its immediate reloading during telophase. This is especially important in metazoans due to cohesin's potential non-canonical role in transcriptional regulation (reviewed by Dorsett & Krantz, 2009). While budding yeast does not remove much, if any, cohesin *via* the prophase pathway, there is a turnover of cohesin on DNA prior to cohesion establishment (Chan *et al.*, 2012). Thus separase-independent cohesin removal does occur in *S. cerevisiae* and several important breakthroughs in understanding its mechanism have been made in this system.

Initially, the mechanism by which Smc3 acetylation promotes cohesion began to be elucidated in budding yeast following a genetic screen to find suppressors of a thermosensitive *eco1* allele (*eco1-1*) (Rolef Ben-Shahar *et al.*, 2008; Rowland *et al.*, 2009; Sutani *et al.*, 2009). Mutations in three cohesin-associated proteins, namely Scc3, Pds5 and Wapl[9], were identified as having the ability to bypass Eco1 function. Since Eco1's function is to promote cohesion, the implication is that these proteins in some way prevent it. Somewhat counterintuitively, both Scc3 and Pds5 have been identified as being essential for sister chromatid cohesion (Tóth *et al.*, 1999; Panizza *et*

9 At the time identified as Rad61, but here referred to as Wapl for consistency between nomenclatures in different species.

al., 2000; Lengronne *et al.*, 2004). While this apparent duality of function is not yet understood, it appears that Wapl, through its association with Pds5 and Scc3, antagonises cohesin's association with DNA, thereby conferring a 'releasing' activity. Recently, Chan *et al.* (2012) found that expressing Smc3 and Scc1 as a fusion protein bypassed the requirement for Eco1, indicating that the role of acetylation is in stabilising this interface. Whereas expressing Wapl in G_2/M in the absence of Eco1 function leads to cohesin's dissociation from chromosomes, Smc3-Scc1 fusion prevents this (Chan *et al.*, 2012). Fusion of Smc3 to Scc1 has also been shown to prevent Wapl-mediated cohesin removal from DNA in *D. melanogaster* (Eichinger *et al.*, 2013). Thus Wapl opposes Eco1 by promoting release of DNA *via* the exit gate formed at the junction between Smc3 and Scc1.

COHESINOPATHIES

Cohesin is best known for its role in building and maintaining sister chromatid cohesion during the cell cycle. Its malfunction in this role can lead to the severe effect of aneuploidy, a hallmark of cancer. Aneuploidy in the germline follows incorrect meiosis and can cause developmental disorders in offspring. Given that the germline of most vertebrate females is maintained in a prolonged prophase I arrest, cohesin is implicated in holding homologous chromosomes together until fertilisation, which may be months, years, or even

decades after it was first loaded. Mice that express mutated *SMC1β* (mammalian meiosis-specific *SMC1*) produce age-related aneuploid oocytes (Hodges *et al.*, 2005). Remarkably it appears from recent studies in mammalian systems that cohesin synthesis is not sustained in oocytes and is indeed not replaced from the time at which it loaded (Revenkova *et al.*, 2010; Tachibana-Konwalski *et al.*, 2010). One might extrapolate from these results that degeneration of cohesin over time and its failure to be replaced provides an explanation as to why incidence of trisomies such as Down syndrome (trisomy 21) increases with maternal age.

However, another class of illnesses is attributed to mutations in cohesin and cohesin-related genes themselves. These are collectively termed cohesinopathies and include Roberts and Cornelia de Lange Syndromes (RBS and CdLS, respectively).

RBS is a rare autosomal recessive disorder caused by mutants in the human *ECO1* orthologue, *ESCO2* (Van Den Berg & Francke, 1993; Vega *et al.*, 2005). RBS patients exhibit severe symptoms, including slow growth, malformed limbs and facial abnormalities. Their cells have clear mitotic chromosome segregation defects (Van Den Berg & Francke, 1993), indicating that cohesin's role in sister chromatid cohesion is compromised.

CdLS is a heterogeneous disorder affecting an estimated 1 in 10,000 births and characterised by slow growth, mental retardation, malformation of limbs and internal organs, hirsutism and distinct facial features (Dorsett & Krantz, 2009). More than half of all cases are caused by a heterozygous

loss-of-function of the human *SCC2* orthologue, *Nipped-B-Like* (*NIPBL*) (Krantz *et al.*, 2004; Tonkin *et al.*, 2004), while heterozygous *SMC1* or *SMC3* mutations have been implicated in up to 5 % of cases (Deardorff *et al.*, 2007). Phenotypic presentations range from mild to severe; patients with nonsense mutations in *NIPBL* normally have the most severe phenotypes while missense mutations, which do not cluster to any appreciable degree, cause milder forms of the disorder (I. Krantz, personal communication). Several CdLS-causing missense mutations in Nipbl's N-terminus negatively affect its binding to the human Scc4 orthologue Mau2 (Braunholz *et al.*, 2012), indicating that compromised kollerin function may be a cause. However, in contrast to RBS, defects in sister chromatid cohesion and segregation are not defining characteristics of this syndrome. It is instead suggested to be *via* a non-canonical role of cohesin that CdLS arises.

Other than sister chromatid cohesion, cohesin is reported to play a role in the regulation of gene transcription. In *D. melanogaster*, cohesin and the Scc2 orthologue Nipped-B associate with actively transcribed genes where the former is suggested to regulate enhancer-promoter interactions (Misulovin *et al.*, 2008). Moreover, in human cells, cohesin is reported to interact and colocalise with the transcriptional repressor CTCF (Parelho *et al.*, 2008; Rubio *et al.*, 2008; Stedman *et al.*, 2008; Wendt *et al.*, 2008). Cohesin has also been implicated in DNA double-strand break repair in *S. cerevisiae* (Sjögren & Nasmyth, 2001), *S. pombe* (Birkenbihl & Subramani, 1992) and mammals (Jessberger *et al.*, 1993; 1996). CdLS being a disorder affecting a

non-canonical function of cohesin highlights the importance of the complex outside of mitosis.

Thesis objective

The aim of this thesis was to investigate the molecular basis for the cohesin loading reaction. Owing to the dearth of structural and functional information about cohesin's dedicated loading complex, kollerin, that existed at the time this project was initiated, the complex was studied biochemically through making mutants with a view to defining functional domains. In addition to this, a genetic screen to determine factors that cooperate with kollerin in the cohesin loading reaction was performed by Dr Maria Demidova and yielded promising results warranting further investigation. This was undertaken here.

Chapter II

A mutation in Smc1 overcomes the requirement for Scc4 and weakens the hinge interface

A mutation in Smc1 overcomes the requirement for Scc4 and weakens the hinge interface

INTRODUCTION

The ring model postulates a topological embrace of sister chromatids within the heterotrimeric annulus formed by cohesin's Smc1, Smc3 and Scc1 subunits (Haering *et al.*, 2002). This embrace ensures that, when cell division occurs, equal copies of genetic material are segregated into each daughter cell by cutting the cohesive ties that bind them in a precise, temporally regulated manner (Uhlmann *et al.*, 1999). Although the sequence of events leading to cohesin's removal from chromosomes at the metaphase-to-anaphase transition is well defined, the process of cohesin loading onto DNA is poorly understood.

Without a complex comprising Scc2 and Scc4, named kollerin, the ring fails to associate with chromatin at all (Tóth *et al.*, 1999; Ciosk *et al.*, 2000). Yet, other than evidence that Scc2 co-immunoprecipitates with with all four members of the core cohesin complex, namely Smc1, Smc3, Scc1 and Scc3 (Tóth *et al.*, 1999; Arumugam *et al.*, 2003), next to nothing is known of how kollerin functions. Unlike the aforementioned members of the core cohesin complex, which are required from the time at which cohesin loads onto DNA in late G_1 until chromosome disjunction in anaphase, kollerin is dispensable following cohesion establishment during S phase (Michaelis *et al.*, 1997; Tóth

et al., 1999; Ciosk *et al.*, 2000). As it appears only to be essential during the early stages of the cohesin cycle rather than for cohesion maintenance, the complex is often referred to as the 'cohesin loading complex'.

Cohesin has a distinct profile of binding to chromosomes. Chromatin immunoprecipitation experiments have shown the complex to be enriched in a region of around 50 kb flanking the centromere (Blat & Kleckner, 1999; Laloraya *et al.*, 2000). Cohesin loading occurs predominantly at the centromeres and, at least in budding yeast, is dependent on functional kinetochores; gene deletion of many of the non-essential central kinetochore proteins in the Ctf19 complex, including Ctf19 itself, results in a cell's failure to become enriched in pericentromeric cohesin (Weber *et al.*, 2004; Eckert *et al.*, 2007; Fernius & Marston, 2009; Ng *et al.*, 2009). Nonetheless, these cells are able to undergo successful mitoses owing presumably to cohesin on chromosome arms (Fernius & Marston, 2009).

A known prerequisite for the stable association of cohesin with chromosomes is the binding and hydrolysis of ATP at the nucleotide-binding head domains of the SMC subunits (Arumugam *et al.*, 2003; Weitzer *et al.*, 2003). Despite the purpose of the energy that is produced in this reaction remaining unclear, one study has addressed the fate of cohesin molecules that have mutated active sites such that they are unable to catalyse ATP hydrolysis (Hu *et al.*, 2011). Not only do these molecules fail to form cohesive structures on DNA, they also exhibit an abnormal localisation on DNA as determined by live cell imaging and ChIP-sequencing. This centromeric, rather than

pericentromeric, enriched pool of cohesin coincides with sites of kollerin enrichment.

Kollerin's localisation is dependent both on the presence of all cohesin subunits and the centromeric accumulation of Dbf4-dependent kinase (DDK), the recruitment of which is, in turn, dependent on the Ctf19 complex (Fernius *et al.*, 2013; Natsume *et al.*, 2013). Thus it is theorised that cohesin loading occurs at the centromere, with ATP hydrolysis being required to form stably associated structures. This would then be followed by translocation of the ring to surrounding sites, presumably through sliding along chromatin, and potentially involving the action of polymerases pushing the molecules to sites of convergent transcription (Lengronne *et al.*, 2004) (Fig. II-1).

Although published data are consistent with a topological model of entrapment, it will not be possible to fully rule out physical models for cohesion

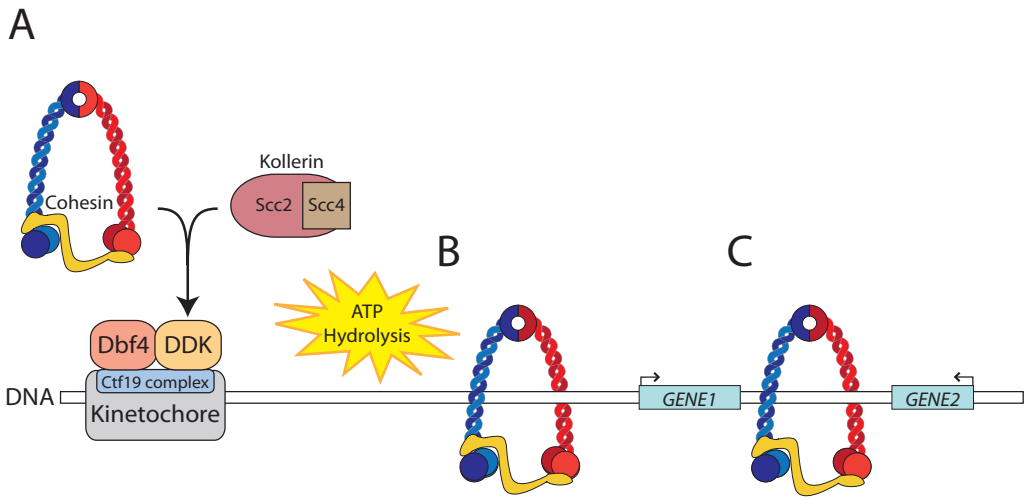

Figure II-1. Current model for cohesin loading and sliding.
A Following Scc1 transcription, cohesin and kollerin are recruited to kinetochores in a DDK-dependent manner. **B** ATP hydrolysis at SMC heads leads to the stable association of cohesin on chromosomes. **C** The complex does not remain at its major centromeric loading site, but instead accumulates at specific pericentromeric loci, which may be a consequence of having been 'pushed' there by polymerases.

without further biochemical evidence. However, assuming the ring model to be correct, a final requirement for cohesin loading is the transient opening of at least one of the three ring interfaces to allow DNA entry. Current evidence points towards the junction between Smc1 and Smc3 hinges being the most plausible entry gate for DNA: in the event of rapamycin-induced closure of the hinge domain, cohesin's association with chromatin is abolished, whereas the covalent closure of either SMC-kleisin interface permits cell proliferation (Gruber *et al.*, 2006). The notion of the existence of more than one potential entry gate, however, has never adequately been addressed and remains a possibility.

Despite the requirement during loading for these constituent elements being widely accepted, the interplay between them is unclear to date. Here, yeast genetics is used with a view to revealing new insights into the process of cohesin loading. Yeast genetics is an incredibly powerful tool in determining components of particular biological processes. To give one notable example, Lee Hartwell and Paul Nurse, using budding and fission yeasts respectively, performed genetic screens that uncovered many of the factors integral to the regulation of the cell cycle (Hartwell *et al.*, 1973; Nurse *et al.*, 1976), resulting in their being awarded the Nobel Prize in Physiology or Medicine in 2001 (together with Tim Hunt for his contribution using sea urchin eggs; Evans *et al.*, 1983). Indeed, the entire core cohesin complex and one essential component of its loading complex, Scc2, were themselves identified using the power of yeast genetics (Strunnikov *et al.*, 1993; Guacci *et al.*, 1997; Michaelis

et al., 1997).

Screening for genetic suppressors of particular phenotypes can elucidate functional relationships between proteins. For example, recent insights into the function of Eco1 were made by suppressing the thermosensitive phenotype of the *eco1-1* allele in *S. cerevisiae* (Rolef Ben-Shahar *et al.*, 2008; Rowland *et al.*, 2009; Sutani *et al.*, 2009). Although Eco1 was previously understood to be an acetyl transferase important for sister chromatid cohesion, no physiologically relevant targets were known (Ivanov *et al.*, 2002). The studies revealed acetylation of lysines 112 and 113 in Smc3's head domain to be crucial for the establishment of sister chromatid cohesion. This discovery has paved the way in understanding the mechanism of cohesion maintenance.

The very same approach of screening for genetic suppressors has now been adopted to shed new light on the mechanism of cohesin loading. A screen for suppressors of the thermosensitive *SCC2* allele, *scc2-4*, has previously been carried out to no avail (M. Demidova, personal communication). At the time that this project commenced, a similar screen was performed by Dr Maria Demidova, instead using the thermosensitive *SCC4* allele, *scc4-4*. This had a surprising outcome: a suppressor mutation that appeared to be genetically linked to *SMC1* could revert *scc4-4*'s thermosensitive lethal phenotype to wild type.

The work presented here investigates the validity of the purported suppressor mutation in *SMC1* and considers its biochemical implications, as well as exploring the role of Scc4 in cohesin loading.

RESULTS

A mutation within Smc1 bypasses the requirement for Scc4

To investigate factors involved in the cohesin loading pathway, naturally arising mutants of a yeast strain containing the *scc4-4*[10] thermosensitive allele that permit growth at the restrictive temperature (35.5 °C) were identified in a genetic screen (Fig. II-2A; screen performed by M. Demidova).

The genetic linkage of suppressors was determined by crossing them to strains into which auxotrophic markers or drug resistance cassettes had been inserted proximally to candidate cohesin and cohesin-related genes. During this process, one extragenic suppressor, isolated from twelve independent clones, manifested the remarkable ability to support growth of not just *scc4-4* cells, but cells harboring a deletion of the essential *SCC4* gene (data not shown). This suppressor displayed a tight linkage to *SMC1*. Sequencing of the gene revealed the single base pair mutation 1762G>T in all cases. This resulted in a change at the level of Smc1's primary structure such that an aspartate residue at position 588 was mutated to tyrosine. The same missense mutation was also independently isolated from similar screens performed with the thermosensitive *SCC4* alleles *scc4-2*[11] and *scc4-6*[12] (K. Kozyrska, personal communication).

To confirm the ability of Smc1(D588Y) to bypass the requirement for Scc4 function, the strain was reconstituted *de novo* (Fig. II-2B). A yeast

10 *scc4-4(Y40N; I77L; K178R; C278S; I314N; S349T; M574I)*
11 *scc4-2(V73A; T104S; I169F; T265I; I432K; Q466R; F492L; Q509R)*
12 *scc4-6(L54M; K94E; S192A; N323Y; W373G; L390F; V397E; D534G; M574L)*

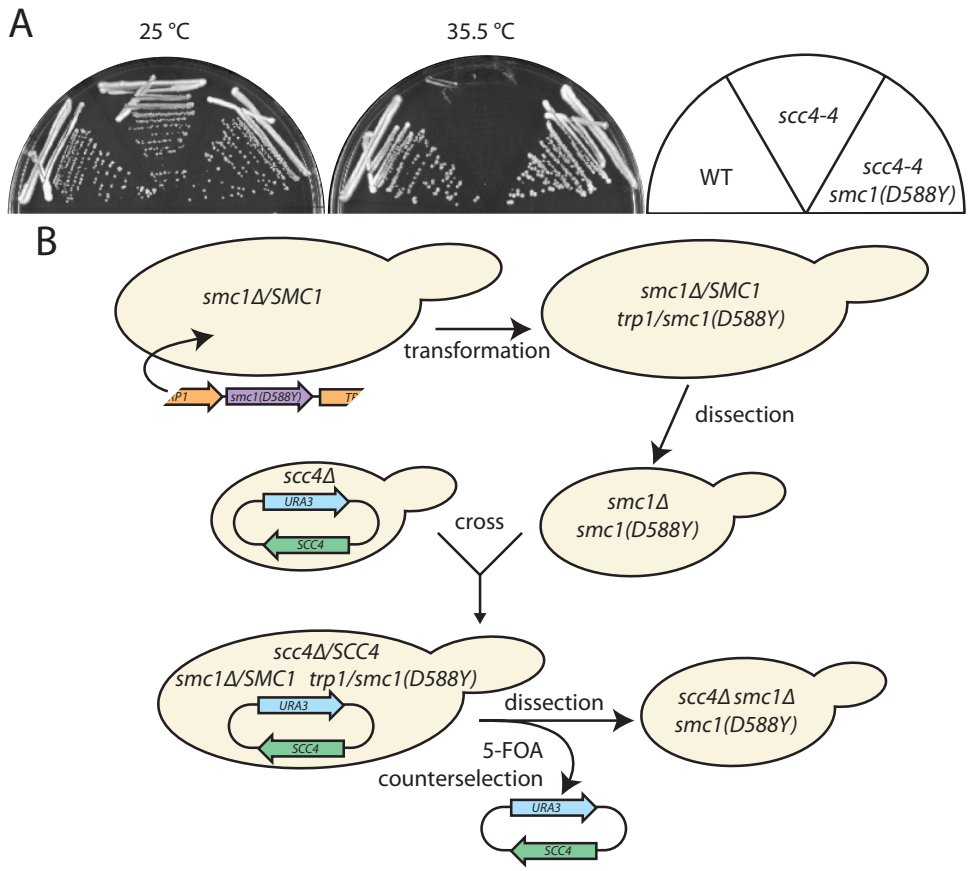

Figure II-2. Identification of a mutation that bypasses the requirement for Scc4.
A A strain harbouring a suppressor mutation, later identified as *smc1(D588Y)*, restores wild type-like growth of *scc4-4* cells at the restrictive temperature. Strains (K699, K8326, K19813) were grown for 2 d on YPD agar at the temperatures displayed.
B Schematic diagram depicting the method by which *scc4Δ smc1(D588Y)* was reconstituted *de novo*.

integrative plasmid harbouring *smc1(D588Y)* under its endogenous promoter was created by site-directed mutagenesis of the wild type gene. Following integration of the gene at the *trp1* locus in an *smc1Δ/SMC1* diploid, dissection of asci revealed that the ectopically expressed *smc1(D588Y)* is able to fully complement the lethality caused by *smc1Δ*, implying that the mutation does not impair Smc1 function (data not shown).

The resulting haploid was crossed to a strain in which a deletion of the essential *SCC4* gene was rescued by a *URA3*-containing plasmid harbouring

wild type *SCC4*. Diploids were then selected on medium containing the drug 5-FOA, which, due to being toxic to strains containing the *URA3* gene, was used to expel the plasmid (Boeke *et al.*, 1984). According to the probabilities predicted by Mendelian genetics, should *smc1(D588Y)* bypass *scc4Δ*, the combination should be present in 25 % of spore clones (12.5 % *smc1Δ*, 12.5 % *SMC1*). Upon dissection, 15.7 % of 108 spore clones contained the markers for *smc1(D588Y)* and *scc4Δ* (12.0 % *smc1Δ*, 3.7 % *SMC1*), thus Smc1D588Y was indeed found to be capable of bypassing Scc4 (Fig. II-3B). In contrast, dissection

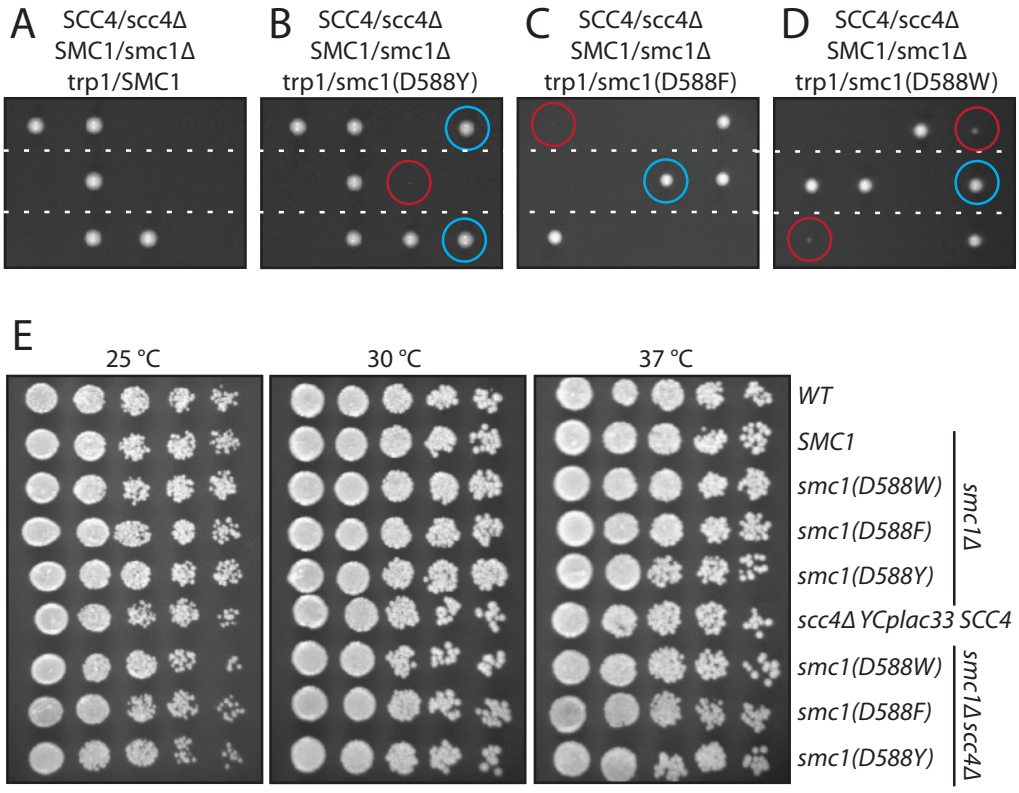

Figure II-3. Uncharged aromatic amino acid substitutions at Smc1's D588 bypass the requirement for Scc4.
Tetrad dissection performed on a heterozygous *smc1Δ/SMC1 scc4Δ/SCC4* strain with **A** *SMC1*, **B** *smc1(D588Y)*, **C** *smc1(D588F)* or **D** *smc1(D588W)* integrated at the *trp1* locus (K21973, K21974, K21990 and K22012, respectively). Spore clones in which *scc4Δ*-related lethality is suppressed by ectopically-expressed *smc1* mutants are circled in blue (*smc1Δ*) and red (*SMC1*). Dissection was performed on YPD agar and plates were incubated at 25 °C for 3 d.
E Five-fold serial dilutions of *smc1(D588)* point mutants and *scc4Δ* mutants were spotted onto YPD agar. Plates were incubated at the temperatures displayed for 2-3 d (K699, K20904, K22011, K20909, K21046, K8290, K21009, K21021, K21118).

of asci derived from *smc1Δ/SMC1 scc4Δ/SCC4* diploids in which wild type *SMC1* had been integrated at the *trp1* locus showed that ectopically expressed *SMC1* was unable to support growth in the absence of *SCC4* (Fig. II-3A). It was noted that only in the absence of *SCC4*, the suppressor mutant-expressing spores that also express endogenous *SMC1* grew more slowly than those with *smc1Δ*. Furthermore, this genetic combination was not seen as often as expected. Thus *SMC1* appears to be partially dominant over *smc1(D588Y)*.

Smc1's D588 is a highly conserved residue within cohesin's hinge interface

Cohesin's stable association with chromosomes occurs *via* an as yet elusive mechanism that requires ATP binding and hydrolysis at Smc1 and Smc3's NBDs, and transient opening of at least one interface of the ring (Haering *et al.*, 2002; Arumugam *et al.*, 2003). Following the identification of a single point mutation in Smc1 that is capable of rescuing *scc4Δ*-related lethality, uncovering the significance of this residue becomes a pertinent challenge.

Through multiple sequence alignment of Smc1 homologues, D588 was found to be a highly conserved acidic residue, not only within the *Saccharomycetaceae* family of fungi, but also throughout multicellular organisms (Fig. II-4A). Furthermore, the residue lies within a highly conserved patch of amino acids sharing the consensus sequence, (S/T)FΦPΦ[-](S/T/Y)Φ[13].

13 Φ = hydrophobic amino acid; [-] = acidic amino acid

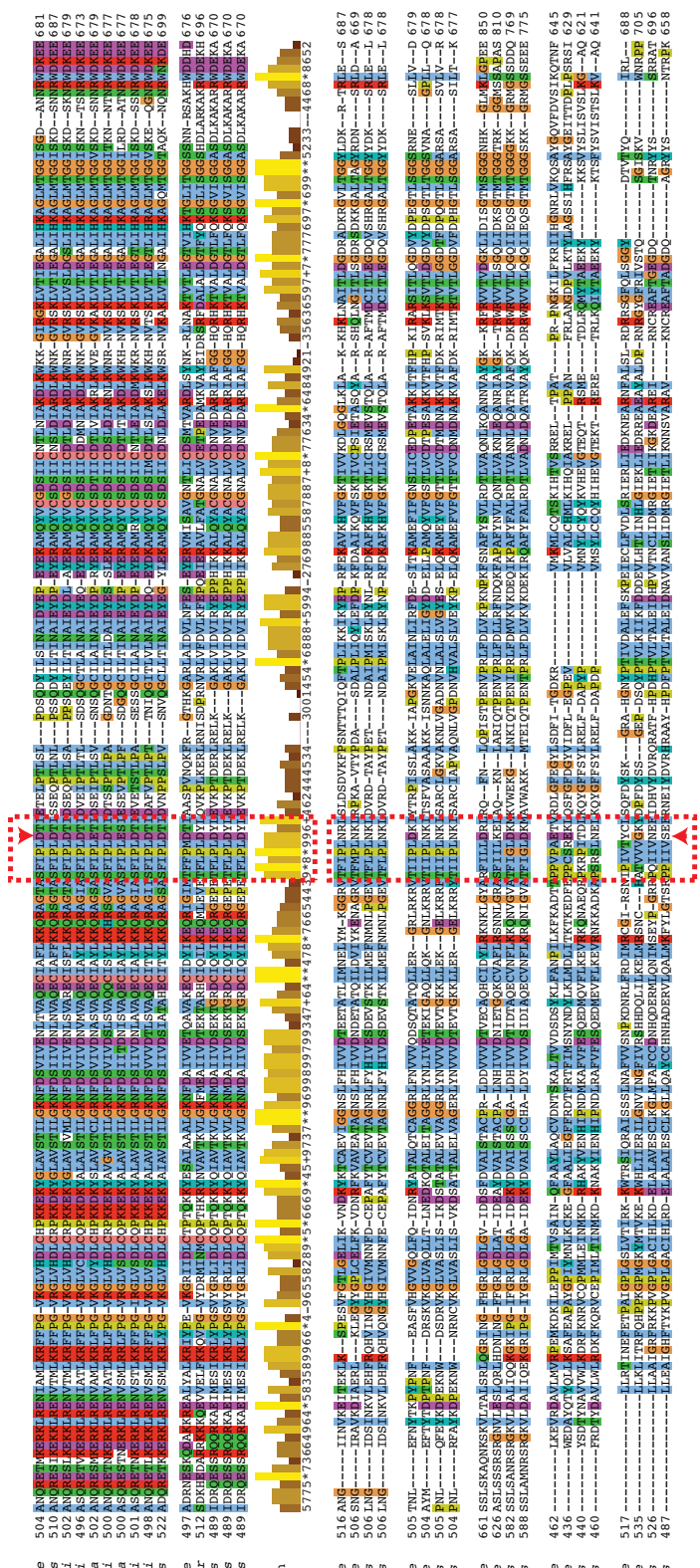

Figure II-4. D588 is a highly conserved Smc1 residue that is located within a patch conserved throughout SMC family members.
Multiple sequence alignments indicating the conservation of the residue D588 from *S. cerevisiae*'s Smc1 subunit in **A** Smc1 orthologues from the *Saccharomycetaceae* family of yeasts (upper panel) and more diverse eukaryotes (lower panel), and **B** SMC family members. Conservation of Smc1 orthologues is shown graphically. Consensus sequence containing residue analogous to D588 (red arrowheads) is outlined in red.

Interestingly the conservation of this patch, though not the negatively charged amino acid, extends to the structurally similar family member Smc3 and its condensin equivalent Smc2. Smc4, perhaps unsurprisingly given that it is the condensin equivalent of Smc1, shows a higher level of conservation of this amino acid throughout evolution. Neither Smc5 nor Smc6, however, exhibit these features (Fig. II-4B).

At position 588, the suppressor residue lies within the central hinge dimerisation domain of Smc1. Since no crystal structure of the *S. cerevisiae* hinge domain exists, *in silico* modelling using the crystal structure from *T. maritima* (PDB identifier 1GXL) was implemented with a view to visualising the molecular context of the aspartate (Fig. II-5). It was found that D588 is N-terminal to a β-strand (S583-P586) that forms an antiparallel, two-stranded β-sheet with a β-strand donated by Smc3 (G670-T673). Furthermore, the acidic D588 residue itself is in close proximity (at 3.7 Å) to a basic residue in Smc3, K652. Since this lysine residue shares the aspartate's high level of conservation (Fig. II-7A) this supports the notion that they may form a salt bridge interaction (Schueler & Margalit, 1995).

Scc2 is not upregulated in the absence of Scc4

Following the discovery that yeast can survive in the absence of Scc4 with the aid of a mutation in Smc1, one might envisage that in order to facilitate cohesin loading, a compensatory upregulation of the other kollerin subunit, namely Scc2, occurs. To test this hypothesis, using exponentially growing

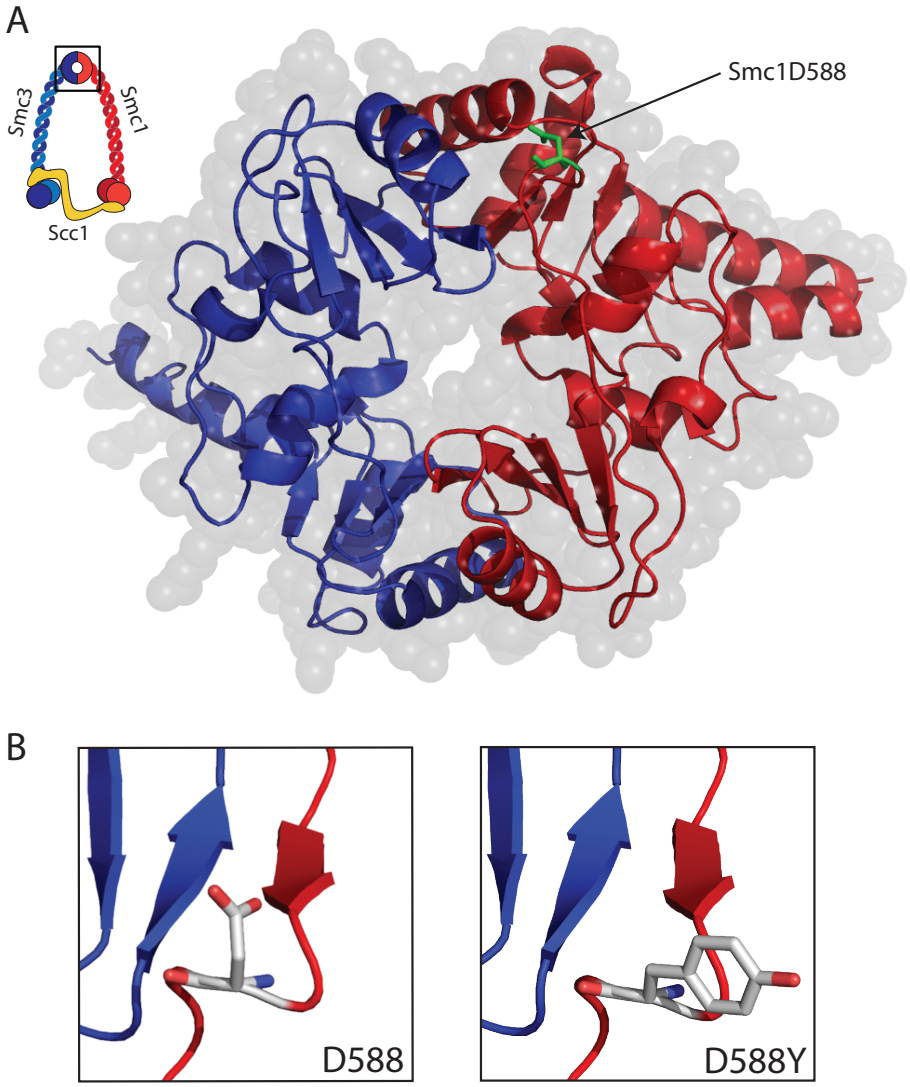

Figure II-5. D588 is positioned at the interface between Smc1 and Smc3 hinge domains.
A Homology model of *S. cerevisiae* Smc1 (red) and Smc3 (blue) hinge structure showing the location of Smc1D588 (green). The model was created using the crystal structure of SMC homodimer from *T. maritima* (PDB identifier 1GXL) as a template.
B Residue D588 is shown in close-up to emphasise its proximity to Smc3 (left panel). The effect of D588Y mutation is simulated (right panel).

strains in which Scc2 was PK epitope-tagged, protein levels were analysed by Western blot (Fig. II-6). In fact, Scc2 protein levels did not vary between wild type cells and cells harbouring the suppressor mutation *smc1(D588Y)*, either in the presence or absence of *SCC4*.

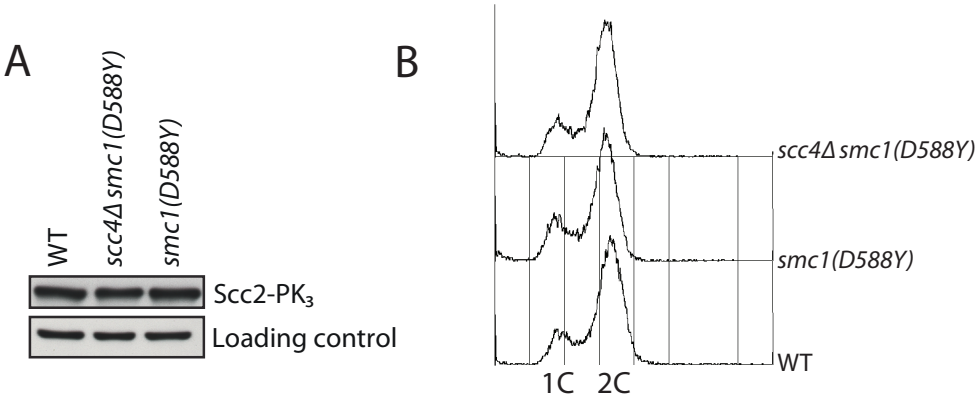

Figure II-6. Scc2 expression levels are unchanged in the absence of Scc4.
A Western blot showing expression of Scc2-PK_3 from exponentially growing cells in the presence and absence of *SCC4* and suppressor mutation *smc1(D588Y)*. Pgk1 is used as a loading control (K18921, K19429, K19431).
B FACS profile from exponentially growing cultures shows the cell cycle profiles to be similar in all strains.

Uncharged aromatic residue substitutions in Smc1 at position 588 can bypass the requirement for Scc4

After observing no modulation of Scc2, Smc1 was investigated biochemically with the intention to establish the nature of *scc4Δ* suppression.

Although an unbiased approach was implemented in the search for factors implicated in the cohesin loading reaction, the screen for suppressors of *scc4-4* is inherently biased towards the most common naturally occurring mutations, namely single base pair point mutations. It may have been a remarkable coincidence that the *SMC1* missense mutation 1762G>T encoding *smc1(D588Y)* was the only extragenic mutation that arose from the screen that could be genetically linked to the cohesin complex. However, perhaps other mutations in Smc1's hinge domain render Scc4 dispensable for cohesin loading. Indeed, perhaps other mutations at position 588 bypass the essential kollerin subunit.

In wild type yeast, Smc1's aspartate 588 is encoded by the codon GAC. Of the seven amino acids capable of arising at this position as a result of a single base pair point mutation (see Table II-1), only tyrosine did. To test the hypothesis that other amino acids may be capable of bypassing Scc4, the effect of mutating D588 to several different amino acids was investigated. The study incorporated amino acids with a wide variety of chemical properties, including both those that may and may not have arisen due to a single base pair point mutation of the D588 codon.

Codon	Translation	Properties
CAC	Asp > His	Aromatic, polar, basic
TAC	Asp > Tyr	Aromatic, polar, uncharged
AAC	Asp > Asn	Polar, uncharged
GGC	Asp > Gly	Non-polar, uncharged
GCC	Asp > Ala	Non-polar, uncharged
GTC	Asp > Val	Non-polar, uncharged
GAG	Asp > Glu	Polar, acidic
GAA	Asp > Glu	Polar, acidic
GAT	Asp (silent mutation)	Polar, acidic

Table II-1. List of amino acids that may arise due to a single base pair point mutation of the GAC codon.

A series of mutant *SMC1* plasmids were created by site-directed mutagenesis of the wild type gene. Strains were generated as depicted in the scheme shown in Fig. II-2B. Each of the mutants tested was able to complement the lethality caused by *smc1Δ* (data not shown). However, only Smc1D588F and Smc1D588W shared Smc1D588Y's ability to support growth in the absence of Scc4 (Fig. II-3C and D, results summarised in Table II-2). Following growth on YPD for 2 d at 30 °C, 27.8 % of 72 spore clones contained the markers for

smc1(D588W) and *scc4Δ* (18.0 % *smc1Δ*, 9.8 % *SMC1*), and 5.6 % of 72 spore clones contained the markers for *smc1(D588F)* and *scc4Δ* (4.2 % *smc1Δ*, 1.4 % *SMC1*). Consistent with what was previously observed with *smc1(D588Y)* (Fig. II-3B), these two mutants conveyed a slow growth phenotype when expressed alongside wild type endogenous *SMC1*.

Residue at 588	Complements *smc1Δ*?	Complements *scc4Δ*?
Asp (D)	YES	NO
Tyr (Y)	YES	YES
Phe (F)	YES	YES
Trp (W)	YES	YES
His (H)	YES	NO
Ala (A)	YES	NO
Glu (E)	YES	NO
Arg (R)	YES	NO
Asn (N)	YES	NO

Table II-2. Observed phenotype of mutations in Smc1 at position 588.

smc3(K652Y) is unable to bypass the requirement for Scc4

The aspartate at position 588 of *S. cerevisiae* Smc1 is a highly conserved acidic residue that lies in close proximity to a highly conserved basic residue: a lysine at position 652 in Smc3. This led to the hypothesis that a salt bridge may be disrupted when D588 is mutated to tyrosine, as it is in the suppressor of *scc4Δ*. If this were the case, then mutations at Smc3's K652 would result in similar suppression. The fact that no mutations in Smc3 arose from the original screen does not necessarily indicate that mutations at K652 are unable to bypass Scc4, rather that it is unlikely that a single base pair point mutation is able to.

In wild type yeast, Smc3's lysine 652 is encoded by the codon AAG. A single base pair change may lead to one of six missense mutations (see Table II-3). Notably, it appears unfeasible that this residue would naturally mutate to an aromatic residue.

Codon	Translation	Properties
ATG	Lys > Met	Non-polar, uncharged
ACG	Lys > Thr	Polar, uncharged
CAG	Lys > Gln	Polar, uncharged
AGG	Lys > Arg	Polar, basic
AAA	Lys (silent mutation)	Polar, basic
AAC	Lys > Asp	Polar, acidic
AAT	Lys > Asp	Polar, acidic
GAG	Lys > Glu	Polar, acidic
TAG	Lys > STOP	N/A (truncated protein)

Table II-3. List of amino acids that may arise due to a single base pair point mutation of the AAG codon.

Whether or not mutation of Smc3's K652 to an aromatic residue has the ability to bypass Scc4 function was investigated genetically, following a scheme similar to that depicted in Figure II-2B. A yeast integrative plasmid harbouring the wild type *SMC3* gene was engineered to encode *smc3(K652Y)* by site-directed mutagenesis. Following integration of the gene at the *leu2* locus in a heterozygous *smc3Δ/SMC3* diploid, tetrad dissection showed that the mutant gene was able to complement *smc3Δ* (data not shown).

The resulting haploid was crossed to a strain in which a deletion of *SCC4* was rescued by a *URA3*-containing plasmid harbouring wild type *SCC4*. This plasmid was expelled by plating cells on medium containing 5-FOA (Boeke *et al.*, 1984). Upon dissection, no spore clones containing the marker for *scc4Δ*

were found to survive, indicating that, unlike *smc1(D588Y)*, but like wild type *SMC3*, *smc3(K652Y)* was unable to bypass Scc4 deletion (Fig. II-7B and C).

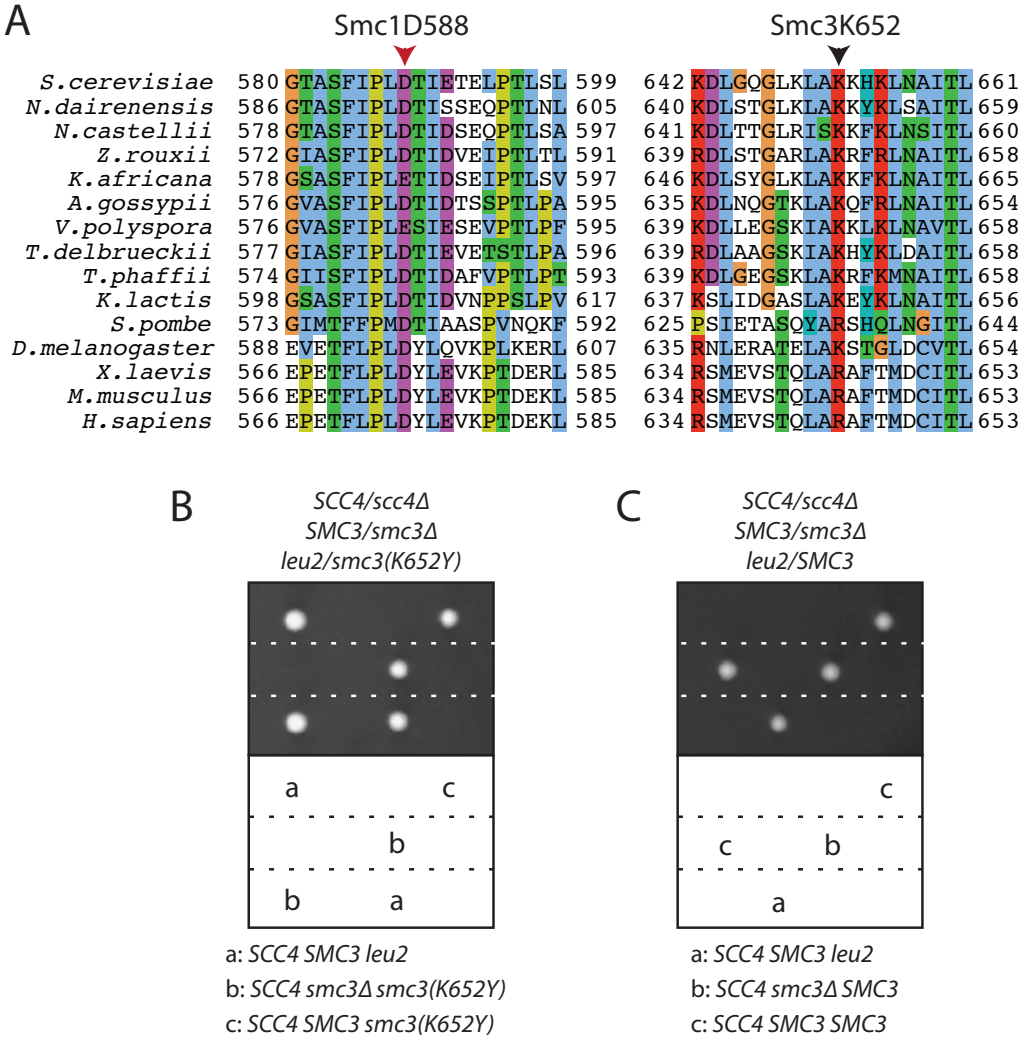

Figure II-7. Mutation of Smc3's conserved lysine 652 to tyrosine does not support yeast growth in the absence of *SCC4*.

A Multiple sequence alignments highlighting the similarity in the evolutionary conservation of the residue D588 from *S. cerevisiae*'s Smc1 subunit (red arrowhead) to K652 from *S. cerevisiae*'s Smc3 subunit (black arrowhead).

B,C Tetrad dissection performed on heterozygous *smc3Δ/SMC3 scc4Δ/SCC4* strains with **B** s*mc3(K652Y)* or **C** *SMC3* integrated at the *leu2* locus (K20205 and K20209, respectively). In both cases, 20 asci were dissected on YPD agar, which was incubated at 25 °C until the appearance of colonies was observed. The genetic marker for *scc4Δ* was never present. In addition, spore viability (38.75 % and 41.25 %, respectively) was consistent with the frequency expected should the ectopically expressed *smc3* be unable to bypass *scc4Δ* (37.5 %).

Suppressor mutations in Smc1 hinge weaken the interaction between Smc1 and Smc3

A number of studies have documented the ability of mutations in the interface between Smc1 and Smc3 hinges to alter the integrity of this dimerisation domain (Hirano & Hirano, 2002; Chiu *et al.*, 2004; Mishra *et al.*, 2010; Kurze *et al.*, 2011). Based on the position of the *scc4Δ* suppressor in Smc1 hinge, and the fact that an interaction between Smc1 and Smc3 may be disrupted by the mutation, the hypothesis that the suppressor mutations alter the interaction between Smc1 and Smc3 was investigated.

A biochemical assay was used to address whether heterodimerisation between the two hinges is affected by the Scc4-bypassing Smc1 mutations. An expression vector containing the wild type Smc1^{hinge} as an MBP fusion[14] (to improve solubility) was engineered by site-directed mutagenesis to encode mutant hinges, Smc1^{hinge}D588Y and Smc1^{hinge}D588W. Wild type and mutant proteins were expressed and purified to homogeneity from *E. coli* (Fig. II-8), and assayed for their ability to bind purified wild type Smc3^{hinge} [15] by *in vitro* co-immunoprecipitation.

Since previous experimental data have determined the dissociation constant of the hinge heterodimer to be approximately 25 nM at 20 °C (Mishra *et al.*, 2010; Kurze *et al.*, 2011), FLAG$_3$-tagged Smc3^{hinge} was incubated with wild type or mutant Smc1^{hinge} in an equimolar concentration of 250 nM (a concentration at which wild type hinge heterodimer formation is favoured

14 MBP-Smc1(S503-E681)-HIS$_6$

15 Smc3(T495-L705)-FLAG$_3$-HIS$_6$

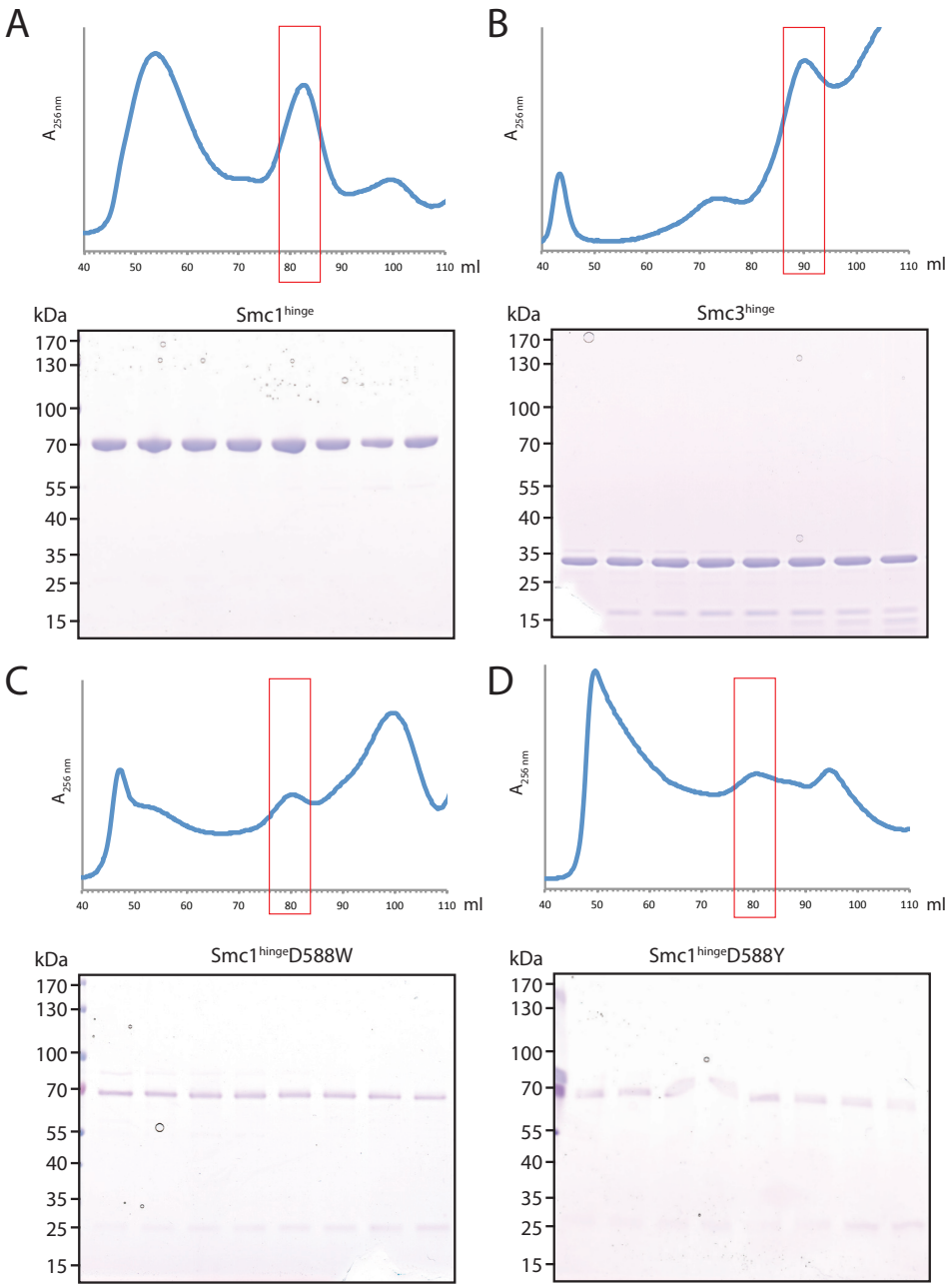

Figure II-8. Purification of Smchinge monomers.
Elution profile of **A** Smc1^{hinge}, **B** Smc3^{hinge}, **C** Smc1^{hinge}D588W and **D** Smc1^{hinge}D588Y proteins following size-exclusion chromotography (upper panels). Fractions taken from elution peaks corresponding to monomeric hinges (red boxes) were analysed by SDS-PAGE (lower panels).

over the monomeric state), then Smc3^{hinge} immunoprecipitated with anti-FLAG antibody-coupled beads, and interaction with Smc1 was determined by Western analysis (Fig. II-9).

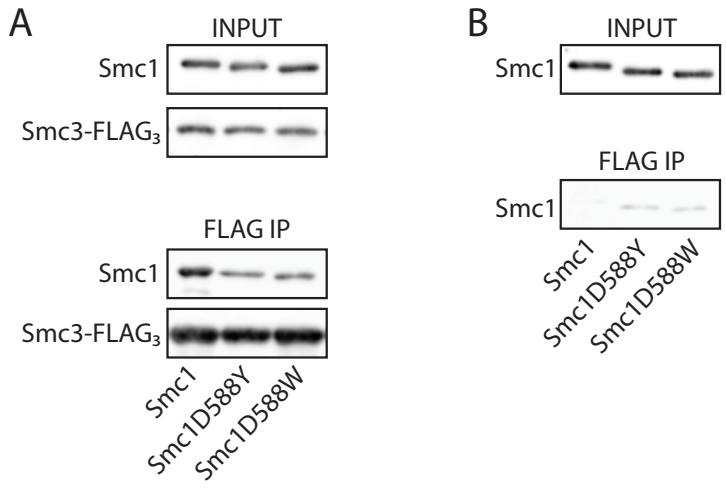

Figure II-9. Aromatic amino acid substitutions in Smc1 hinge lead to a weaker interaction with Smc3.
A Smc1 (wild type, D588Y or D588W) and Smc3-$FLAG_3$ monomeric hinge proteins were mixed together in equimolar ratio (250 nM each) and incubated for 15 min at 16 °C, then added to anti-FLAG beads and incubated for a further 15 min at 16 °C before being washed quickly three times. The amount of protein bound to beads was determined by Western blot using anti-HIS antibody to detect Smc proteins.
B Non-specific binding of wild type and mutant Smc1 hinges (250 nM each) to anti-FLAG beads, under the same conditions as in **A**.

As expected, wild type $Smc1^{hinge}$ successfully co-immunoprecipitated with $Smc3^{hinge}$. Although the mutant proteins also co-immunoprecipitated with $Smc3^{hinge}$, the level of interaction between $Smc3^{hinge}$ and $Smc1^{hinge}$D588Y appeared to be reduced compared to wild type, and to a similar extent as the reduction in binding observed between $Smc3^{hinge}$ and $Smc1^{hinge}$D588W, indicating a weaker interaction between Smc1 and Smc3 hinges in the presence of the mutated residues.

Hinge mutations predicted to weaken Smc1/Smc3 interaction are not able to bypass Scc4

Given that *smc1(D588Y)* and *smc1(D588W)* both display the ability to bypass Scc4 *in vivo* and have similar reductions in their affinity to Smc3 *in*

vitro, perhaps there are other mutations in the Smc1/Smc3 hinge interface that reduce the affinity between Smc1 and Smc3, and also make it possible to bypass Scc4.

A series of mutations have previously been designed in the 'north' and 'south' poles of the hinge heterodimer, aiming to disrupt the interaction between Smc1 and Smc3 (Mishra *et al.*, 2010). Several mutations[16] were described to weaken the interaction between isolated hinge domains as measured by gel filtration chromatography and co-immunoprecipitation experiments, but these mutations also caused lethal defects in sister chromatid cohesion. However, several other hinge mutants[17] that were created in the same study did not have such severe phenotypes and were not investigated further. These are depicted in Figure II-10A. Perhaps these mutants may weaken the interface sufficiently to bypass Scc4 but not so severely as to cause defects in sister chromatid cohesion.

In another study relating to the interface between cohesin's hinge domains, mutations were made in both Smc proteins with a view to neutralising the highly conserved, negatively charged inner pore (Kurze *et al.*, 2011). These mutations[18] had a lethal effect on yeast and were in fact surprisingly found to strengthen the interaction between Smc1 and Smc3 as measured by an *in vitro* competition assay. A genetic screen was later performed by Dr Alexander Kurze to find suppressors of the 'low dissociation rate' hinges. This yielded

16 *smc1(F584R)*, *smc1(M665R)*, *smc3(M577K)*, *smc3(F590R)*
17 *smc1(L635K; K639E)*, *smc1(I590K)*, *smc1(L564K)*, *smc3(E570K)*, *smc3(L672R)*
18 *smc1(K554D; K661D)*; *smc3(K668A; R665A; R669A)*

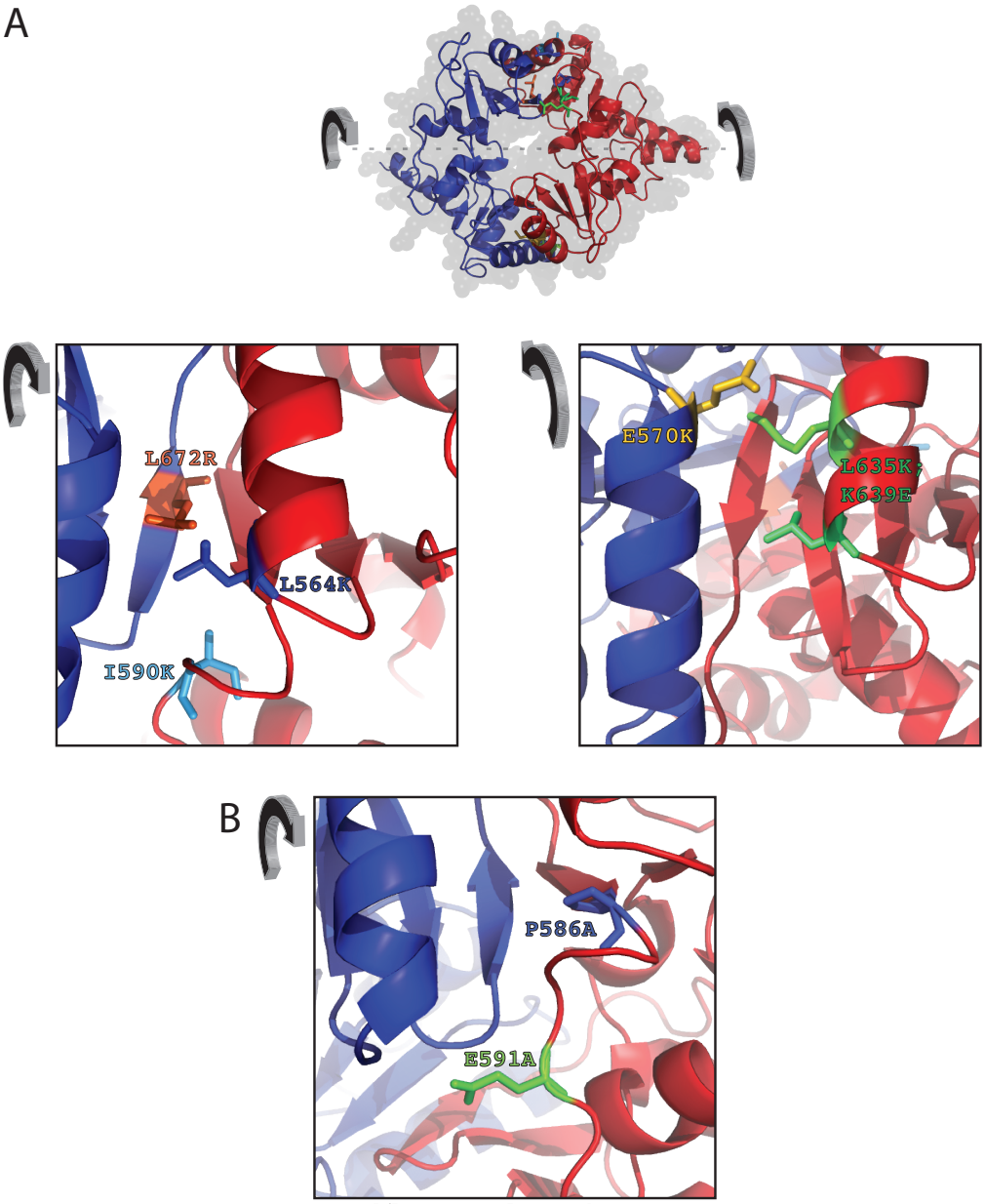

Figure II-10. Location of supposed 'hinge weakening' mutations.
Mutations **A** *smc1(L564K)*, *smc1(I590K)*, *smc1(L365K; K639E)*, *smc3(E570K)* and *smc3(L672R)* designed as reported by Mishra *et al.* (2010), and **B** *smc1(P586A)* and *smc1(E591A)* resulting from a screen for suppressors of the 'low dissociation rate hinges' reported by Kurze *et al.* (2011) are depicted on Smc1/Smc3 hinge heterodimer modelled on *T. maritima* crystal structure (PDB identifier 1GXL).

two independent mutations within Smc1's hinge[19], which to date have not been investigated further (A. Kurze, personal communication). The location of these mutations is shown in Figure II-10B. Since these mutations, in theory,

19 *smc1(E591A)*, *smc1(P586A)*

might be predicted to cause an increase in the dissociation rate of Smc1/Smc3 hinges, their presence may too weaken the hinge sufficiently to render Scc4 dispensable without greatly affecting sister chromatid cohesion.

The ability of the mutations depicted in Figure II-10 to overcome the deletion of *SCC4* was investigated essentially by following the scheme shown in Figure II-11. Dissection of *smc1Δ/smc1(D588Y) scc4Δ/SCC4* diploids in which *smc1* hinge mutants had been integrated at the *trp1* locus, or of *smc1(D588Y)/SMC1 smc3Δ/SMC3 scc4Δ/SCC4* diploids in which *smc3* hinge mutants had been integrated at the *leu2* locus did not reveal any additional suppressors of *scc4Δ*-related lethality. These results are summarised in Table II-4.

Interestingly, this dissection revealed that the two suppressors of 'low dissociation rate' hinges, *smc1(E591A)* and *smc1(P586A)*, much like wild type *SMC1*, were dominant over *smc1(D588Y)*, since no spores grew in the

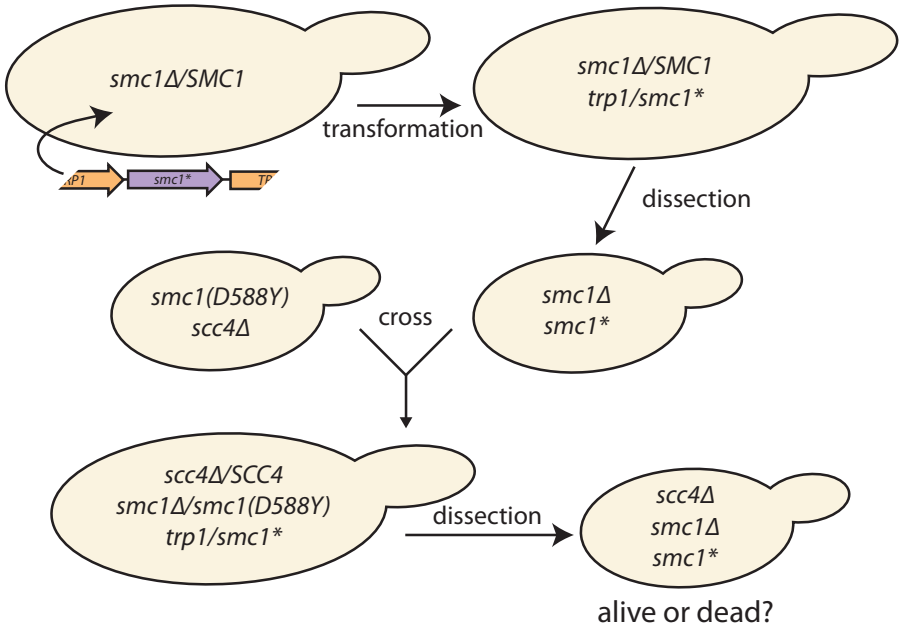

Figure II-11. Yeast cross scheme.
Schematic diagram depicting the method by which *scc4Δ smc1Δ* strains harbouring ectopically expressed *smc1* hinge mutants were constructed.

absence of *SCC4* when both the endogenous *smc1(D588Y)* and the additional ectopic mutated copy of *smc1* were present. The mutations in Smc1 and Smc3 previously published by Mishra *et al.*, however, did not affect the ability of *smc1(D588Y)* to permit growth in the absence of *SCC4*.

Mutation	Complements *smc1Δ/smc3Δ*?	Complements *scc4Δ*?
smc1(L635K; K639E)	YES	NO
smc1(I590K)	YES	NO
smc1(L564K)	YES	NO
smc3(E570K)	YES	NO
smc3(L672R)	YES	NO
smc1(E591A)	YES	NO
smc1(P586A)	YES	NO

Table II-4. Observed phenotype of predicted 'hinge weakening' mutations in Smc1 and Smc3 hinge domains.

The ability of smc1(D588Y/W/F) to bypass Scc4 cannot be reversed by complementary mutations in Smc3

Mutating Smc1's D588 to the aromatic amino acids tyrosine, tryptophan or phenylalanine has the remarkable effect of suppressing the lethal phenotype of *scc4Δ*. Due to the positioning of this residue at a critical interaction surface, and bearing in mind the bulkiness of the side chains of the suppressor mutants, it is perhaps unsurprising that these amino acids, or at least tyrosine and tryptophan, also weaken the interaction between Smc1 and Smc3 hinges.

Although the evidence presented in this chapter thus far suggests that mutations in Smc3 hinge that may also weaken the hinge interface are not able

to overcome the deletion of *SCC4*, perhaps mutation of Smc3's K652 to small, hydrophobic residues could minimise any steric effect caused by mutating Smc1's D588 to the large bulky *scc4Δ* suppressor residues, and as a result in fact prevent suppression of *scc4Δ*. To investigate this, strains were created in which a deletion of the endogenous copy of *SMC3* was rescued by ectopically expressed *smc3* in which K652 had been mutated to either alanine or valine. Following essentially the scheme of crosses depicted in Figure II-11, it was found that all three suppressors of *scc4Δ* were able to support spore growth in the absence of *SCC4*, even when Smc3's K652 was mutated. These results are summarised in Table II-5.

Complements *scc4Δ*?	*smc3(K652A)*	*smc3(K652V)*
smc1(D588Y)	YES	YES
smc1(D588W)	YES	YES
smc1(D588F)	YES	YES

Table II-5. Observed phenotype of combinations of mutations in Smc1 and Smc3 hinges.

smc1(D588Y) mutation does not facilitate an interaction between kollerin and cohesin

Despite that fact that two Smc1 hinge mutants have been shown to bypass the requirement for Scc4 *in vivo* and weaken the interface between Smc1 and Smc3 *in vitro*, this 'hinge weakening' may not necessarily be the mechanism by which suppression is achieved. Since kollerin has been shown to be able to co-immunoprecipitate with all four core cohesin subunits (Tóth *et al.*,

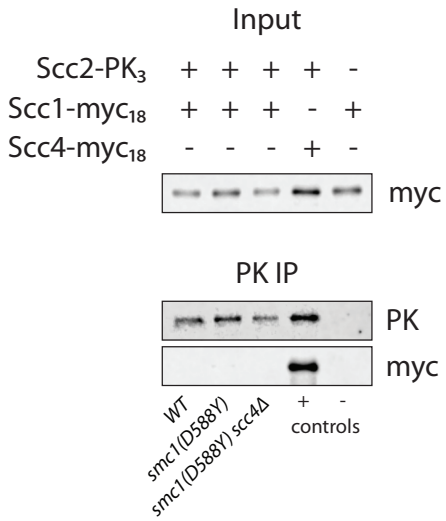

Figure II-12. The interaction between kollerin and cohesin is not affected by Smc1's hinge mutation.
Scc1-myc$_{18}$ fails to co-immunoprecipitate with Scc2-PK$_3$, either in the presence or absence of Scc4 and Smc1D588Y mutation (K19820, K19822, K19824, K18946, K19825).

1999; Arumugam *et al.*, 2003), an alternative mechanism might be to facilitate the interaction between the ring and its loader. This hypothesis was tested by observing whether an epitope-tagged Scc1 is able to co-immunoprecipitate with Scc2-PK$_3$ in a *smc1(D588Y) scc4Δ* or *smc1(D588Y)* background (Fig. II-12). Despite using relatively mild wash conditions (two washes with 100 mM NaCl) it was not possible to detect any co-immunoprecipitation between Scc1 and Scc2, either in wild type or mutant strains. Thus, Smc1D588Y does not detectably modify any potential interaction between cohesin and kollerin.

smc1(D588Y) rescues Smc3 acetylation defect of cells in which Scc4 is inactivated

Earlier in this chapter, it was seen that *scc4-4* cells harbouring the *smc1(D588Y)* mutation grow well following the loss of Scc4 function, forming

colonies of wild type morphology (Fig. II-2), indicating no catastrophic defects in sister chromatid cohesion. In addition, cell cycle dynamics appear identical to wild type, even in the complete absence of Scc4 (Fig. II-6B). However, grave defects in sister chromatid cohesion have previously been described in cells in which Scc4 has been inactivated using the *scc4-4* temperature-sensitive allele (Ciosk *et al.*, 2000). It is therefore necessary to further characterise the ability of *smc1(D588Y)* to suppress the loss of Scc4 function.

Another way of ascertaining whether or not cohesion has been compromised in a genome-wide manner is to measure the level of Smc3 acetylation using Western blotting. Acetylation of Smc3 by Eco1 occurs during S phase and may be used as a marker for sister chromatid cohesion (Rolef Ben-Shahar *et al.*, 2008). In cells in which cohesin fails to load properly onto DNA, Smc3 acetylation is compromised (Mishra *et al.*, 2010).

Here, the kollerin subunit Scc4 was inactivated by temperature shift upon exit from G_1 and Smc3 acetylation was monitored during the cell cycle. In wild type cells, Smc3 became acetylated during S phase, whereas cells with *scc4-4* thermosensitive allele failed to acetylate Smc3 during S phase at the restrictive temperature of 35.5 °C. This effect was reversed to a large extent, although not fully, by *smc1(D588Y)* (Fig. II-13).

Defects in sister chromatid cohesion are observed in the absence of Scc4

Given that, in the absence of Scc4 function, Smc3 acetylation is not restored to wild type levels by suppressor mutation *smc1(D588Y)*, it was

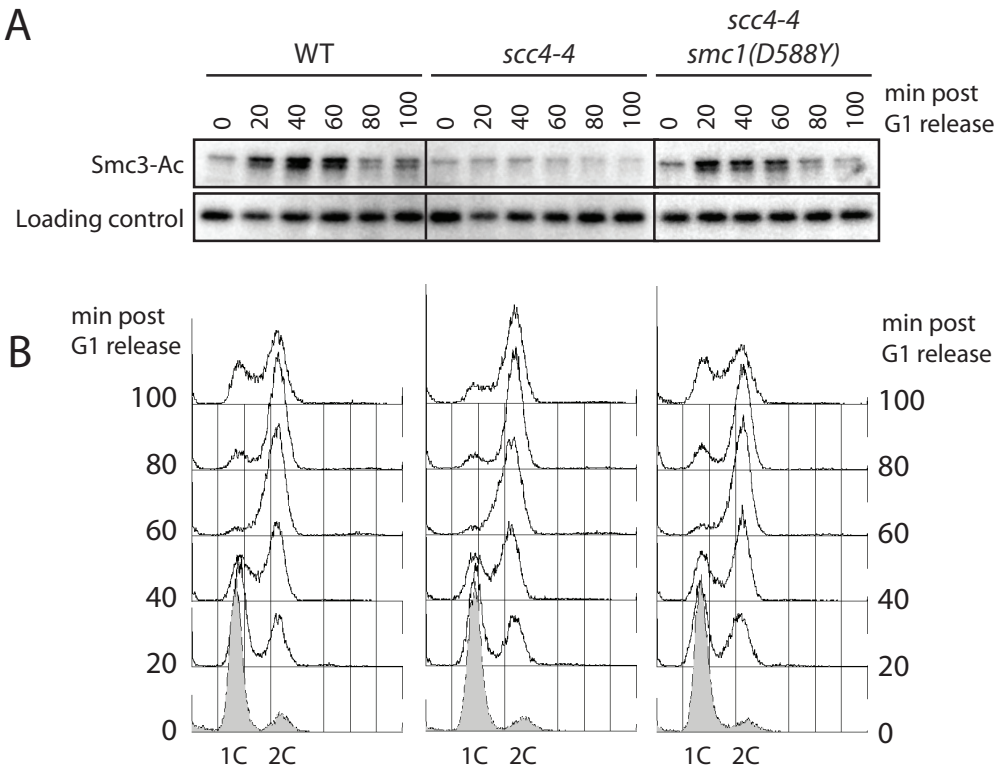

Figure II-13. *smc1(D588Y)* restores the Smc3 acetylation defect of *scc4-4*.
A The ability of *smc1(D588Y)* to rescue *scc4-4* cohesion defect was determined by monitoring Smc3 acetylation level. Strains (K21988, K21989, K22021) were grown to exponential phase in YPD at 23 °C, then arrested in G_1 by addition of α-factor for 2.5 h. Inactivation of *scc4-4* was achieved by temperature shift to 35.5 °C concurrent with G_1 release. Samples were taken every 20 min to measure Smc3 acetylation by Western blot. A non-specific band recognised by anti-Smc3 K112,113 acetylation antibody is used as a loading control.
B Cell cycle progression during experiment shown in **A** as measured by FACS.

hypothesised that cells lacking Scc4 entirely have compromised sister chromatid cohesion.

An established technique exists whereby sister chromatid cohesion can be measured according to the presence of either one or two green fluorescent dots in the nucleus (Michaelis *et al.*, 1997). This assay relies on cells expressing the recombinant Tet repressor protein fused to GFP (TetR-GFP) and having 336 Tet operators (*tetO*) integrated at the *URA3* locus (36 kb from *CEN5*). The fluorescent green nuclear foci result from the binding of TetR-GFP molecules to the *tetO* array. In wild type cells, in which metaphase arrest is achieved by

methionine-induced repression of the APC/C activator Cdc20 (Yeong *et al.*, 2000), duplicated chromosomes are usually held tightly together such that the two dots are indistinguishable. In cells with defects in sister chromatid cohesion, however, the two chromosomes tend not to be held together so tightly and as a result, the two dots can be visually distinguished. Using this assay, the contribution of Scc4 to sister chromatid cohesion can be addressed in a system in which the protein is entirely absent, albeit in the presence of one of three Smc1 point mutations.

In the presence of wild type *SCC4*, the proportion of cells that experienced cohesion loss was low (approximately 5 %). The same background cohesion loss was observed when Smc1D588 was mutated to tyrosine or phenylalanine. Combined with *scc4Δ*, however, a modest increase in split dots is observed; 24 % of tyrosine mutants and 35 % of phenylalanine mutants exhibit premature loss of sister chromatid cohesion at the *URA3* locus (Fig. II-14). It was not possible to investigate cohesion loss in *scc4Δ* cells owing to their being non-viable.

Defects in mitotic chromosome segregation are observed in the absence of Scc4

Since sister chromatid cohesion is required to ensure accurate mitotic chromosome segregation, the above observation that cohesion is compromised in the absence of Scc4 led to the hypothesis that the faithful segregation of chromosomes during mitosis may too be compromised in these conditions.

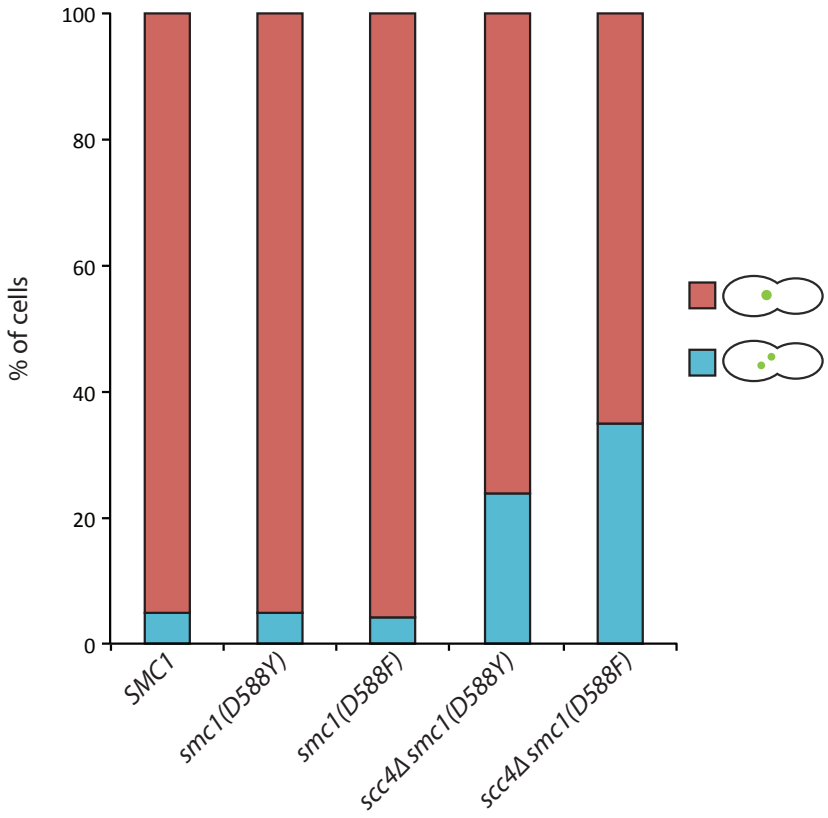

Figure II-14. Deletion of *SCC4* leads to premature cohesion loss.
Cells were assayed for cohesion using a method in which the *URA3* locus (~ 35 kb from *CEN5*) is marked with GFP. The presence of one nuclear focus in metaphase-arrested cells indicates cohesion, whereas the presence of two distinct foci indicates loss of cohesion. Strains (K21468, K21474, K21476, K21478, K21480) were grown to exponential phase in synthetic medium lacking methionine at 25 °C, before being transferred to YPD plus methionine for 2.5 h to induce metaphase arrest through Cdc20 depletion (n = 100).

To address whether *SCC4* deletion, in combination with each of the Smc1 hinge suppressor mutations, causes chromosome segregation defects, a colony-sectoring assay was performed (Hieter *et al.*, 1985). This visual assay relies on the red pigment phenotype conferred by the *ade2-101* ochre allele of laboratory wild type yeast. This phenotype can be suppressed by the presence of the stably segregating chromosome fragment *CFIII*, which contains the ochre-suppressing tRNA gene *SUP11*. Thus, cells capable of accurate chromosome segregation appear white, even when plated on adenine-deficient medium, whereas cells with decreased chromosome stability, such as strains

deficient in cohesion (Lengronne *et al.*, 2006), lose the *CFIII* fragment, resulting in the appearance of red sectors.

Since *CFIII* loss in the first cell division after plating cells causes colonies to appear half red and half white, the rate of chromosome loss per cell division

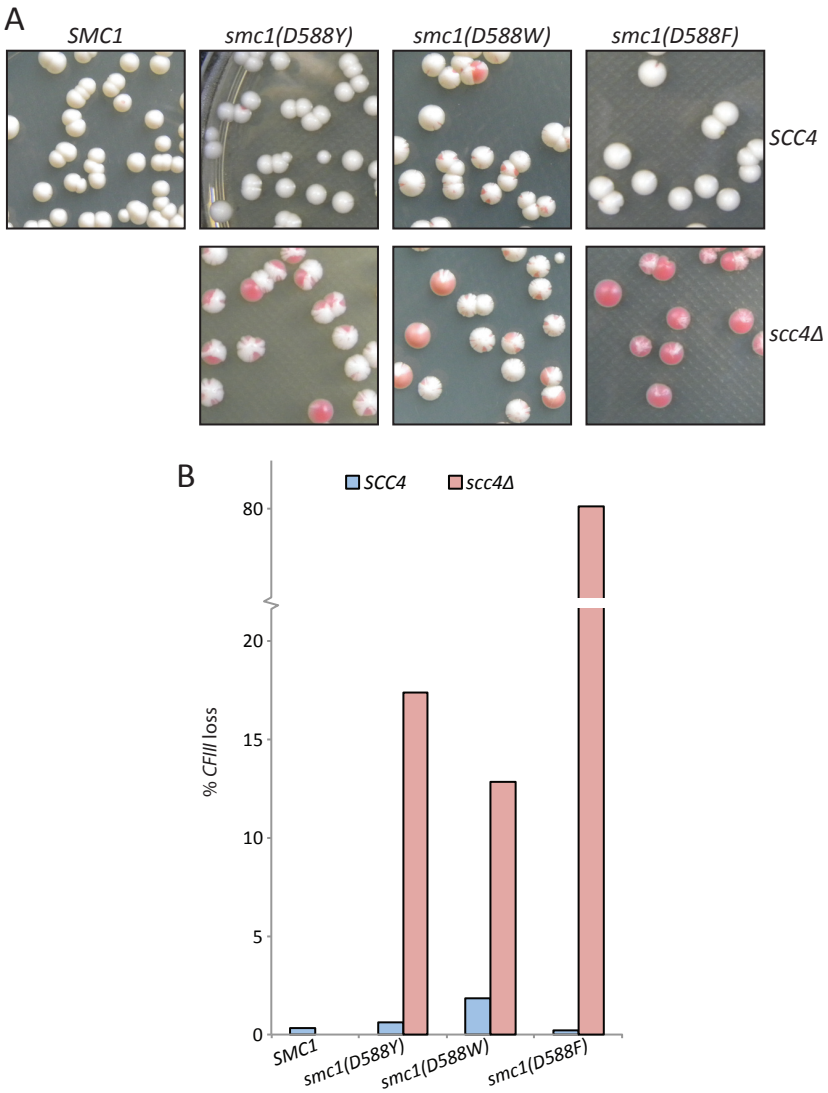

Figure II-15. Cells lacking *SCC4* display elevated levels of chromosome loss.
A Sectoring assay performed using strains harbouring the supernumerary chromosome fragment *CFIII*. In these strains, endogenous *smc1Δ* is complemented by *SMC1*, *smc1(D588Y)*, *smc1(D588W)* or *smc1(D588F)* integrated at the *trp1* locus, and *SCC4* is either present (*SCC4*; K21483, K21492, K21485, K21489, respectively) or absent (*scc4Δ*; K21494, K21487, K21491, respectively). Cells were grown in medium lacking uracil to maintain *CFIII*, then plated on rich medium deficient in adenine.
B Percentage of colonies in which *CFIII* was lost in the first cell division (half red sectors) is displayed (n > 1000).

may be determined by measuring the frequency of half-sectored colonies (Fig. II-15). Unsurprisingly, wild type control had a very low rate of chromosome loss (0.3 %). The presence of Smc1 hinge mutations alone (Smc1D588Y; Smc1D588W; Smc1D588F) had little effect on the rate of chromosome loss (0.6 %, 1.8 % and 0.2 %, respectively), whereas in combination with *scc4Δ*, these mutations caused a marked increase in the rate of chromosome loss (17.4 %, 12.8 % and 80.1 %, respectively). The combination of *SMC1* hinge mutation and *SCC4* deletion clearly has a negative impact on a cell's ability to perform faithful chromosome segregation during mitosis.

Cohesin's pericentromeric chromatin enrichment is aberrant in the absence of Scc4

After observing the sister chromatid cohesion and chromosome segregation defects noted above, it was hypothesised that the correct functioning of the cohesin complex is compromised in the absence of Scc4. For this reason, the intracellular localisation and genome-wide distribution of cohesin were investigated.

Diploid yeast strains, in which cohesin and kinetochores were marked with fluorescent proteins (Smc3-GFP; Mtw1-RFP), were observed by fluorescence microscopy (Fig. II-16; experiment conducted with Dr Kok-Lung Chan). Wild type cells displayed the characteristic cylindrical or barrel-shaped cohesin structure between sister kinetochores that is typical during metaphase (Yeh *et al.*, 2008). This pattern of enrichment was shared by cells

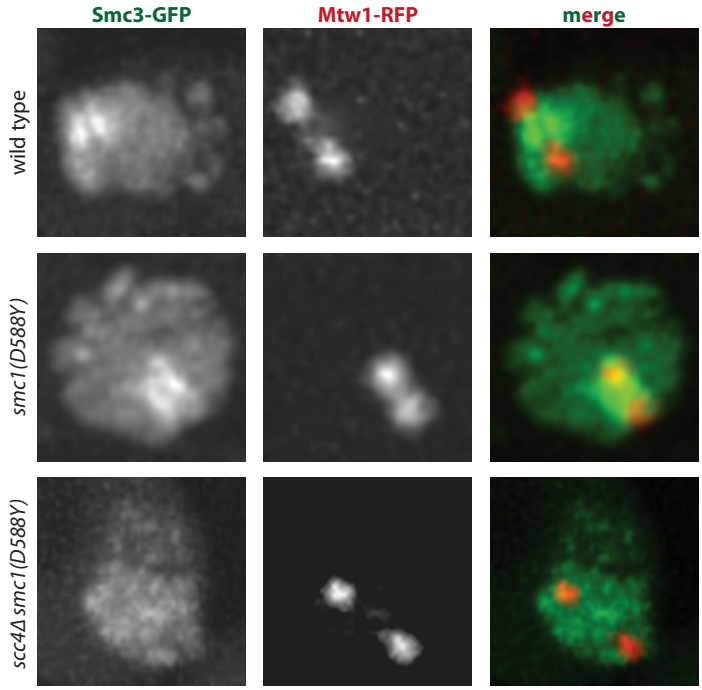

Figure II-16. Pericentromeric localisation of cohesin is aberrant in the absence of Scc4. Wild type, *smc1(D588Y)* and *smc1(D588Y) scc4Δ* cells were grown to exponential phase and observed by live cell imaging. Shown is a representative nucleus from a cell in G_2/M phase (K19457, K19456, K19471). Performed in collaboration with Dr Kok-Lung Chan.

with suppressor mutation *smc1(D588Y)* and wild type *SCC4*. However, in cells in which *SCC4* was not present, although nuclear fluorescence was detected, this structure was not observed. In addition, on visual inspection the distance between sister kinetochores, when viewed along the sagittal plane of the mitotic spindle, appeared greater than in wild type and single mutant cells.

To extend this finding, the genome-wide distribution of cohesin (Scc1-PK_6) in exponentially growing cells was compared in the presence and absence of *SCC4* and/or *smc1(D588Y)*, as detected by ChIP-sequencing (Fig. II-17; experiment performed by Dr Yuki Katou). As expected, wild type cells display a characteristic enrichment of cohesin in the 10-15 kb region surrounding the centromere. In agreement with the observation in live

cell imaging, *smc1(D588Y)* single mutant cells share this pericentromeric enrichment, whereas in the *scc4Δ smc1(D588Y)* double mutant, the enrichment was absent (Fig. II-17A). On the other hand, cohesin localisation on chromosome arms overall did not appear to be affected either by *smc1(D588Y)* mutation or by the additional deletion of *SCC4* (Fig. II-17B). This was true of

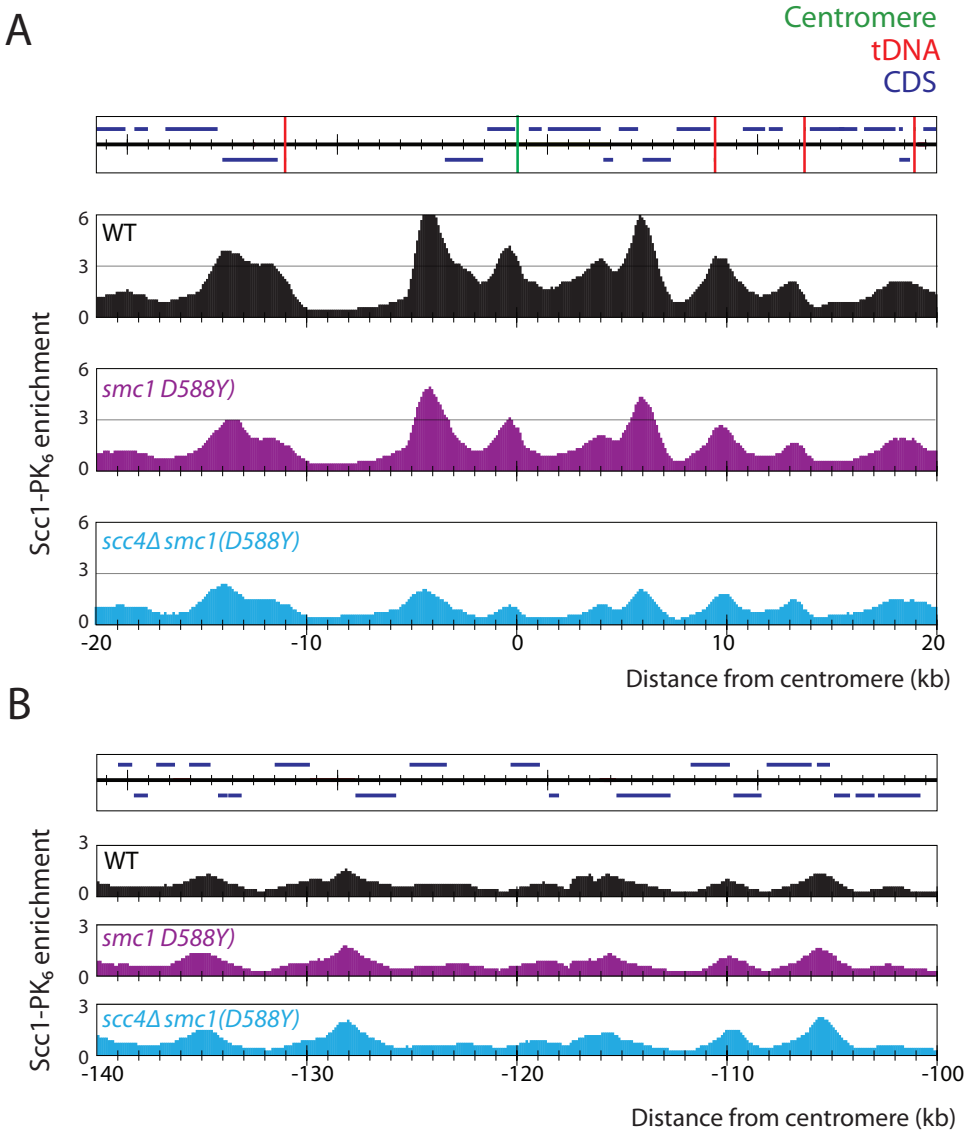

Figure II-17. Pericentromeric cohesin enrichment is aberrant in the absence of Scc4, while arm loci remain unaffected.
The genome-wide distribution of Scc1-PK_6 was measured by ChIP-sequencing using exponetially growing cells (K19641, K19647, K19624). Shown here are representative **A** pericentromeric and **B** arm regions from chromosome *VI*. See Appendix I for full data from a representative chromosome.

all chromosomes. Variability in cohesin enrichment at tRNA-encoding genes was observed in some cases between the strains, but this appears to occur in a manner that is unrelated to the presence or absence of *SCC4* (see Appendix A1 for full data from a representative chromosome).

Scc2 is not enriched at centromeric chromatin in the absence of Scc4

Kollerin is known to predominantly localise at the centromere and, although its localisation is distinct from and proximal to the major sites of cohesin localisation, it is required for this pericentromeric cohesin enrichment to occur (Ciosk *et al.*, 2000; Lengronne *et al.*, 2004). Since, in the absence of Scc4, cohesin fails to localise correctly at the pericentromere, the hypothesis that, under these circumstances, Scc2 also fails to localise correctly at the centromere was investigated.

Firstly, the intracellular localisation of Scc2 was determined by live cell imaging. Diploid yeast strains, in which Scc2 and kinetochores were marked with fluorescent proteins (Scc2-GFP; Mtw1-RFP), were observed by fluorescence microscopy (Fig. II-18; experiment conducted with Dr Kok-Lung Chan). As expected, Scc2 in wild type cells formed a focus that co-localised with Mtw1 at the kinetochores in metaphase. *smc1(D588Y)* single mutants displayed the same phenotype. In the absence of Scc4, however, no Scc2 focus was observed and, in accordance with data presented previously, on visual inspection these cells appear to have greater inter-sister kinetochore distance than wild type and single mutant cells.

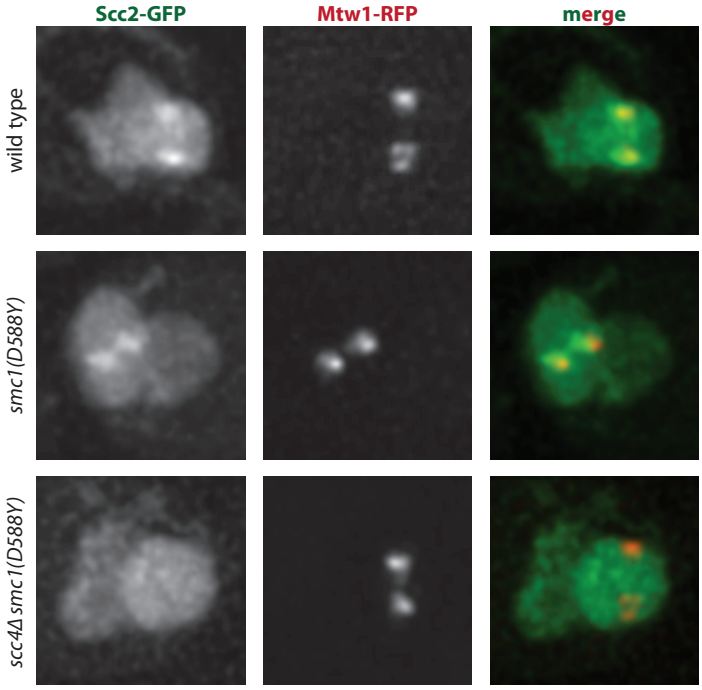

Figure II-18. Centromeric localisation of Scc2 is aberrant in the absence of Scc4.
Wild type, *smc1(D588Y)* and *smc1(D588Y) scc4Δ* cells were grown to exponential phase and observed by live cell imaging. Shown is a representative nucleus from a cell in G_2/M phase (K16442, K22057, K22055). Performed in collaboration with Dr Kok-Lung Chan.

In addition, the genome-wide distribution of Scc2-PK_3 in nocodazole-arrested metaphase cells was examined by ChIP-sequencing (Fig. II-19; experiment performed by Dr Yuki Katou). The results support the prior observation of centromeric Scc2 enrichment in both wild type and *smc1(D588Y)* single mutant cells, as well as the lack of Scc2 enrichment at centromeres in the double mutant (Fig. II-19A). Neither at tRNA-encoding regions nor elsewhere along all chromosomes does Scc2 localisation appear to be affected either by the presence of *smc1(D588Y)* mutation alone or coupled with *scc4Δ* (Fig. II-19B; see Appendix A2 for full data from a representative chromosome).

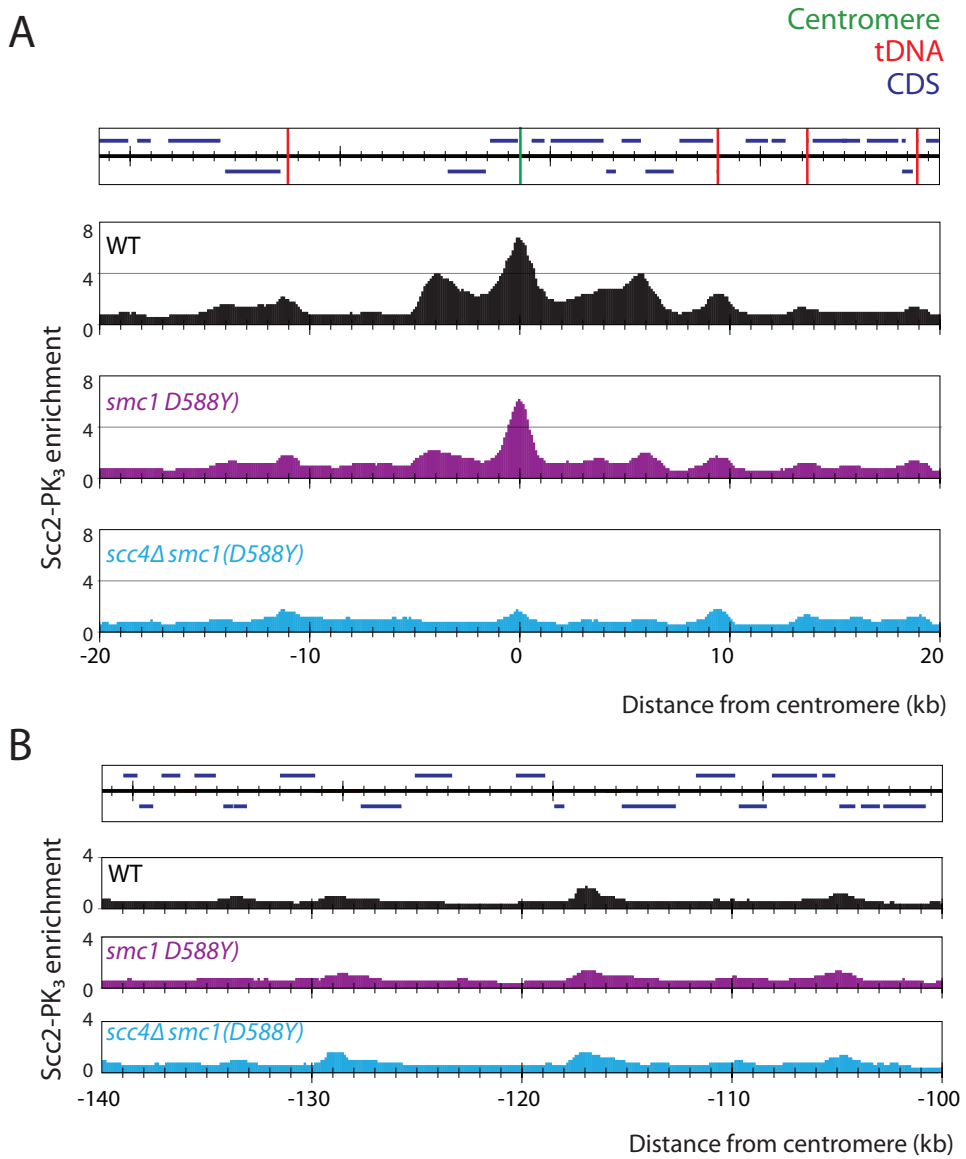

Figure II-19. Centromeric Scc2 enrichment is aberrant in the absence of Scc4, while arm loci remain unaffected.
The genome-wide distribution of Scc2-PK_3 was measured by ChIP-sequencing using nocodazole-arrested G_2/M phase cells (K18920, K19431, K19429). Shown here are representative **A** pericentromeric and **B** arm regions from chromosome *VI*. See Appendix II for full data from a representative chromosome.

smc1(D588Y) scc4Δ confers a meiotic defect

Following the observation that cohesin fails to become enriched at centromeric loci in *smc1(D588Y) scc4Δ* cells, the ability of homozygous diploids to undergo meiosis was investigated. Meiosis presents a more

complex challenge than mitosis in that it involves two rounds of cell division. Centromeric cohesion, mediated by meiotic cohesin, must persist throughout meiosis I in order for cells to be able to coordinate the segregation of sister chromatids during meiosis II (Klein *et al.*, 1999; Marston *et al.*, 2004). That the level of centromeric cohesin is diminished in mitotic cells might indicate that chromosome segregation defects may be encountered during meiosis.

Homozygous diploids were plated on nitrogen-deficient medium to induce meiosis. Dissection of 54 wild type asci resulted in a spore viability rate of 96.3 %. The mutation *smc1(D588Y)* led to a significant decrease in the level of spore survival to 90.0 % (of 60 asci; $p < 0.01$). Only 75.0 % of spores arising from 90 diploids that were homozygous for both *smc1(D588Y)* and *scc4Δ* were viable (Fig. II-20). It therefore appears that meiosis is compromised in both single and double mutant cells.

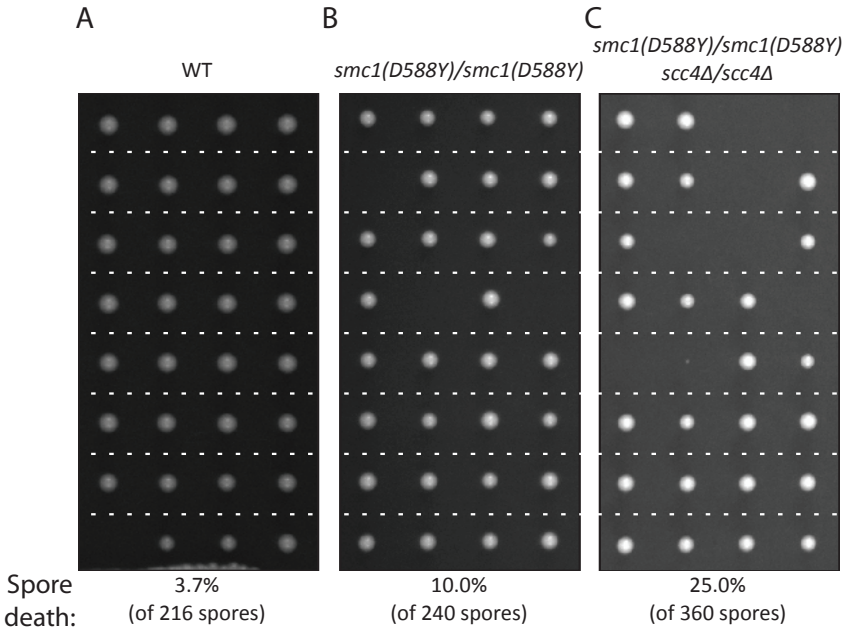

Figure II-20. *smc1(D588Y)* and *smc1(D588Y) scc4Δ* cells suffer meiotic defects.
Representative spore growth following dissection of homozygous **A** wild type, **B** *smc1(D588Y)* or **C** *smc1(D588Y) scc4Δ* diploid yeast strains. Percentage spore death is shown below (K842, K21418, K21419).

DISCUSSION

The ring model, whereby sister chromatids are held together by a topological embrace within cohesin's tripartite ring, is currently the best-supported mechanism for sister chromatid cohesion. However, the question of how DNA enters the ring has not yet been adequately answered. One envisages that transient opening at one of the three interfaces is necessary. The strongest evidence to date suggests that it is the interface between Smc1 and Smc3 hinges that acts as a DNA entry gate, although models whereby more than one interface may open to permit DNA entry have not yet satisfactorily been ruled out (Gruber *et al.*, 2006). Indeed, the notion of DNA entry occurring *via* transient ring opening is even more conceivable since the discovery that the interface between non-acetylated Smc3 heads and the N-terminus of Scc1 transiently opens to allow DNA exit in a separase-independent manner (Chan *et al.*, 2012; Buheitel & Stemmann, 2013; Eichinger *et al.*, 2013).

Also required for cohesin's association with chromatin is the kollerin complex, consisting of Scc2 and Scc4 (Tóth *et al.*, 1999; Ciosk *et al.*, 2000). Scc2 has been shown to interact with the core cohesin complex in a sub-stoichiometric manner by co-immunoprecipitation (Tóth *et al.*, 1999; Arumugam *et al.*, 2003). This, together with the fact that both Scc2 and Scc4 are predicted to possess structural motifs commonly found in scaffold proteins (Andrade & Bork, 1995; Blatch & Lässle, 1999; Neuwald & Hirano, 2000; Panizza *et al.*, 2000; Watrin *et al.*, 2006), suggests that kollerin might act as a platform with which cohesin may need to transiently associate to permit

its loading onto chromatin. Despite a mounting body of evidence, the specific roles of both Scc2 and Scc4, and the way in which they relate to cohesin are very poorly understood.

A screen for suppressors of the *scc4-4* thermosensitive phenotype (performed by Dr Maria Demidova) uncovered a mutation in Smc1's hinge that could bypass the otherwise essential kollerin subunit entirely. Although this screen required no assumptions to be made about the mechanism of cohesin loading, it was remarkably able to uncover the first ever genetic link between not merely the cohesin complex and its loader, but the exact interaction interface within cohesin that has been suggested to be a DNA entry gate. The work presented in this chapter confirms this discovery, investigates the phenotype of yeast cells in which Scc4 is entirely absent and explores the biochemical nature of mutations in the cohesin hinge.

It was found that not only tyrosine, but also tryptophan and phenylalanine substitutions in Smc1's hinge at position 588 had the ability to overcome *scc4Δ*-related yeast lethality. In addition, both tyrosine and tryptophan mutations weakened the interaction between Smc1 and Smc3. Further investigation is required to determine the effect of Smc1D588F on the stability of the hinge heterodimer, which was not possible during the time constraints of this project, but the result is consistent with the notion that cohesin loading requires transient dissociation of the hinge.

It was observed that *SMC1* is partially dominant over *smc1(D588Y/F/W)* in the absence of *SCC4*. Given that these hinge mutants, in the absence of wild

type *SMC1*, permit *scc4Δ* cell growth like wild type yeast, why might this be the case? According to the ring model, cohesin must form stable rings to mediate cohesion. This is supported by evidence that mutations which disrupt the interaction at the hinge, or indeed at the other interfaces, cause lethal defects in sister chromatid cohesion (Arumugam *et al.*, 2006; Mishra *et al.*, 2010). Evidence is presented in this chapter that isolated Smc1 hinges bearing mutations that render the full-length protein able to bypass the requirement for Scc4 interact less strongly with Smc3 hinges than wild type Smc1 does. It is likely due to the fact that the mutants have, effectively, a reduced ability to bind Smc3 that they suffer this partial loss-of-function phenotype.

It was postulated that the mutation *smc1(D588Y)* may disrupt a salt bridge between Smc1 and Smc3. This hypothesis is supported by the similar patterns of conservation of acidic residues in Smc1 and basic residues in Smc3, a characteristic of non-surface accessible salt bridges (Schueler & Margalit, 1995), and the fact that Scc4-bypassing mutants in D588 display weaker interactions to Smc3 *in vitro*. However it was demonstrated by mutagenesis of both hinges that neither mutation of Smc1D588 to histidine, alanine, arginine or asparagine, nor mutation of the opposing residue in Smc3 (K652) to alanine, valine or tyrosine, (all of which would have disrupted the potential salt bridge interaction), conferred the ability to cells to survive in the absence of Scc4. Moreover, a series of mutations in both Smc1 and Smc3 hinges that were predicted to weaken this interface (listed in Table II-4) were tested to see if they shared the ability of Smc1D588Y to bypass deletion of Scc4; none

did. From this, it may be concluded that D588 mutations do not function *via* disruption of an intramolecular salt bridge. Thus it is not clear, from a structural point of view, what causes the hinge weakening that was measured *in vitro*. Can anything be learnt from the crystal structure of the hinge that indicates what might occur on a molecular level?

Here, *S. cerevisiae*'s hinge domain was modelled on the crystal structure from *T. maritima* (Haering *et al.*, 2008). In this structure, the residue corresponding to yeast Smc1's D588 is 3.2 Å from the residue corresponding to Smc3's K652. Thus the residues are on the upper limit (4 Å) of being close enough to be able to form a salt bridge (Barlow & Thornton, 1983). The more recently published structure of the mouse cohesin hinge (Kurze *et al.*, 2011) shows a more open conformation, in which the residue corresponding to yeast Smc1's D588 is 7.1 Å from the mouse equivalent of Smc3's K652. However, the distance from these residues to the main-chain NH group at the N-terminus of an α-helix in Smc1 (L564-Q577 in *S. cerevisiae*), at just 1.8 and 2.3 Å respectively, and the orientation of these residues, permit hydrogen bonding (Fig. II-21). Thus it is more likely that D588 participates in an intra- rather than intermolecular interaction. The mutation of D588 may then have structural consequences for the α-helix it stabilises, affecting its interaction with the neighbouring helix from Smc3.

However, if an intramolecular hydrogen bond is required to stabilise the α-helix, why then do only mutations of this aspartate to tyrosine, tryptophan and phenylalanine cause cohesin to become resistant to *SCC4* deletion? By

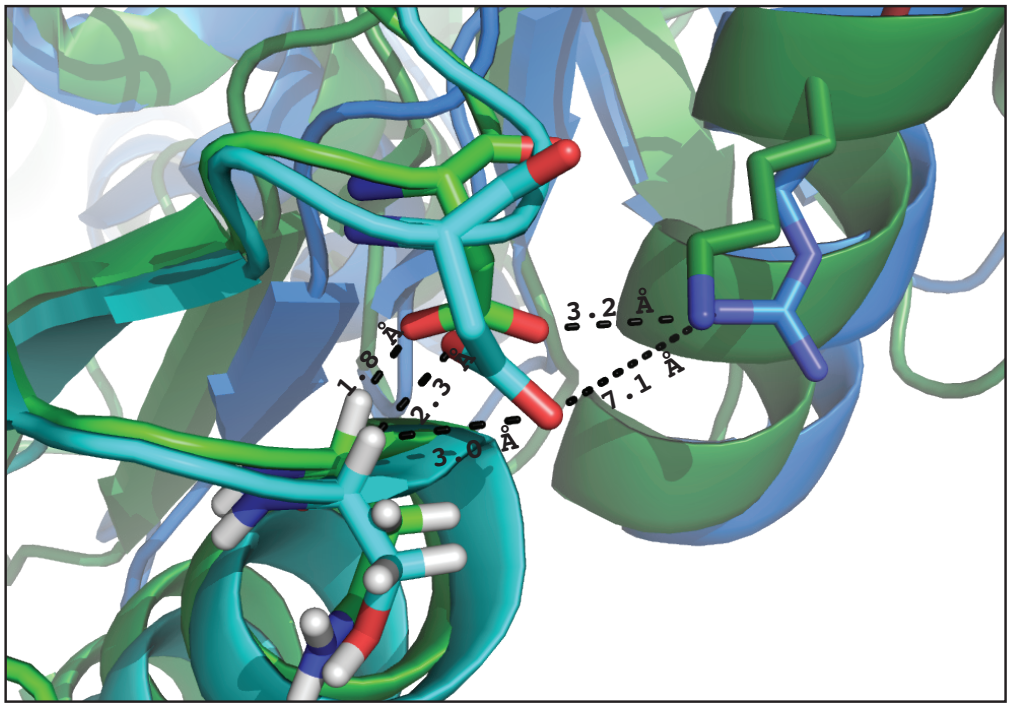

Figure II-21. Orientation of D588 and distance from K652 cast doubt upon salt bridge formation.
An overlay of the SMC hinge dimerisation domains from *T. maritima* (in light and dark green; PDB identifier 1GXL) and *M. musculus* (in light and dark blue; PDB identifier 2WD5) showing the distance between residues analagous to *S. cerevisiae*'s Smc1D588. Measurements are shown between the residue corresponding to Smc1 D588 to the residue corresponding to Smc3 K652 and show that, while the residues from the bacterial SMC are close enough to form a salt bridge (3.2 Å), the orthologous residues from mouse cohesin are not (7.1 Å). More likely is the formation of an intramolecular hydrogen bond between D588 and main chain hydrogens as depicted (*T. maritima*: 1.8 Å, *M. musculus*: 2.3 and 3.0 Å)

no means were all twenty amino acids tested in this position for their ability to bypass Scc4 function, but of those investigated, only bulky, uncharged aromatic residues could, and in a manner that does not reflect their hydrogen bond-accepting propensity. Furthermore, all D588 mutants described in this chapter were able to support yeast cell growth in the absence of wild type Smc1, suggesting that any structural consequences of mutations in this position on the hinge itself were minor. The best strategy to study the structural effect of such mutations would be through X-ray crystallography. Although the hinge domain from *S. cerevisiae* does not perform well in crystallisation trials,

in both *T. maritima* and *M. musculus*, which have both successfully yielded hinge crystals, the aspartate residue in question is conserved. Purifying and crystallising mutant hinge domains from one of these organisms could thereby reveal structural consequences of Smc1D588 mutations on a molecular level.

Although it is now apparent that an intramolecular salt bridge is not disrupted by the *scc4Δ* suppressor mutations, the fact remains that both Smc1D588Y and Smc1D588W weaken the hinge dimerisation interface and render Scc4 non-essential, but none of the other hinge mutations that were predicted to weaken this interaction were able to bypass Scc4 function. Either none of the hinge mutations described here succeed in weakening the hinge interface in the manner that D588Y, D588W and, presumably, D588F do, or weakening of the hinge interface is not the mechanism by which the suppressor mutation works *per se*.

The effect on Smc1/Smc3 interaction of Smc1 and Smc3 hinge mutations that were unable to bypass the requirement for *SCC4* was not investigated. The possibility that 'hinge weakening' does not occur in these cases may be investigated using the approach implemented with Smc1^{hinge}D588Y and Smc1^{hinge}D588W to determine whether the Smc1/Smc3 interaction is affected by the presence of each mutation. In addition, quantitative measurements of isolated hinge heterodimer affinity may be made, as they have been previously, using isothermal titration calorimetry (Mishra *et al.*, 2010; Kurze *et al.*, 2011). Unfortunately, due to low yields and concentrations of mutant proteins,

this was not applicable within the time constraints of the project. These experiments could be realised following optimisation of protein expression and purification conditions.

Nevertheless, if 'hinge weakening' really is a requirement for bypassing Scc4 function, why then, in the screen for suppressors of *scc4-4* thermosensitive phenotype, is the very same mutation within Smc1 hinge implicated on no fewer than twelve independent occasions? Bearing in mind that the screen held no assumptions about the mechanism of cohesin loading, one would envisage several mutations within both Smc1 and Smc3 hinges would have the same effect of Smc1D588Y. As noted in this chapter, the suppressor screen is inherently biased towards substitutions that may occur as a result of a single base pair mutation; phenylalanine and tryptophan substitutions in Smc1 hinge are equally as capable of bypassing Scc4 as tyrosine, but these did not arise naturally, presumably because they cannot result from a single base pair point mutation of the wild type codon, whereas tyrosine can. Even given the codon limitations of the screen, it is hard to conceive that no other mutations within either Smc1 or Smc3 can cause such a generic effect as weakening the affinity between the two molecules and thereby bypassing Scc4. Do such mutations exist? Mutagenesis of both Smc1 and Smc3 hinges, for example by error-prone PCR, would remove codon bias from the screen and make it possible to uncover whether or not they do.

It is equally as plausible that *scc4Δ* suppression does not depend on, nor is it caused by, the reduced affinity between Smc1/Smc3 hinges. If this is

the case, what then is the ability conferred by a mutation in Smc1's hinge? The possibility that the interaction between cohesin and its loader was modified by this mutation was investigated by co-immunoprecipitation, but no effect was seen. However, any interaction between the wild type cohesin complex and kollerin is reported to be weak or transient (Tóth *et al.*, 1999; Arumugam *et al.*, 2003). This is supported by FRAP experiments in live cells, which have shown kollerin to be more rapidly turning over at the centromere than even ATP hydrolysis-defective cohesin, which is unable to stably bind DNA (Hu *et al.*, 2011). It is entirely possible, therefore, that any interaction is still too weak/transient to be measured by co-immunoprecipitation and Western blot.

Likewise, the D588Y mutation within Smc1's hinge may facilitate loading through enhancing an interaction between cohesin and factors that are present on chromatin at loading sites, or indeed DNA itself. Multiple studies suggest that the SMC hinge is more than just a dimerisation domain; the homodimeric SMC complex from *B. subtilis* binds to DNA *via* the coiled coils, but in a manner that is dependent on dimerisation at the hinge (Hirano & Hirano, 2002). However, both isolated bovine cohesin hinges and, more recently, mouse condensin hinges have demonstrated the ability to bind DNA *in vitro* (Chiu *et al.*, 2004; Griese *et al.*, 2010). Either way, the Smc1 hinge mutations presented here have been shown to affect the dimerisation of Smc1 and Smc3, and one might postulate that the DNA binding ability of said heterodimers, either directly *via* the hinges, or indirectly *via* the coiled coils, is also altered by this change. This may be investigated by carrying out DNA

binding assays, such as those described in the above studies.

However, these *in vitro* assays do not accurately represent the chromatin environment that is faced by cohesin as it loads onto DNA. The predominant site of cohesin loading is at the centromere. One envisages an interaction between cohesin and protein components of or around the kinetochore is necessary for cohesin loading, especially since Scc2 targeted to an arm locus (36 kb from *CEN5*) is sufficient to recruit Scc4, but not cohesin, whereas Scc4 targeted to a pericentromeric locus (500 bp from *CEN4*) recruits both Scc2 and cohesin (Hu *et al.*, 2011; Fernius *et al.*, 2013). It is currently unclear as to what these protein components may be, but perhaps the mutation within Smc1 hinge that renders Scc4 dispensible for loading might facilitate cohesin's association with such proteins. By comparing the silver staining profiles of TAP-purified wild type and D588Y Smc1 molecules and performing mass spectrometry, it may be possible to uncover such binding partners. If, however, as seems more likely, interaction partners are only weak or transient, and since candidate approaches, such as yeast two-hybrid screening, Förster resonance energy transfer (FRET) and Bimolecular Fluorescence Complementation (BiFC) are not applicable, an alternative would be to use *para*-benzoyl-L-phenylalanine (BPA)-mediated crosslinking. Incorporating the non-natural, photo-crosslinkable amino acid BPA into the Smc1 hinge, at and around the residue of interest, followed by UV irradiation leads to *in vivo* site-specific crosslinks between the BPA residue and binding partners within ~7 Å radius (Dormán & Prestwich, 1994; Chin *et al.*, 2003; Chen *et al.*, 2007).

The novel suppressor of *scc4Δ* may be considered a revolutionary tool with which the mechanism of cohesin loading may be investigated. Many past studies addressing the mechanism of cohesin loading have focused on Scc2, using the thermosensitive *scc2-4* allele to inactivate kollerin, perhaps considering it to be the more important subunit due to its larger size and greater level of conservation than Scc4. Now the roles of Scc2 and Scc4 have been unequivocally divorced. Through studying of the pathology of *scc4Δ* cells, Scc4's unique role as a subunit of the essential kollerin complex is beginning to be uncovered.

First, the data presented in this chapter demonstrate that a major role of Scc4 is the recruitment of Scc2 to the centromeric loci at which cohesin is predominantly loaded. Scc4 is an essential protein; presumably global loss of cohesion occurs in its absence. However, in the absence of Scc4, arm loading can be restored by a single point mutation in Smc1 hinge, whereas loading at the centromere cannot. Perhaps though, the mutation in Smc1 hinge prevents centromeric cohesin loading. It is shown by both ChIP-sequencing and live cell imaging that this is not the case; in the presence of wild type *SCC4*, *smc1(D588Y)* does not prevent the pericentromeric accumulation of cohesin. Thus, loading of cohesin onto chromosome arms must occur *via* a different mechanism than that at the centromere.

It may be postulated that additional factors are required for cohesin loading at the centromere, and that Scc4 itself interacts with these factors. One candidate is DDK, which has recently been implicated in the enrichment

of kollerin at this locus (Natsume *et al.*, 2013). Should DDK be involved in an interaction with Scc4, one would envisage Scc4 mutants that are defective only in their ability to interact with DDK, thus resulting in their failure to load cohesin only at the centromere. One would predict such mutants to be viable, since the otherwise functional kollerin complex should presumably remain able to load cohesin, like in the case of *scc4Δ smc1(D588Y)*, on chromosome arms.

Is the function of Scc4 solely in bringing Scc2 to the centromere? Would, therefore, the targeting of Scc2 to the centromere in the absence of Scc4 be sufficient to restore cohesin loading at this locus? Even in the absence of Smc1D588Y? Answering these questions should provide greater insight not merely into the mechanism of centromeric loading, but also *scc4Δ* suppression by Smc1D588Y.

Like the kinetochore component Chl4, Scc4 is required for the pericentromeric enrichment of cohesin, and in accordance with data presented by Fernius *et al.* (2009), the results presented here imply that pericentromeric cohesion is not essential for proliferation of yeast. However, cells deficient in centromeric cohesion display cohesion and mitotic chromosome segregation defects. Although all *scc4Δ*-bypassing mutants displayed no mitotic defects in the presence of *SCC4*, it has not been possible to determine whether defects seen in *smc1(D588Y/F/W) scc4Δ* cells were the result of *SCC4* deletion or the combination of both *SCC4* deletion and *SMC1* hinge mutation. However, based on the chromosome segregation and loss of cohesion assays presented in

Figures II-8 and 9, it appears that cells expressing *smc1(D588F)* in addition to *scc4Δ* have noticeably greater cohesion defects than those expressing *smc1(D588Y)* and *scc4Δ*. Thus, Smc1D588Y is a better suppressor than Smc1D588F. Future biochemical investigation of these mutants is required to understand the cause of this difference.

In addition to mitotic defects, defects in meiotic chromosome segregation are seen in the presence of *smc1(D588Y)* and *scc4Δ*. This is perhaps unsurprising given the facts that enrichment of pericentromeric cohesin fails to occur in these mutants, and that this population of cohesin is important to maintain cohesion between centromeres of univalent chromosomes until their segregation at the metaphase-anapase II transition (Kiburz *et al.*, 2005). The precise nature of the meiotic defect observed here requires further investigation.

What does suppression of *scc4Δ* mean on a grander scale? The kollerin complex has been implicated in loading not only of cohesin, but also of the two other SMC protein-containing complexes, namely condensin and the Smc5/6 complex (Tóth *et al.*, 1999; Ciosk *et al.*, 2000; Lindroos *et al.*, 2006; D'Ambrosio *et al.*, 2008). Despite this, and the fact that all three SMC complexes are essential in yeast, it is shown here that deletion of *SCC4* is tolerated with only a single point mutation in cohesin. The possibility remains that Scc2 is involved in condensin and Smc5/6 loading, in a manner that is independent of Scc4. Alternatively, under normal conditions, condensin and the Smc5/6

complex may require both Scc2 and Scc4 for their loading indirectly, i.e. *via* cohesin: when cohesin is modified such that it no longer requires Scc4 for its loading, nor too do condensin and Smc5/6. Given that cohesin appears essential for Scc2's recruitment, at least to kinetochores (Fernius *et al.*, 2013), the latter possibility is surely more feasible. Nevertheless, the contribution of both Scc2 and Scc4 to condensin and Smc5/6 complex loading may need to be readdressed in light of the results here presented.

Finally, it will be interesting to determine whether or not the phenomenon whereby *scc4Δ* may be suppressed by a mutation in Smc1's hinge is evolutionarily conserved. *ECO1* is an essential gene; it encodes an acetyl transferase required to acetylate two lysines on Smc3's N-terminal head. In budding yeast, should these two targets be mutated to non-acetylatable arginine residues, cell proliferation is not supported (Rolef Ben-Shahar *et al.*, 2008; Ünal *et al.*, 2008; Zhang *et al.*, 2008a; Rowland *et al.*, 2009). In fission yeast, however, this is not the case; cells survive in the absence of acetylation on Smc3 head residues but *ESO1* remains essential (Feytout *et al.*, 2011). This indicates that *S. pombe*'s Eco1 orthologue has additional functions that are yet to be elucidated. Although Scc4's function in budding yeast still requires much further investigation, the use of additional model systems may shed yet more light on the mechanism of cohesin loading.

Chapter III

Biochemical studies of kollerin

Biochemical studies of kollerin

INTRODUCTION

In all eukaryotes, the process of sister chromatid cohesion is mediated by a highly conserved protein complex called cohesin (Hirano, 2006; Peters *et al.*, 2008; Nasmyth & Haering, 2009). The association of cohesin with chromatin occurs during late G_1/S and depends on a large cohesin-associated protein complex comprising Scc2 and Scc4 proteins (Ciosk *et al.*, 2000). Like cohesin, this complex, named kollerin, is conserved in almost all eukaryotes throughout evolution[20] (Nasmyth & Haering, 2009). Unlike most other key components involved in the phenomenon of sister chromatid cohesion, these two proteins remain largely structurally and functionally unstudied.

Scc2 is the largest cohesin-associated protein known; its size ranges from approximately 170 kDa in budding yeast to over 300 kDa in humans (Tóth *et al.*, 1999; Tonkin *et al.*, 2004). Budding yeast Scc2 has been reported to possess a known kinase motif and, in accordance with this, phosphorylation of the fission yeast Scc1 orthologue is diminished in Scc2 thermosensitive mutant cells (Tomonaga *et al.*, 2000; Jones & Sgouros, 2001). However, no kinase activity has been measured of the protein *in vitro*, and no essential targets have been described.

20 Kollerin is one of several cohesin-associated factors (including Pds5, Eco1 and Wapl) that to date has not been identified in the eukaryotic intracellular parasite *E. cuniculi*. While this may indicate kollerin-independent loading of cohesin in one of the most anciently diverged eukaryotic species known, equally, the loading factor may be provided by the host cell.

Scc2 is predicted to be composed of repeating helical structural motifs, called HEAT (Huntingtin, Elongation factor 3, Protein Phosphatase 2A, TOR1) repeats (Andrade & Bork, 1995; Neuwald & Hirano, 2000). These repeating units consist of two antiparallel helices connected *via* a hairpin loop (Fig. III-1A). Tandem HEAT repeats form flexible structures, typically acting as scaffolds that promote protein-protein interactions. Scc2 has been reported to co-immunoprecipitate, albeit sub-stoichiometrically, with the cohesin subunits Smc1, Smc3, Scc1 and Scc3 (Tóth *et al.*, 1999; Arumugam *et al.*, 2003). May any of these be targets of the purported kinase?

Like Scc2, prediction algorithms estimate Scc4 to comprise a repeating helical motif, called a tetratricopeptide repeat (TPR), which too is implicated in facilitating protein-protein interactions (Fig. III-1B) (Blatch & Lässle, 1999; D'Andrea & Regan, 2003; Watrin *et al.*, 2006). On reviewing the literature, it appears that Scc4 is less well studied than even Scc2. It is not immediately clear

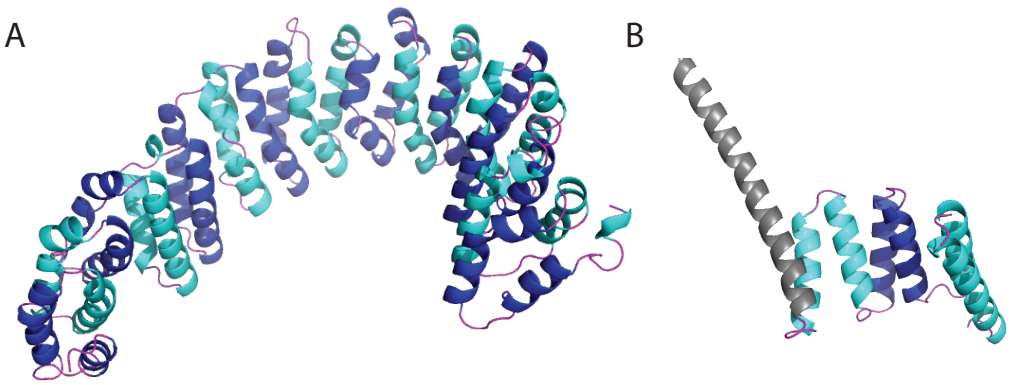

Figure III-1. Kollerin's predicted structural motifs.
A Scc2 is predicted to contain several HEAT repeats. The HEAT repeats of PP2A, shown here, fold to make a solenoid structure. Each HEAT motif consists of a helix-turn-helix. Fifteen HEAT motifs are shown in alternating colours (PDB identifier 1B3U; Groves *et al.*, 1999).
B Scc4 is predicted to be composed of TPR motif. This is a 34-residue helix-turn-helix repeating structure, first described in Protein Phosphatase 5, shown here. Three TPRs are shown in alternating colours. In grey is a non TPR helix (PDB identifier 1A17; Das *et al.*, 1998).

why this may be. Perhaps due to its smaller size it has been considered less important than Scc2. Maybe the fact that Scc4, unlike its binding partner, is not implicated in the developmental disorder, Cornelia de Lange Syndrome (CdLS), has made it a less appealing candidate for study. One factor that must have precluded the study of Scc4 is that its primary sequence is not well conserved throughout evolution, and orthologues of the budding yeast protein were not discovered until relatively recently. Nevertheless, Scc4 orthologues have now been identified in plants, fungi, invertebrates and vertebrates, in which it has an essential role in cohesin loading, suggesting it is of as critical importance as Scc2 (Watrin *et al.*, 2006; Seitan *et al.*, 2006; Nasmyth & Haering, 2009).

Multiple studies claim that Scc2 and Scc4 interact through their respective N-termini (Seitan *et al.*, 2006; Takahashi *et al.*, 2008; Braunholz *et al.*, 2012). Other than this, the functions of the rest of both proteins remain unknown. In the previous chapter, it was seen that Scc2's function could successfully be uncoupled from Scc4 through deletion of the latter subunit in the presence of a mutation in Smc1's hinge. Must Scc2 and Scc4 even interact with each other to perform their role in cohesin loading? Perhaps they are able to act independently of each other.

In this chapter, claims that Scc2 might possess kinase activity are investigated. In addition, the nature of the interaction between Scc2 and Scc4 is explored biochemically. Mutations are made in Scc2 and Scc4 that prevent kollerin complex assembly with catastrophic effects.

RESULTS

Putative kinase in Scc2 is not essential for cell viability

Yeast Scc2 shares 9 of the 13 residues that comprise the serine/threonine kinase signature motif of Chk1 and Pkh1, including the active site aspartate[21] (Jones & Sgouros, 2001). In addition, fission yeast Mis4 (Scc2) thermosensitive lethal mutants show diminished levels of Rad21 (Scc1) phosphorylation (Tomonaga *et al.*, 2000). Might Scc2 exhibit kinase activity? To date, no mechanistic evidence exists to explain the way in which Scc2 functions, so this hypothesis was investigated. Alignment of Scc2 orthologues from the *Saccharomycetaceae* family of yeasts shows poor conservation of this motif and of the purported active site residue (Fig. III-2A). Mutating the active site aspartate residue to alanine should prevent any kinase activity; if Scc2 has an essential function as a kinase, this mutation should be lethal.

The mutation D468A was introduced into the wild type gene on a stably segregating yeast centromeric plasmid by site-directed mutagenesis. The plasmid, marked with the *LEU2* auxotrophic marker, was transformed into a yeast strain in which *scc2Δ* is complemented by a *URA3*-marked yeast centromeric plasmid containing the wild type *SCC2* gene. The wild type gene was counter-selected by plating cells on medium containing 5-FOA (Boeke *et al.*, 1984), thus leaving *scc2(D468A)* as the only source of Scc2. Figure III-2B shows that cells expressing *scc2(D468A)* have similar growth to wild type cells. In contrast, cells transformed with empty vector control cannot survive

21 [LIVMFYC]X[HY]X**D**[LIVMFY]KXXN[LIVMFYCT]$_3$, where X means any amino acid and **D** is the active site residue.

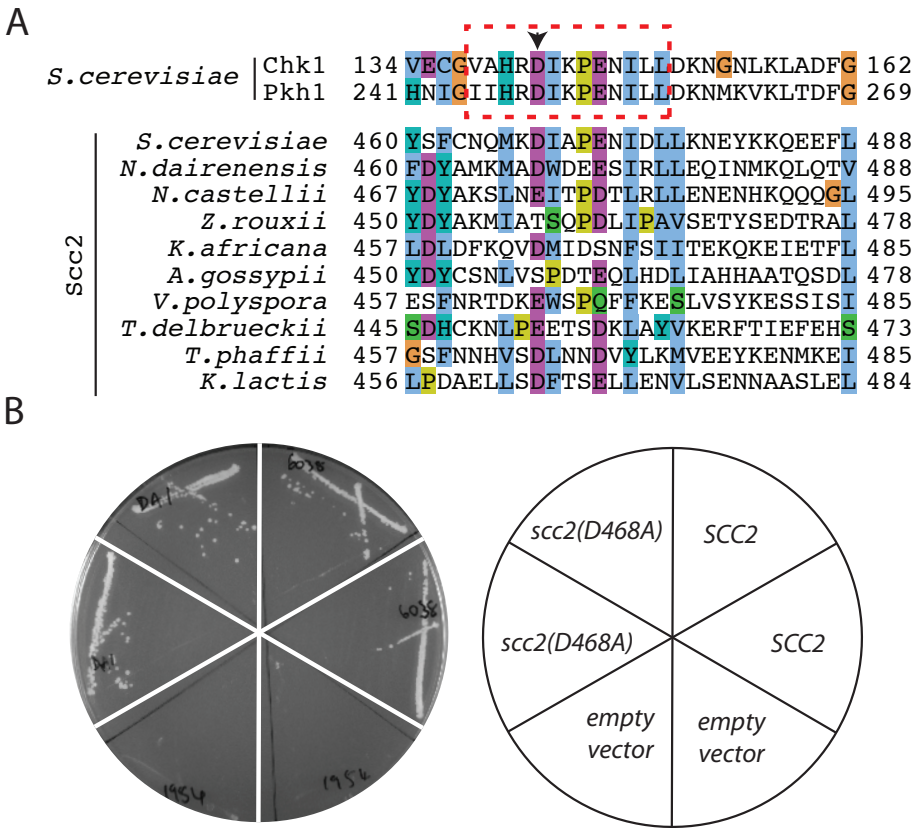

Figure III-2. Scc2's putative kinase is not essential.
A Mulitple sequence alignment showing the conservation of the serine/threonine kinase motif of *S. cerevisiae*'s Chk1 and Pkh1 to Scc2 and orthologues from the *Saccharomycetaceae* family of yeasts. The black arrowhead denotes the active site aspartate residue. Outlined in red is the kinase motif [LIVMFYC]X[HY]XD [LIVMFY]KXXN[LIVMFYCT]$_3$.
B *scc2Δ* strains, kept alive by a *URA3* plasmid encoding *SCC2*, were transformed with an empty *LEU2* plasmid or one encoding either *SCC2* or *scc2(D468A)*. Strains were streaked on medium containing 5-FOA and assessed for growth after incubation for 3 d at 25 °C (K22133, K22134, K22135, K22136, K22137, K22138).

in the absence of the wild type gene. Whilst it cannot be ruled out that Scc2 has kinase activity, these data suggest that any potential phosphorylation performed by this putative kinase motif in Scc2 is non-essential.

Kollerin is a heterodimeric complex

In order to study the interaction between Scc2 and Scc4, one must first determine the stoichiometry of the complex. It is currently unclear if Scc2

and Scc2 can interact with themselves, as well as each other; binding assays between Scc2 and Scc4 mutants can only be performed in the presence of the wild type proteins if kollerin is heterodimeric, rather than a higher order complex.

According to silver staining, Scc2 immunoprecipitates with Scc4 in a roughly 1:1 ratio (Ciosk *et al.*, 2000), but the actual stoichiometry of the yeast kollerin holocomplex has never been addressed. To clarify this matter, co-immunoprecipitations were performed with lysates from diploid yeast strains expressing two differently tagged copies of the same kollerin subunit, the rationale being that these should co-immunoprecipitate if kollerin is a multimer, but not if forms a truly heterodimeric holocomplex. Following immunoprecipitation of Scc2-PK_3, Scc2-HA_6 was not detected by Western blot, while Scc4-myc_{18} was. Likewise, Scc4-GFP did not co-immunoprecipitate with

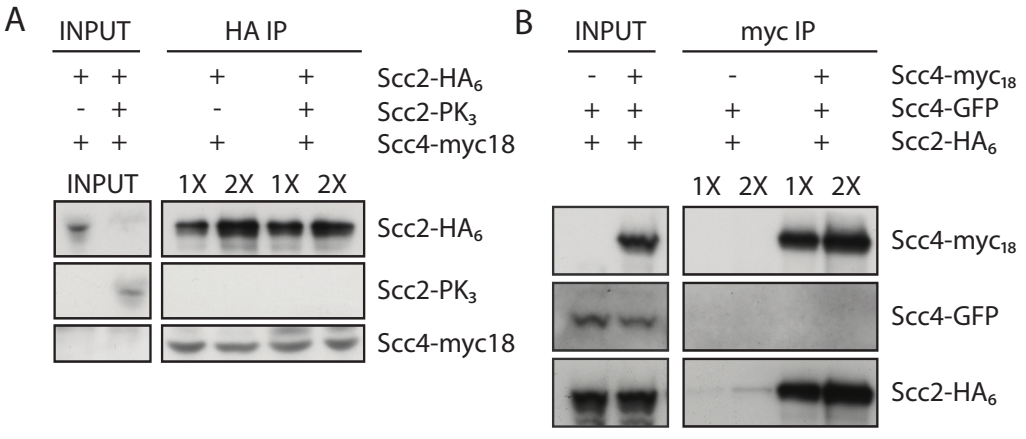

Figure III-3. Kollerin forms a heterodimeric complex.
A Immunoprecipitation of Scc2-HA_6 from cells also expressing Scc2-PK_3 and Scc4-myc_{18} shows that Scc2-PK_3 does not co-immunopreciptiate with Scc2-HA_6 (K18948, K18970). N.B. despite immunoprecipitating Scc2-HA_6 rather than Scc2-PK_3 (the relevant negative control being therefore absent) no Scc2-PK_3 binding is seen upon Scc2-HA_6 immunoprecipitation.
B Immunoprecipitation of Scc4-myc_{18} from cells also expressing Scc4-GFP and Scc2-HA_6 shows that Scc4-GFP does not co-immunopreciptiate with Scc4-myc_{18} (K18977, K18922).

Scc4-myc$_{18}$, whereas Scc2-HA$_{6}$ did (Fig. III-3). These data are consistent with the hypothesis that kollerin is a heterodimeric complex

Mutation of Scc4's moderately well-conserved Y40 confers the thermosensitive phenotype of scc4-4

The *scc4-4* allele was created by error-prone PCR and contains several mutations (Ciosk *et al.*, 2000). As well as the extragenic suppressor mutation uncovered in a screen for suppressors of *scc4-4* thermosensitive phenotype (performed by Dr Maria Demidova; outlined in Chapter II) several intragenic revertants were found. Gene sequencing revealed that both reversion of the *scc4-4* mutant Y40N residue to tyrosine and its substitution to histidine restored wild type growth, implying that this mutation is responsible for the thermosensitive phenotype.

Fungal Scc4 orthologues display a high level of conservation of this tyrosine residue, which often is found neighbouring an additional aromatic amino acid. Although this high level of conservation is not so clearly shared by metazoans, many possess tandem aromatic residues at this position, which may be indicative of the residue's structural or functional importance (Fig. III-4A).

To test whether *scc4(Y40N)* was alone sufficient to cause thermosensitivity, site-directed mutagenesis was implemented to introduce the mutation into a plasmid harbouring the wild type *SCC4-myc$_{18}$* gene. The mutant gene was integrated into a yeast strain that was then crossed such that

it was the only source of Scc4. Also tested were *scc4(Y40A)*, since alanine is a structurally simple amino acid that can reveal functionally important sites, and the partial revertant *scc4(Y40H)*. These strains were streaked on YPD agar and incubated at permissive (25 °C) and restrictive (37 °C) temperatures to determine thermosensitivity. All strains grew well at both temperatures, except *scc4(Y40N)-myc*$_{18}$, which was thermosensitive, albeit to a slightly lesser degree than *scc4-4* (Fig. III-4B).

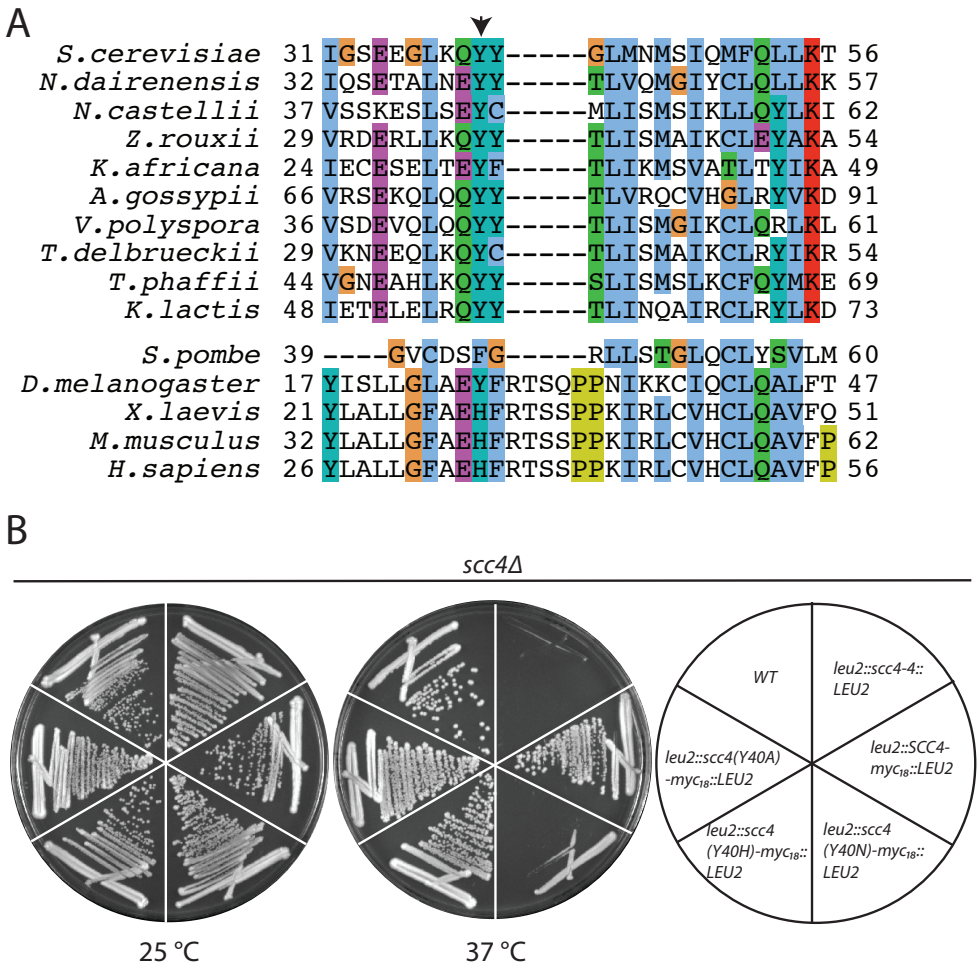

Figure III-4. Mutation of a conserved tyrosine residue in Scc4 causes thermosensitive lethality.

A Mulitple sequence alignment showing conservation of *S. cerevisiae* Scc4's Y40 (black arrowhead) in Scc4 orthologues from the *Saccharomycetaceae* family of yeasts (upper panel) and more diverse eukaryotes (lower panel).

B Yeast strains ectopically expressing *scc4(Y40)* mutants in an *scc4Δ* genetic background (K699, K8326, K20338, K20339, K20340, K20341) were streaked on YPD and assessed for growth after incubation for 2 d at permissive (25 °C) and restrictive (37 °C) temperatures.

Scc4Y40 mutants are defective in Scc2 binding

The molecular basis for the thermosensitive phenotype of *scc4-4* is unknown. Indeed, very little is known about the molecular mechanism of how the kollerin complex pursues its function. Since it is long established that Scc2 and Scc4 interact (Ciosk *et al.*, 2000), and the genetic and evolutionary evidence (presented above) is consistent with a functional role of Scc4Y40, it is postulated that the point mutation that confers the thermosensitive phenotype may affect the binding between Scc2 and Scc4.

To test the hypothesis that Scc4Y40 is an important residue in Scc2 binding, *scc4(Y40N/H/A)-myc*$_{18}$ mutants were crossed with a strain expressing

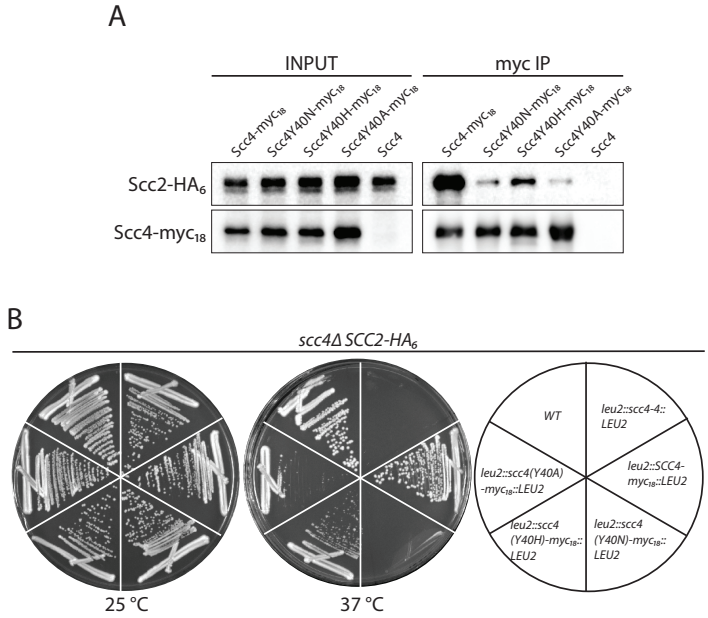

Figure III-5. *scc4(Y40)* mutants have a reduced ability to interact with Scc2-HA$_6$.
A Immunoprecipitation of myc$_{18}$-tagged Scc4Y40 mutants from cells also expressing Scc2-HA$_6$ (K20110, K20111, K20112, K20113, K7564). While wild type Scc4 co-immunoprecipitates with Scc2, Scc4Y40 mutants exhibit a reduced level of interaction.
B Yeast strains ectopically expressing *scc4(Y40)* mutants in an *scc4Δ SCC2-HA*$_6$ genetic background (K7564, K8504, K20350, K20351, K20352, K20353) were streaked on YPD and assessed for growth after incubation for 2 d at permissive (25 °C) and restrictive (37 °C) temperatures.

SCC2-HA$_6$ in order to perform co-immunoprecipitation between the two proteins (Fig. III-5A). The interaction between Scc4Y40N and Scc2 was seen to be severely diminished compared to the wild type protein. In accordance with the partial reversion phenotype seen *in vivo*, Scc4Y40H displayed an intermediate level of binding to Scc2 between the thermosensitive and wild type proteins. Somewhat surprisingly, Scc4Y40A bound Scc2 as poorly as Scc4Y40N. However, it became apparent upon streaking strains at restrictive temperature that the C-terminal epitope tag on Scc2 has a synthetic sick effect with all Scc4Y40 mutants in a manner that broadly reflects what is observed by co-immunoprecipitation (Fig. III-5B).

N-terminally truncated Scc2 is unable to bind Scc4

Past studies have looked into the interaction between Scc2 and Scc4 from different organisms. Although three groups (Seitan *et al.*, 2006; Takahashi *et al.*, 2008; Braunholz *et al.*, 2012) have produced results consistent with the notion that the N-terminus of Scc2 is involved in the interaction with Scc4, two use the yeast two-hybrid system, which is notorious for giving false positive readouts (Serebriiskii & Golemis, 2001). The other does, however, detect an interaction between the two *in vitro*-translated truncated *X. laevis* kollerin subunits by co-immunoprecipitation. The issue is readdressed here with yeast kollerin. The interaction between Scc4 and several different truncated versions of Scc2 was measured by co-immunoprecipitation. Although this technique, too, may detect indirect interactions between proteins, it has the advantage of

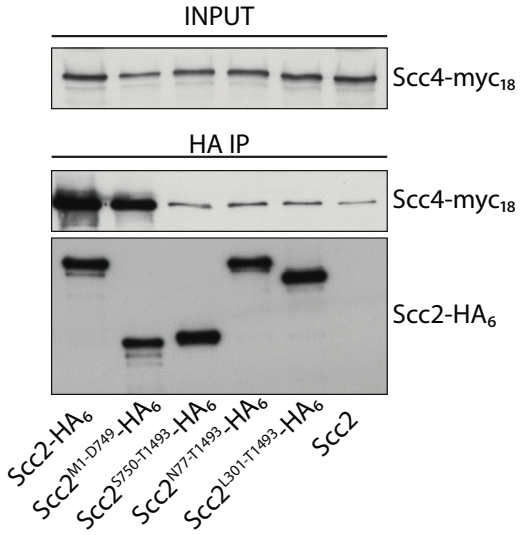

Figure III-6. Scc2's N-terminus is essential for Scc4 interaction.
Immunoprecipitation of truncated forms of Scc2-HA_6 from cells also expressing Scc4-myc_{18} (K19586, K19588, K19587, K19590, K19589, K18971). While Scc4 co-immunoprecipitates with full length and C-terminally truncated Scc2 constructs, it exhibits a level of interaction with N-terminally truncated Scc2 constructs close to the level of background binding.

using conditions that are closer to a physiological state than both the methods described above.

Truncated *SCC2-HA_6* constructs were created by overlapping PCR and integrated into an ectopic locus in *SCC4-myc_{18}*-expressing cells for performing co-immunoprecipitation. While both the full length ($Scc2^{M1\text{-}T1493}$) and N-terminal half ($Scc2^{M1\text{-}D749}$) of Scc2 interact with Scc4, the C-terminal half ($Scc2^{S750\text{-}T1493}$) does not. Indeed, deletion of as few as the first 76 amino acids ($Scc2^{N77\text{-}T1493}$) was sufficient to prevent the interaction (Fig. III-6). These first 76 amino acids are therefore crucial for Scc4 interaction.

N-terminally truncated Scc2 is unable to support yeast growth

It has been shown earlier in this chapter that a point mutation in Scc4

disrupts Scc2 binding and prevents cell proliferation. It might therefore be hypothesised that N-terminally truncated versions of Scc2 that may no longer bind Scc4 are similarly unable to support growth.

The ability of the N-terminally truncated proteins to support growth in the presence of wild type Scc2 was addressed after having removed the C-terminal HA_6 tag and integrated the genes at the endogenous *SCC2* locus due to a problem that was encountered with the tag (described later). As predicted by Mendelian genetics for genes that do not support proliferation, approximately half of all spores originating from diploids heterozygous for truncated versions of *scc2* were non-viable. In addition, the drug resistance cassette that marked these modified genes was never present in viable spore clones. In contrast, almost all spore clones originating from *SCC2/SCC2* diploids were viable and half of these spores conferred drug resistance (Fig. III-7A). Thus, the Scc4-binding N-terminus of Scc2 appears to be essential.

Growth of cells expressing N-terminally truncated Scc2 is restored by scc4Δ suppressor mutation smc1(D588Y)

N-terminally truncated Scc2 can no longer bind Scc4, and can no longer support growth. Is it merely the ability of Scc2 to bind Scc4 that has been disrupted, or is another function of Scc2 perturbed by these truncations? The *scc4Δ* suppressor mutation *smc1(D588Y)* can be used to investigate this, since Scc2 obviously does not need to interact with Scc4 in a genetic background where *SCC4* may be deleted. Other functions of Scc2 should, however, still be

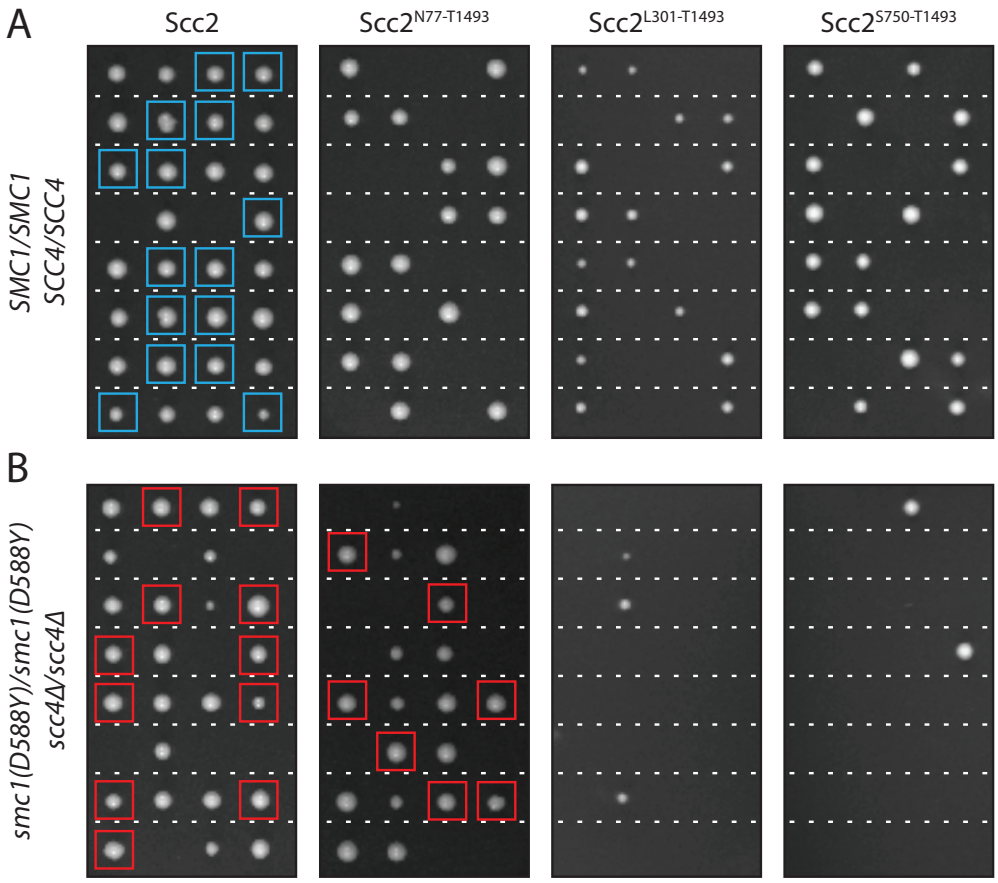

Figure III-7. Deletion of the essential N-terminus of Scc2 can be rescued by *scc4Δ* suppressor mutation *smc1(D588Y)*.
Dissection of diploids expressing at the endogenous locus either full length or N-terminally truncated Scc2 in **A** an otherwise wild type genetic background (K21600, K21598, K21633, K21631), or **B** a homozygous *smc1(D588Y) scc4Δ* background (K21599, K21597, K21632, K21630). Dissection was performed on YPD agar and plates were incubated at 25 °C for 3 d. Spore clones exhibiting the antibiotic resistance marker, indicating presence of either full length or a truncated form of Scc2 are marked in blue (wild type background) or red (*smc1(D588Y) scc4Δ* background).

required since this subunit remains essential. It is therefore hypothesised that the suppressor mutation *smc1(D588Y)* should rescue the lethality of Scc2 truncations if Scc4 binding is the only Scc2 function that has been disrupted.

Dissection of a diploid yeast strain expressing an ectopic copy of *SCC2-HA*$_6$ revealed that the gene was able to complement *scc2Δ*, both in the presence and absence of *smc1(D588Y)* in a wild type *SCC4* background, but

not when *SCC4* was deleted. Further investigation revealed that, in agreement with the prior indication that *Scc2-HA*$_6$ does not behave like the wild type protein (Fig. III-5B), it was the presence of the C-terminal tag on Scc2, rather than its being expressed from an ectopic locus that conferred the synthetic lethal phenotype (data not shown).

Integrating untagged full length *SCC2* at the endogenous locus of homozygous *scc4Δ smc1(D588Y)* diploids and dissection revealed that this gene, unlike the tagged version, supports growth in this genetic background. Remarkably, cells expressing *smc1(D588Y)* alongside *scc2*$^{N77\text{-}T1493}$ were also able to grow in the absence of *SCC4*. Neither *scc2*$^{L301\text{-}T1493}$ nor *scc2*$^{S750\text{-}T1493}$ conferred growth in the presence of the *scc4Δ* suppressor mutation (Fig. III-7B).

DISCUSSION

The kollerin complex comprises Scc2 and Scc4 proteins, and is essential for cohesin's association with DNA. Its mechanism of action is unclear. Here, a biochemical approach was implemented with a view to better understanding the way in which cohesin loading is achieved.

By co-immunoprecipitation, it was shown that kollerin is a heterodimeric complex. While this work was in progress, the same was reported of human kollerin, a predicted heterodimer of 382 kDa, using sucrose gradient sedimentation (Bermudez *et al.*, 2012). Previously published studies,

using proteins from different model organisms, suggest that the N-terminus of Scc2 interacts with the N-terminus of Scc4 (Seitan *et al.*, 2006; Takahashi *et al.*, 2008; Braunholz *et al.*, 2012). Through N-terminal truncation of Scc2 and a point mutation in the N-terminus of Scc4 both interfering with the formation of stable kollerin heterodimers, the data presented in this chapter support these studies.

Firstly, a screen for suppressors of *scc4-4*'s thermosensitive phenotype (performed by Dr Maria Demidova) uncovered an intragenic mutation that could fully revert the lethal phenotype seen at restrictive temperature. This mutation was revealed to be a reversion of the thermosensitive Scc4Y40N residue to wild type Scc4Y40. In addition, partial reversion was achieved by mutation of the same residue to histidine (Scc4Y40H), a residue that bears moderate structural similarity to the wild type tyrosine. The ability of a single, fairly well conserved residue to confer the thermosensitive phenotype of *scc4-4* was confirmed, and these data were interpreted as the residue having structural and/or functional importance for Scc4. This notion was supported by co-immunoprecipitation showing that mutations in Scc4Y40 severely impacted on the protein's ability to bind Scc2. Secondly, deletion of the N-terminal 76, 299, or 749 amino acids of Scc2 prevented its Scc4 binding, whereas deletion of its C-terminal 743 amino acids permits the interaction.

While the Scc4 point mutation allows normal protein function at permissive temperatures, N-terminal Scc2 truncations do not. It might therefore be postulated that the resultant truncated proteins suffer grave defects such

as erroneous protein folding. However, at least for Scc2$^{N77\text{-}T1493}$, this cannot be the case; this mutant protein can support yeast growth in the presence of *scc4Δ* suppressor mutation *smc1D588Y*. Thus, the only essential role of Scc2's N-terminal 76 amino acids is in forming a complex with Scc4. Since the truncated protein appears only defective in its ability to form a complex with Scc4, it must presumably remain able to perform its other enigmatic functions, for example interacting with DNA, chromatin or cohesin. Indeed, the fact that Scc2$^{N77\text{-}T1397}$ is essential even in the presence of *smc1(D588Y)* is indicative of a vital Scc4-independent function being conferred by this truncated protein. One might postulate that part of the remaining Scc2 molecule is required to interact with the cohesin complex.

Deletions of 299 or more amino acids from Scc2's N-terminus prevent its interaction with Scc4 but, in contrast to a smaller deletion, are not rescued by *smc1(D588Y)*. It is not possible to conclude at this time whether the amino acids between 77-299 contribute an essential role or whether the truncated protein fails to fold correctly. It remains unclear as to whether there is a direct interaction between Scc2 and sites of cohesin loading. Might a reported leucine zipper motif defined by residues L694-L715 mediate Scc2's chromatin binding (Jones & Sgouros, 2001; Sigrist *et al.*, 2002)? Further work to determine the maximum Scc2 N-terminal deletion that supports growth in the presence of *smc1(D588Y)* is required to define a minimal Scc2.

The facts that Scc4Y40N causes temperature sensitive lethality and that, under normal circumstances, Scc2$^{N77\text{-}T1493}$, Scc2$^{L300\text{-}T1493}$ and Scc2$^{S750\text{-}T1493}$ do not

support yeast proliferation whatsoever, are consistent with the notion that Scc2 and Scc4 must interact in order to carry out their essential role in cohesin loading. Depending on the rate of kollerin subunit exchange, it may be possible to use the data presented here to engineer a conditional method of inactivating kollerin that, unlike currently established methods, would not depend on temperature shift. By placing a DNA sequence encoding the 76-amino acid N-terminal fragment of Scc2 under a strong conditional promoter (e.g. *pGAL*), its inducible overexpression should introduce competition with full length Scc2 for Scc4 binding. Since it is shown in this chapter that the binding of full length Scc2 to Scc4 is essential for kollerin function, its titration out of complex by the N-terminal fragment should therefore render kollerin inactive. This may be transferrable to other model organisms, for example through mRNA injection in fruit fly or mouse.

Is it possible to draw any relation to disease from the findings presented here? Strikingly, G15R and P29Q are two CdLS (Cornelia de Lange Syndrome)-causing mutations in the N-terminus of NIPBL, the human orthologue of Scc2, that are described to negatively affect its heterodimerisation with MAU2 (Scc4) (Braunholz *et al.*, 2012). Might it be that these mutant proteins, through failing to interact with Scc4, prevent their own, and thereby cohesin's loading?

How then does *scc4Δ* suppressor *smc1(D588Y)* rescue the lethality of $Scc2^{N77\text{-}T1493}$ truncation? While the mechanism of *scc4Δ* suppression by *smc1(D588Y)* remains unexplained as yet, it was shown in the previous chapter

that cells expressing *smc1(D588Y)* no longer require Scc2's enrichment at centromeres for sufficient cohesin loading to take place globally to support proliferation. Presumably in the absence of an interaction between Scc2 and Scc4, cohesin loading, both at the centromere and along chromosome arms, does not take place. Moreover, since in the absence of Scc4, Scc2 is no longer directed to the centromere (Chapter II), one might predict that when Scc2 is unable to interact with Scc4, such as in strains expressing *scc4-4* or *scc4Y40N* at restrictive temperature, or $scc2^{N77\text{-}T1493}$, $scc2^{L300\text{-}T1493}$ or $scc2^{S750\text{-}T1493}$ at any temperature, it is also unable to become enriched at the centromere. This may be investigated using one of many methods, including live cell imaging.

Interestingly, although *smc1(D588Y)* is unable to complement *scc2Δ*, it does raise the restrictive temperature of the *scc2-4* thermosensitive allele (M. Demidova, personal communication). The precise defect of the protein encoded by *scc2-4* has not been investigated, but if it were to be defective in either its interaction with Scc4 or its localisation to the centromere, the fact that *smc1(D588Y)* bypasses the requirement for both these abilities would go some way to explaining why this effect is seen.

A final observation arising from the work presented in this chapter is that ectopically expressed *SCC2-*HA_6 is unable to complement *scc2Δ* in an *scc4Δ smc1(D588Y)* background. In addition, *SCC2-*HA_6 expressed from its endogenous locus conferred a synthetic sick phenotype to *SCC4(Y40N/A/H)-*myc_{18} mutants. Removal of the C-terminal HA_6 tag resolved both issues. These data imply that the epitope tag on the C-terminus of Scc2 interferes with its function. Perhaps

a function such as interaction with cohesin, DNA/chromatin or kinetochore proteins is conveyed by the C-terminus of Scc2, and is disrupted upon C-terminal tagging.

May a parallel be drawn here to the fact that Scc4-GFP but not cohesin (Smc1-GFP) can be recruited to a *tetO* array on chromosome arms by Scc2-TetR (Hu *et al.*, 2011)? Another group has reported that Scc4-LacI is able to recruit C-terminally epitope tagged Scc2-HIS_6-$FLAG_3$ and cohesin (Scc1-HA_6) to a *lacO* array close to the centromere (Fernius *et al.*, 2013). An explanation of this discrepancy (alternative to that presented in the discussion of Chapter II) is that Scc2's C-terminal fusion to TetR may prevent its function in recruiting cohesin to the chromosomal arm locus. It would be interesting to see whether Scc2-TetR is functional in recruiting both Scc4 and cohesin to a pericentromeric *tetO* array as per this study, or whether its C-terminal fusion to the large (22 kDa) TetR protein affects its function.

Chapter IV

Summary and future directions

Summary and future directions

SUMMARY

The association of cohesin's heterotrimeric ring with chromatin is an essential requisite for the faithful transmission of chromosomes from mother to daughter cell during mitosis and meiosis. The kollerin complex, composed of a large (Scc2) and small (Scc4) subunit, is a regulator of cohesin; without kollerin, cohesin fails to load onto DNA. Here, the mechanism of cohesin loading was investigated, both genetically and biochemically, and the following original conclusions have been made:

1) Mutation of Smc1D588 to an uncharged aromatic residue renders Scc4 dispensable for yeast proliferation;

2) Uncharged aromatic residue substitutions at Smc1D588 weaken the interaction between Smc1/Smc3 hinge dimers;

3) Scc4 is required for the centromeric enrichment of both cohesin and Scc2;

4) The interaction between Scc2 and Scc4 is essential for kollerin's function.

FUTURE DIRECTIONS

The data presented here are consistent with the hypothesis that the Smc1/Smc3 hinge interface is more than just a dimerisation domain. Sister chromatid cohesion is likely conferred through a topological mechanism (Haering *et al.*, 2008). In light of this, the transition between cohesin's soluble state that exists prior to loading, and the chromatin bound state that exists following DNA replication, must involve opening of at least one of the three interfaces. Strengthening this hypothesis, separase-independent removal of cohesin is prevented by fusion of Smc3 to Scc1, implying that this junction acts as a 'DNA exit gate' (Chan *et al.*, 2012). The combination of genetic and biochemical evidence presented here strongly support the notion that the hinge interface acts as the 'DNA entry gate', which is in accordance with the previously published results and model proposed by Gruber *et al.* (2006). However, this raises questions as to the nature of cohesin loading and the establishment of cohesion. Primarily, focus should be placed on answering the following questions:

How is the hinge opened and how is it locked?

While the ring model predicts transient ring opening to allow cohesin's loading onto DNA, it also makes the apparently contradictory prediction that all three interfaces must remain closed following cohesion establishment. In the case of separase-independent removal of cohesin, which involves opening of the interface between Smc3 and Scc1, Wapl is an essential factor in release,

whereas post-translational modification of Smc3's NBD by the acetyltransferase Eco1 provides the antagonistic function of 'locking' the interface.

The fact that a mutation in Smc1's hinge weakens the interaction between Smc1 and Smc3 hinges (shown biochemically, and inferred from genetic data as discussed in Chapter II) whilst also overcoming the requirement for Scc4 function suggest that Scc4 itself may play a role in opening Smc1's hinge. Perhaps post-translational modification of the ring is therefore required to lock it. One candidate modification is SUMOylation, which occurs on all cohesin subunits and is required for the establishment of cohesion *via* an as yet undefined mechanism (Almedawar *et al.*, 2012). Equally, the Eco1-dependent acetylation of Smc3's NBD, which occurs concomitantly with cohesion establishment and is already implicated in locking the Smc3-Scc1 interface (Chan *et al.*, 2012), may have a secondary role in locking the hinge.

Alternatively, since ATP hydrolysis is required for the stable, and presumably topological, association of cohesin with DNA (Arumugam *et al.*, 2003; Weitzer *et al.*, 2003; Hu *et al.*, 2011), the energy produced by this reaction might be transmitted along the coiled coils to modify the hinge interaction in a manner analogous to the way in which ABC transporters are proposed to transmit their energy to a distal site *via* a transmembrane domain (Jones & George, 2002). While a model has been proposed whereby the role of ATP hydrolysis is in opening the hinge (Hu *et al.*, 2011), it is equally, if not more plausible given the novel findings presented here, that it is instead required to lock it.

At what point(s) is hinge opening required?

The question of how cohesion is established during S phase remains one of the most pertinent unanswered questions in the cohesin field. Cohesion establishment is linked to the progression of the replication fork through Eco1, which interacts with fork-associated PCNA (Moldovan *et al.*, 2006) and promotes the stability of cohesin on DNA through acetylation of its Smc3 subunit (Rolef Ben-Shahar *et al.*, 2008; Ünal *et al.*, 2008; Zhang *et al.*, 2008a; Rowland *et al.*, 2009; Chan *et al.*, 2012). However, several gaps remain in our understanding of replication-coupled establishment. Might topologically associated G_1 cohesin rings dissociate from DNA and be reloaded following passage of the replication fork? Or is this dynamically bound population of cohesin that exists prior to replication, reported by Gerlich *et al.* (2006), representative of a non-topological state, thus requiring the hinge to open only after passage of the fork? While kollerin is not required during G_2 phase (Ciosk *et al.*, 2000), the exact moment at which it becomes dispensable is not defined. It has been suggested that cohesion may be established by passage of the replication machinery through the topologically-bound rings deposited in G_1 (Haering *et al.*, 2002; Lengronne *et al.*, 2004). However, the notion of the replication machinery being able to pass through the ring without its opening is difficult to reconcile with the observation that the transcription machinery is not able to pass through the ring but instead relocates it to sites of convergent transcription (Lengronne *et al.*, 2004).

It remains to be elucidated whether the cohesin that associates with DNA

prior to replication does so topologically or not. Is the cohesin that is associated with DNA prior to passage of the replication fork the same population that is associated afterwards? Establishing the number of times that hinge opening is required and at which points it occurs during the cohesin cycle will provide fundamental clues as to the mechanism of cohesion establishment.

Chapter V

Materials and methods

Materials and methods

Yeast strains and growth conditions

All strains are derived from W303 and were grown at 25 °C unless otherwise stated. Rich growth medium (YEP) was supplemented with 2 % glucose (YPD). Liquid cultures were agitated at 200 rpm (Multitron Standard, Infors HT).

Arrest in G_1 was achieved through addition of α-factor (Bücking-Throm *et al.*, 1973) at 2 mg/L/h, half-hourly for 2.5 h. Subsequent release from G_1 was achieved through harvesting cells by centrifugation and washing cell pellets with a volume of 1X PBS equal to three times the volume of culture before resuspending in the appropriate growth medium.

Inactivation of *scc4-4* was achieved through harvesting cells by centrifugation and resuspending in pre-warmed growth medium (at 35.5 °C). Liquid cultures were agitated at 200 rpm (Aquatron, Infors HT).

Metaphase arrest was achieved through methionine-induced repression of Cdc20 (Yeong *et al.*, 2000). Methionine was added to a concentration of 2 μM for 2.5 h.

Fluorescence-activated cell sorting

1 mL culture was harvested by centrifugation for 1 min at 16 000 *g*, resuspended in 1 mL of 70 % (v/v) ethanol and stored at 4 °C overnight.

Following an additional centrifugation step, the supernatant was discarded and the pellet was resuspended in 1 mL of 50 mM Tris-HCl, pH 7.5 containing 200 µg/mL RNase A (Roche). RNase treatment was performed at 37 °C for 2 h with agitation at 1 000 rpm. Cells were then pelleted and resuspended in 400 µL FACS buffer.

FACS buffer	
Tris-HCl, pH 7.5	180 mM
$MgCl_2$	70 mM
Propidium iodide	50 µg/mL
NaCl	190 mM

Cells in FACS buffer were dispersed by sonication for 5 s at 40 % output (Vibra-Cell™ VCX 130FSJ, Sonics & Materials Inc.). A 1:200 dilution into 1 mL of 50 mM Tris-HCl, pH 7.5 was made, the suspension transferred to FACS tubes and analysis performed by measuring 10 000 events per sample using FACSCalibur™ flow cytometer (BD Biosciences).

Yeast transformation

Salmon sperm DNA (10 mg/mL) was heat-inactivated at 95 °C for 5 min and cooled on ice before use. Exponentially growing cells (approximately 10 mL at OD_{600} = 0.4 per transformation) were harvested by centrifugation and washed with 1 M lithium acetate before being resuspended in 300 µL of transformation buffer. To this, DNA (approximately 200 ng - 2 µg) was added and the mixture incubated for 20 min at 42 °C.

Following heat shock, cells were pelleted by centrifugation and

resuspended in 300 µL of sterile ddH_2O, then plated on selective drop-out agar medium. In the case of a heterologous drug resistance cassette being the marker for successful transformation, a 2-h recovery in YPD was performed prior to plating on YPD agar medium supplemented with the appropriate antibiotic.

Transformation buffer	
Lithium acetate	150 mM
Inactivated salmon sperm DNA	1.5 mg/mL
PEG-2 000	33% (w/v)

Genomic integration

Integrative plasmids (YIplac128, YIplac204, YIplac211) were linearised by restriction digest with an appropriate endonuclease (New England Biolabs) at a single site within the selective auxotrophic marker gene (*LEU2*, *TRP1*, *URA3* respectively) prior to transformation. Integration into the *leu2*, *trp1* and *ura3* loci was verified using extracted genomic DNA as a template for PCR using specific primer sets to indicate single-copy, multiple-copy or no integration.

For C-terminal tagging of genes at their endogenous loci, tagging cassettes containing 50 bp homology regions flanking the required insertion site were PCR amplified from pFA6a plasmids prior to their transformation as described previously.

For integration of mutant genes at the endogenous locus, constructs were created that contained the gene of interest and a selective marker between regions of homology to the desired insertion site. The entire cassette

was isolated by restriction digest or amplified by PCR, as appropriate, prior to transformation as described above. Correct integration was confirmed by PCR from genomic DNA using primers flanking the insertion site.

Yeast genomic DNA preparation

Exponentially growing cells were harvested by centrifugation. The pellet was washed with ddH_2O, then resuspended in 200 µL of spheroplasting buffer and incubated at 37 °C with agitation at 1 000 rpm.

Spheroplasting buffer	
Sorbitol	850 mM
Sodium citrate	85 mM
EDTA, pH 7.0	50 mM
β-mercaptoethanol	100 mM
Zymolase® 100T	1.5 mg/mL

When spheroplasts could be visualised microscopically (after approximately 1 h), 200 µL of SDS lysis buffer was added, and the mixture was incubated at 65 °C for 5 min.

SDS lysis buffer	
SDS	2 % (w/v)
Tris HCl, pH 9.0	100 mM
EDTA	50 mM

Following lysis, 200 µL of 5 M potassium acetate was added to precipitate cell debris. Following centrifugation (10 min, 16 000 *g*), 300 µL of the soluble fraction was added to 800 µL of ice cold 100 % ethanol to precipitate DNA. A further centrifugation step (10 min, 16 000 *g*) was performed, the liquid

removed and the DNA pellet was washed with 1 mL of ice cold 70 % (v/v) ethanol before being air dried at 65 °C. The thereby obtained DNA pellet was dissolved in 200 µL of TE buffer, pH 7.5, and stored at -80 °C

Tetrad dissection

Diploid strains were patched on nitrogen-deficient medium to induce meiosis. When sporulation could be visualised microscopically (after approximately 48 h at 30 °C), cells were spheroplasted by incubation for 20 min at room 20 °C in 300 µL of tetrad dissection buffer. Ten microlitres of this suspension were transferred to an agar plate for microscopic dissection (MSM 300, Singer Instruments).

Tetrad dissection buffer	
Sorbitol	1 M
Zymolase® 20T	1.5 mg/mL

Preparation of denatured yeast cell extracts

4 OD units of exponentially growing cells (e.g. 10 mL culture at OD_{600} = 0.4) were harvested by centrifugation and washed with 1 mL of 20 % TCA, then resuspended in 200 µL of 20 % TCA and transferred to 2 mL screw-top microcentrifuge tubes. A bed volume of 100 µL of acid-washed glass beads, 425-600 µm (Sigma) was added and lysis was performed using a FastPrep®-24 benchtop homogenizer at 4 °C (2 x 60 s at 4.5 m/s, or until lysis could be confirmed microscopically). The precipitated protein suspension

was separated from the beads, which were then washed with 400 uL 5% TCA. The supernatants were combined then the insoluble material was pelleted by centrifugation for 5 min at 8 000 *g*. The supernatant was discarded and the pellet was resuspended in 100 µL of 2X SDS sample buffer.

2X SDS sample buffer	
Tris-HCl pH 6.8	250 mM
SDS	4 % (w/v)
Glycerol	20 % (v/v)
β-mercaptoethanol	1.43 M
Bromophenol blue	0.025 % (w/v)

Preparation of native yeast cell extracts

Cells were grown in liquid culture as described previously before being harvested by centrifugation and washed with 1X PBS. Cell pellets were resuspended in 200 µL of yeast lysis buffer.

Yeast lysis buffer	
NaCl	150 mM
Tris-HCl pH 7.5	50 mM
NP-40	0.5 % (v/v)
EDTA	5 mM
DTT	1.25 mM
PMSF (Fisher Scientific)	1 mM
Protease inhibitor cocktail (Roche)	1 tablet/50 mL

The cell suspension was transferred to 2 mL screw-top microcentrifuge tubes containing 100 µL of acid-washed glass beads, 425-600 µm (Sigma), and lysis was performed using a FastPrep®-24 benchtop homogenizer at 4 °C (2 x 60 s at 4.5 m/s, or until lysis could be confirmed microscopically).

Insoluble material was pelleted by centrifugation at 16 000 *g* for 15 min. Soluble extract was decanted and protein concentration measured.

Quantitation of protein concentration in crude extracts

Crude extract protein concentration was determined using the Bradford protein assay (Bradford, 1976). Bradford® reagent (dye concentrate; Bio-Rad), diluted 1:4, was added to samples to a volume of 1 mL and allowed to stand at room temperature for 5 min. Sample absorbance at 595 nm was measured for each sample relative to a blank, containing lysis buffer, using an Ultrospec 3 300 pro spectrophotometer (Amersham Biosciences). Concentration of samples was calculated from a standard curve that was created using serially diluted BSA.

Immunoprecipitation

Cells were grown, lysed and crude extract protein concentration was quantified as above. Concentration of lysates were adjusted with lysis buffer before equal volumes of each sample were pre-cleaned by being added to 100 µL of pre-equilibrated lgG Sepharose® 6 Fast Flow beads (GE Healthcare) and incubated at 4 °C with rotation for 1 h. Following centrifugation at 850 *g* for 30 s, lysates were decanted. To these were added the appropriate antibody (PK: 1.5 µL of V5, AbD Serotec; myc: 3 µL of A-14, Santa Cruz Biotech) for 1 h 30 min then 100 µL of pre-equilibrated rmp Protein A Sepharose® Fast Flow beads (GE Healthcare) for 2 h at 4 °C with rotation. For immunoprecipitation

of HA-tagged proteins, pre-cleaned lysates were incubated with 50 µL of pre-antibody-coupled Anti-HA Affinity Matrix (Roche) for 2 h at 4 °C with rotation. Beads were washed 3 times with 1 mL of lysis buffer before being resuspended in a volume equal to the bead bed volume of 2X SDS sample buffer for immunoblotting.

Protein gel electrophoresis, gel staining and Western blotting

Samples were loaded onto SDS polyacrylamide gels and separated using an appropriate current. For gel staining, gels were washed three times for 5 min with deionised water before staining with Imperial™ protein stain (Pierce Biotechnology) as per the manufacturer's instructions. For Western blotting, samples separated by SDS-PAGE were transferred to 0.45 µm PVDF membrane (Millipore) or 0.2 µm nitrocellulose membrane (Bio-Rad) using a wet transfer.

Ponceau S stain was used to assess the transfer, and was removed by incubation of the membrane in PBS + 0.05 % TWEEN® 20 (Sigma; PBST). Membrane blocking was achieved through incubation of the membrane for 1 h with 3 % milk powder (w/v) in PBST, then incubation with primary antibody, diluted as indicated in PBST + 3 % milk powder was performed for 1 h 30 min.

Primary antibody	Immunogen	Origin	Dilution (WB)
His-tag antibody (GenScript)	HIS6	Rabbit	1:5 000
V5 (AbD Serotec)	PK	Mouse	1:1 000
3F10 (Roche)	HA	Rat	1:5 000
4A6 (Millipore)	c-MYC	Mouse	1:2 500
GFP (Roche)	GFP	Mouse	1:1 000
PGK1	PGK1	Mouse	1:5 000

The membrane was washed three times for 5 min with PBST before incubation for 45 min with secondary antibody, diluted as indicated in PBST + 3 % milk powder.

Secondary antibody	Conjugate	Dilution
Goat anti rabbit (Millipore)	HRP	1:5 000
Goat anti mouse (Millipore)	HRP	1:5 000
Goat anti rat (Millipore)	HRP	1:5 000
Goat anti rabbit (LI-COR)	IRDye® 800CW	1:15 000
Goat anti mouse (LI-COR)	IRDye® 680RD	1:15 000
Goat anti rat (LI-COR)	IRDye® 800CW	1:15 000

The membrane was washed three times for 5 min with PBST, then finally with PBS. Blots probed with HRP-conjugated secondary antibody were incubated with Immobilon™ Western Chemiluminescent HRP Substrate (Millipore) prior to detection. Proteins were detected using an ODYSSEY® Fc Imaging System (LI-COR).

Site-directed mutagenesis

Forward and reverse primers of 25-30 bp were designed such that the complementary overlapping region between them was 13-15 bp in length and contained the mutant bases centrally within this region. A mutagenesis

PCR mix using Phusion® DNA Polymerase (New England Biolabs) was set up according to the manufacturer's instructions and using 50 ng template DNA. Thermal cycling conditions were as indicated below. Following the PCR reaction, products were digested with DpnI (New England Biolabs) prior to transformation into competent *E. coli* strain XL1 Blue

Reaction parameters		
Initial denaturation	98 °C, 1 min	
Denaturation	72 °C, 10 s	
Annealing	Primer T_m, 20 s	
Extension	72 °C, 6 min 40 s	
Denaturation	98 °C, 10 s	⎫ 35 cycles
Annealing and extension	72 °C, 4 min 30 s	⎭
Final extension	72 °C, 10 min	

Overlapping PCR

Two PCR products (A and B) with 18-20 bp overlapping homology regions (at the 3' end of A and the 5' end of B) were created in separate PCR reactions. Following QIAquick® PCR cleanup reaction (QIAgen), products A and B were mixed in an equimolar ratio in a new PCR mix using Phusion® DNA Polymerase (New England Biolabs) set up according to the manufacturer's instructions but lacking primers. A two-step PCR reaction program (98 °C denaturation; 72 °C annealing and extension) was run for 20 cycles before the addition of primers (product A forward primer; product B reverse primer) and the reaction was continued with a three-step program (98 °C denaturation; T_m annealing; 72 °C extension).

Protein purification

BL21 DE3 strains containing plasmids encoding proteins for purification were grown at 37 °C in 2XTY liquid medium supplemented with the appropriate antibiotic until an OD_{600} of 0.6 was reached. Expression was induced by addition of IPTG to a concentration of 1 mM for 16 h at 20 °C. Cells were harvested by centrifugation and mixed with 5 times the cell pellet volume of lysis buffer.

E. coli lysis buffer	
NaCl	250 mM
Tris-HCl, pH 7.5	50 mM
EDTA	1 mM
β-mercaptoethanol	2 mM
Protease inhibitor cocktail (Roche)	1 tablet/50 mL

Cells were lysed by passage through a cell disrupter (Constant Systems) at 20 kpsi. PMSF (Fisher) in isopropanol was added to lysate to a final concentration of 1 mM. Sonication was performed on ice for 1 min/50 mL in 30 s intervals with a Vibra-cell sonicator (VCX 130FSJ; Sonics & Materials) at 80 % amplitude to reduce lysate viscosity by shearing DNA. Lysate was cleared by centrifugation at 50 000 *g* for 90 min in an Avanti J-26S XP centrifuge (Beckman Coulter).

Affinity purification was performed by incubating cleared lysates with pre-equilibrated Talon® Superflow Metal Affinity Resin (500 µL/50 mL lysate; Clontech) for 1 h at 4 °C. Beads were sedimented by centrifugation at 700 *g* for 2 min and the supernatant decanted and discarded. The resin was washed 5 times with 50 mL lysis buffer containing 10 mM imidazole. Proteins were

eluted with a volume of elution buffer (lysis buffer supplemented with 250 mM imidazole) equal to twice the volume of resin.

Size-exclusion chromatography was performed by injecting up to 2 mL of eluent onto a HiLoad™ 16/60 Superdex™ 200 prep grade column (equilibrated with Buffer A) connected to an ÄKTApurifier™ 100 purification system controlled by UNICORN™ software (GE Healthcare). Peak fractions containing purified protein were concentrated using Vivaspin™ columns (Sartorius Stedim Biotech) with a molecular weight cut-off of 10 kDa.

Buffer A	
NaCl	95 mM
HEPES, pH 7.5	20 mM
β-mercaptoethanol	2 mM

Concentration of purified protein was achieved based on its absorbance at 280 nm, measured using a NanoDrop-1000™ (Thermo Fisher Scientific). Measurements were made relative to buffer and based on the protein's calculated extinction coefficient and molecular mass (Gasteiger *et al.*, 2005).

In vitro hinge binding assay

Wild type and mutant MBP-Smc1^{hinge}-HIS$_6$ and Smc3^{hinge}-FLAG$_3$-HIS$_6$ proteins were expressed and purified as described above. Proteins were mixed at an equimolar concentration of 250 mM in Buffer A and incubated at 16 °C with shaking at 1000 rpm for 15 min. 400 µL of protein mixture was added to 20 µL of pre-equilibrated ANTI-FLAG® M2 affinity gel and incubated at 16 °C with shaking at 1000 rpm for 15 min. Resin was sedimented by centrifugation

for 1 min at 850 *g* then washed three times with Buffer A + 1 % Triton™ X-100 (Sigma) before being boiled in 2X SDS sample buffer prior to immunoblotting.

Chromosome loss assay

Strains carried an artificial chromosome containing *SUP11*, a tRNA gene capable of suppressing the defective *ade2-101* allele. Cells were grown to exponential phase in medium lacking uracil (to retain the artificial chromosome) before being transferred to rich medium and cultured for 2-3 h. Cells were dispersed by mild sonication prior to an approximate cell count being taken by measuring optical density at 600 nm (OD_{600}). Based on an OD_{600} of 1 being approximately equal to 3 x 10^7 cells, over 1 000 cells were plated on YPD sectoring plates lacking adenine. The percentage of colonies that were at least half red, indicating that the *SUP11*-containing chromosome was lost during the first cell division after plating, was scored.

GFP dots assay

Chromosomes were marked at the *URA3* locus by a *tetO* array, to which TetR-GFP fusion protein was recruited. Exponentially growing cells, in which Cdc20 was placed under the control of the methionine-repressible *MET3* promoter, were arrested in metaphase by the addition of 2 mM methionine. An aliquot of cells was fixed by a 10-min incubation with formaldehyde at a final concentration of 3.7 % (v/v). Cells were pelleted and permeabilised by resuspension in 100 % ethanol, then rehydrated and dispersed by sonication

for 5 sec at 40 % output (Vibra-Cell™ VCX 130FSJ, Sonics & Materials Inc.). Samples were concentrated by centrifugation before being resuspended in VECTASHIELD® Mounting Medium with DAPI (Vector Laboratories). Cells were immobilised on a slide and the number of cells with split GFP dots was determined microscopically. 100 cells were analysed per sample.

Live cell imaging

Exponentially growing cells were immobilised on 2 % agarose pads mounted on glass slides. All imaging was carried out at 25 °C using a spinning disk confocal system controlled by the Volocity™ program (Perkin Elmer UltraVIEW) with an EMCCD camera (Hamamatsu) mounted on an Olympus IX8 microscope with an Olympus 100X 1.35 N.A. objective.

Multiple sequence alignment

Multiple sequence alignments were performed using Clustal Omega (Sievers *et al.*, 2011) and were processed using Jalview (Waterhouse *et al.*, 2009). Uniprot identifiers of proteins used in multiple sequence alignments are displayed in the following table.

Organism	Smc1	Smc3	Smc2	Smc4	Smc5	Smc6	Scc4	Scc2	Chk1	Pkh1
S. cerevisiae	P32908	P47037	P38989	Q12267	Q08204	Q12749	P40090	Q04002	P38147	Q03407
N. dairenensis	G0WE98	J7S4N2					G0WBN4	G0W382		
N. castellii	G0VD28	G0V7P3					G0V655	G0VBR9		
Z. rouxii	C5DXC1	C5E1I6					C5E0Q6	C5DSY3		
K. africana	H2ASG2	H2AMJ9					H2AQ80	H2ARA6		
A. gossypii	Q750H4	Q75FB3					Q74ZR5	Q750S2		
V. polyspora	A7TQW2	A7TDK5					A7TGY9	A7TMS7		
T. delbrueckii	G8ZR43	G8ZT02					G8ZPJ9	G8ZXH2		
T. phaffii	G8C214	G8BXI7					G8BN16	G8BZW7		
K. lactis	Q6CRP2	Q6CYH7					Q6CNT3	Q6CQC3		
S. pombe	O94383	O42649	P41003	P41004	O13710	P53692	O94459			
D. melanogaster	Q9VCD8	Q9VMA0					Q9VFC0			
X. laevis	O93308	O93309	P50533	P50532	Q805A1	Q6P9I7	B4ZIX8			
M. musculus	Q9CU62	Q9CW03					Q9D2X5			
H. sapiens	Q14683	Q9UQE7	O95347	Q9NTJ3	Q8IY18	Q96SB8	Q9Y6X3			

Homology modelling

SWISS-MODEL (Arnold *et al.*, 2006) was used to create a structure-based homology model of the *S. cerevisiae* hinge domains, using the hinge crystal structure from *T. maritima* with PDB identifier 1GXL.

List of strains

K699	*MATa, W303 wildtype*
K842	*MATa/α, W303 wildtype*
K7564	*MATα, SCC2-HA$_6$::HIS3*
K8290	*MATa, scc4Δ::HIS3, YCplac33-SCC4*
K8326	*MATa, scc4Δ::HIS3, leu2::scc4-4::LEU2*
K8504	*MATa, scc4Δ::HIS3, leu2::scc4-4::LEU2, SCC2-HA$_6$::HIS3*
K16442	*MATa/α, SCC2-GFP::KanMX4/SCC2-GFP::KanMX4, MTW1-RFP::KanMX4/MTW1-RFP::KanMX4, ADE+*
K18920	*MATa, SCC2-PK$_3$::KanMX4, ADE+*
K18921	*MATα, SCC2-PK$_3$::KanMX4, ADE+*
K18922	*MATa, SCC2-HA$_6$::HIS3, SCC4-GFP::KanMX4*
K18946	*MATα, SCC2-PK$_3$::KanMX4, SCC4-myc$_{18}$::URA3*
K18948	*MATa/α, SCC2-PK$_3$::KanMX4/SCC2-HA$_6$::HIS3, SCC4-myc$_{18}$::URA3/SCC4-myc$_{18}$::URA3*
K18970	*MATα, SCC4-myc$_{18}$::URA3, SCC2-HA$_6$::HIS3*
K18971	*MATa, SCC4-myc$_{18}$::URA3*
K18977	*MATa/α, SCC4-GFP::KanMX4/SCC4-myc$_{18}$::URA3, SCC2-HA$_6$::HIS3/SCC2-HA$_6$::HIS3*
K19429	*MATa, scc4Δ::HIS3, smc1(D588Y)::HphNT1, SCC2-PK$_3$::KanMX4, ADE+*
K19431	*MATa, smc1(D588Y)::HphNT1, SCC2-PK$_3$::KanMX4, ADE+*
K19456	*MATa/α, SMC3-GFP::URA3/SMC3-GFP::URA3, MTW1-RFP::ADE2/MTW1-RFP::ADE2, smc1(D588Y)::HphNT1/smc1(D588Y)::HphNT1*
K19457	*MATa/α, SMC3-GFP::URA3/SMC3-GFP::URA3, MTW1-RFP::ADE2/MTW1-RFP::ADE2*
K19471	*MATa/α, SMC3-GFP::URA3/SMC3-GFP::URA3, MTW1-RFP::ADE2/MTW1-RFP::ADE2, smc1(D588Y)::HphNT1/smc1(D588Y)::HphNT1, scc4Δ::HIS3/scc4Δ::HIS3*
K19586	*MATa, SCC4-myc$_{18}$::URA3, leu2::SCC2-HA$_6$::LEU2*
K19587	*MATa, SCC4-myc$_{18}$::URA3, leu2::scc2(S750-T1493)-HA$_6$::LEU2*
K19588	*MATa, SCC4-myc$_{18}$::URA3, leu2::scc2(M1-D749)-HA$_6$::LEU2*
K19589	*MATa, SCC4-myc$_{18}$::URA3, leu2::scc2(L301-T1493)-HA$_6$::LEU2*
K19590	*MATa, SCC4-myc$_{18}$::URA3, leu2::scc2(N77-T1493)-HA$_6$::LEU2*
K19624	*MATa, SCC1-PK$_6$::KanMX4, smc1(D588Y)::HphNT1, scc4Δ::HIS3*
K19641	*MATa, SCC1-PK$_6$:KanMX4*
K19647	*MATa, SCC1-PK$_6$::KanMX4, smc1(D588Y)::HphNT1*
K19813	*MATa, scc4Δ::HIS3, leu2::scc4-4::LEU2, smc1(D588Y)*
K19820	*MATα. scc4Δ::HIS3 smc1(D588Y)::HphNT1. SCC1-myc$_{18}$::TRP, SCC2-PK$_3$::KanMX4, ADE+*
K19822	*MATα, smc1(D588Y)::HphNT1, SCC1-myc$_{18}$::TRP, SCC2-PK$_3$::KanMX4, ADE+*

K19824	*MATα, SCC1-myc$_{18}$::TRP, SCC2-PK$_3$::KanMX4, ADE+*
K19825	*MATα, SCC1-myc$_{18}$::TRP, ADE+*
K20110	*MATα, SCC2-HA$_6$::HIS3, leu2::SCC4-myc$_{18}$::LEU2*
K20111	*MATα, SCC2-HA$_6$::HIS3, leu2::scc4(Y40N)-myc$_{18}$::LEU2*
K20112	*MATα, SCC2-HA$_6$::HIS3, leu2::scc4(Y40H)-myc$_{18}$::LEU2*
K20113	*MATα, SCC2-HA$_6$::HIS3,leu2::scc4(Y40A)-myc$_{18}$::LEU2*
K20205	*MATa/α, SCC4/scc4Δ::HIS3, SMC3/smc3Δ::HphNT1, LEU2/ leu2::smc3(K652Y)::LEU2*
K20209	*MATa/α, SCC4/scc4Δ::HIS3, SMC3/smc3Δ::HphNT1, LEU2/leu2::SMC3::LEU2*
K20338	*MATα, scc4Δ::HIS3, leu2::SCC4-myc18::LEU2*
K20339	*MATa, scc4Δ::HIS3, leu2::scc4(Y40N)-myc$_{18}$::LEU2*
K20340	*MATa. scc4Δ::HIS3, leu2::scc4(Y40H)-myc$_{18}$::LEU2*
K20341	*MATa, scc4Δ::HIS3, leu2::scc4(Y40A)-myc$_{18}$::LEU2*
K20350	*MATα, scc4Δ::HIS3, SCC2-HA$_6$::HIS3, leu2::SCC4-myc$_{18}$::LEU2*
K20351	*MATα, scc4Δ::HIS3, SCC2-HA$_6$::HIS3, leu2::scc4(Y40N)-myc$_{18}$::LEU2*
K20352	*MATα, scc4Δ::HIS3, SCC2-HA$_6$::HIS3, leu2::scc4(Y40H)-myc$_{18}$::LEU2*
K20353	*MATa, scc4Δ::HIS3, SCC2-HA$_6$::HIS3, leu2::scc4(Y40A)-myc$_{18}$::LEU2*
K20904	*MATa, scc4Δ::HIS3, smc1Δ::KanMX4, trp1::SMC1::TRP1*
K20909	*MATa, smc1::KanMX4, trp1::smc1(D588F)::TRP1*
K20995	*MATa/α, SMC1/smc1Δ::KanMX4, SMC3/smc3Δ::HphNT1, SCC4/scc4Δ::HIS3, trp1/ trp1::SMC1::TRP1, leu2/leu2::SMC3::LEU2*
K20996	*MATa/α, SMC1/smc1Δ::KanMX4, SMC3/smc3Δ::HphNT1, SCC4/scc4Δ::HIS3, trp1/ trp1::SMC1::TRP1, leu2/leu2::smc3(K652V)::LEU2*
K20997	*MATa/α, SMC1/smc1Δ::KanMX4, SMC3/smc3Δ::HphNT1, SCC4/scc4Δ::HIS3, trp1/ trp1::SMC1::TRP1, leu2/leu2::smc3(K652A)::LEU2*
K20998	*MATa/α, SMC1/smc1Δ::KanMX4, SMC3/smc3Δ::HphNT1, SCC4/scc4Δ::HIS3, trp1/ trp1::SMC1::TRP1, leu2/leu2::smc3(K652Y)::LEU2*
K20999	*MATa/α, SMC1/smc1Δ::KanMX4, SMC3/smc3Δ::HphNT1, SCC4/scc4Δ::HIS3, trp1/ trp1::smc1(D588E)::TRP1, leu2/leu2::smc3(K652V)::LEU2*
K21000	*MATa/α, SMC1/smc1Δ::KanMX4, SMC3/smc3Δ::HphNT1, SCC4/scc4Δ::HIS3, trp1/ trp1::smc1(D588E)::TRP1, leu2/leu2::smc3(K652A)::LEU2*
K21001	*MATa/α, SMC1/smc1Δ::KanMX4, SMC3/smc3Δ::HphNT1, SCC4/scc4Δ::HIS3, trp1/ trp1::smc1(D588W)::TRP1, leu2/leu2::SMC3::LEU2*
K21002	*MATa/α, SMC1/smc1Δ::KanMX4, SMC3/smc3Δ::HphNT1, SCC4/scc4Δ::HIS3, trp1/ trp1::smc1(D588W)::TRP1, leu2/leu2::smc3(K652V)::LEU2*
K21003	*MATa/α, SMC1/smc1Δ::KanMX4, SMC3/smc3Δ::HphNT1, SCC4/scc4Δ::HIS3, trp1/ trp1::smc1(D588W)::TRP1, leu2/leu2::smc3(K652A)::LEU2*
K21004	*MATa/α, SMC1/smc1Δ::KanMX4, SMC3/smc3Δ::HphNT1, SCC4/scc4Δ::HIS3, trp1/ trp1::smc1(D588F)::TRP1, leu2/leu2::smc3(K652V)::LEU2*
K21005	*MATa/α, SMC1/smc1Δ::KanMX4, SMC3/smc3Δ::HphNT1, SCC4/scc4Δ::HIS3, trp1/ trp1::smc1(D588F)::TRP1, leu2/leu2::smc3(K652A)::LEU2*
K21006	*MATa/α, SMC1/smc1Δ::KanMX4, SMC3/smc3Δ::HphNT1, SCC4/scc4Δ::HIS3, trp1/ trp1::smc1(D588F)::TRP1, leu2/leu2::smc3(K652Y)::LEU2*
K21007	*MATa/α, SMC1/smc1Δ::KanMX4, SMC3/smc3Δ::HphNT1, SCC4/scc4Δ::HIS3, trp1/ trp1::smc1(D588R)::TRP1, leu2/leu2::smc3(K652V)::LEU2*
K21008	*MATa/α, SMC1/smc1Δ::KanMX4, SMC3/smc3Δ::HphNT1, SCC4/scc4Δ::HIS3, trp1/ trp1::smc1(D588R)::TRP1, leu2/leu2::smc3(K652A)::LEU2*
K21009	*MATa, scc4Δ::HIS3, smc1Δ::KanMX4, trp1::smc1(D588W)::TRP1*
K21021	*MATa, scc4Δ::HIS3, smc1Δ::KanMX4, trp1::smc1(D588F)::TRP1*
K21027	*MATa/α, SMC1/smc1Δ::KanMX4, SMC3/smc3Δ::HphNT1, SCC4/scc4Δ::HIS3, trp1/ trp1::smc1(D588E)::TRP1, leu2/leu2::smc3(K652Y)::LEU2*
K21028	*MATa/α, SMC1/smc1Δ::KanMX4, SMC3/smc3Δ::HphNT1, SCC4/scc4Δ::HIS3, trp1/ trp1::smc1(D588W)::TRP1, leu2/leu2::smc3(K652Y)::LEU2*

K21029	*MATa/α, SMC1/smc1Δ::KanMX4, SMC3/smc3Δ::HphNT1, SCC4/scc4Δ::HIS3, trp1/trp1::smc1(D588R)::TRP1, leu2/leu2::smc3(K652Y)::LEU2*
K21030	*MATa/α, SMC1/smc1Δ::KanMX4, SMC3/smc3Δ::HphNT1, SCC4/scc4Δ::HIS3, trp1/trp1::smc1(D588N)::TRP1, leu2/leu2::SMC3::LEU2*
K21031	*MATa/α, SMC1/smc1Δ::KanMX4, SMC3/smc3Δ::HphNT1, SCC4/scc4Δ::HIS3, trp1/trp1::smc1(D588N)::TRP1, leu2/leu2::smc3(K652V)::LEU2*
K21032	*MATa/α, SMC1/smc1Δ::KanMX4, SMC3/smc3Δ::HphNT1, SCC4/scc4Δ::HIS3, trp1/trp1::smc1(D588N)::TRP1, leu2/leu2::smc3(K652A)::LEU2*
K21033	*MATa/α, SMC1/smc1Δ::KanMX4, SMC3/smc3Δ::HphNT1, SCC4/scc4Δ::HIS3, trp1/trp1::smc1(D588N)::TRP1, leu2/leu2::smc3(K652Y)::LEU2*
K21046	*MATα, smc1::KanMX4, trp1::smc1(D588Y)::TRP1*
K21058	*MATa/α, SMC1/smc1Δ::KanMX4, SMC3/smc3Δ::HphNT1, SCC4/scc4Δ::HIS3, trp1/trp1::smc1(D588E)::TRP1, leu2/leu2::smc3::LEU2*
K21059	*MATa/α, SMC1/smc1Δ::KanMX4, SMC3/smc3Δ::HphNT1, SCC4/scc4Δ::HIS3, trp1/trp1::smc1(D588R)::TRP1, leu2/leu2::smc3::LEU2*
K21118	*MATα, scc4Δ::HIS3, smc1Δ::KanMX4, trp1::smc1(D588Y)::TRP1*
K21129	*MATa/α, SMC1/smc1Δ::KanMX4, SMC3/smc3Δ::HphNT1, SCC4/scc4Δ::HIS3, trp1/trp1::smc1(D588A)::TRP1, leu2/leu2::smc3(K652V)::LEU2*
K21130	*MATa/α, SMC1/smc1Δ::KanMX4, SMC3/smc3Δ::HphNT1, SCC4/scc4Δ::HIS3, trp1/trp1::smc1(D588A)::TRP1, leu2/leu2::smc3(K652A)::LEU2*
K21136	*MATa/α, SMC1/smc1Δ::KanMX4, SMC3/smc3Δ::HphNT1, SCC4/scc4Δ::HIS3, trp1/trp1::smc1(D588Y)::TRP1, leu2/leu2::smc3(K652Y)::LEU2*
K21137	*MATa/α, SMC1/smc1Δ::KanMX4, SMC3/smc3Δ::HphNT1, SCC4/scc4Δ::HIS3, trp1/trp1::smc1(D588Y)::TRP1, leu2/leu2::smc3(K652A)::LEU2*
K21138	*MATa/α, SMC1/smc1Δ::KanMX4, SMC3/smc3Δ::HphNT1, SCC4/scc4Δ::HIS3, trp1/trp1::smc1(D588Y)::TRP1, leu2/leu2::smc3(K652V)::LEU2*
K21139	*MATa/α, SMC1/smc1Δ::KanMX4, SMC3/smc3Δ::HphNT1, SCC4/scc4Δ::HIS3, trp1/trp1::smc1(D588Y)::TRP1, leu2/leu2::SMC3::LEU2*
K21140	*MATa/α, SMC1/smc1Δ::KanMX4, SMC3/smc3Δ::HphNT1, SCC4/scc4Δ::HIS3, trp1/trp1::smc1(D588A)::TRP1, leu2/leu2::smc3(K652Y)::LEU2*
K21141	*MATa/α, SMC1/smc1Δ::KanMX4, SMC3/smc3Δ::HphNT1, SCC4/scc4Δ::HIS3, trp1/trp1::smc1(D588H)::TRP1, leu2/leu2::smc3(K652Y)::LEU2*
K21142	*MATa/α, SMC1/smc1Δ::KanMX4, SMC3/smc3Δ::HphNT1, SCC4/scc4Δ::HIS3, trp1/trp1::smc1(D588H)::TRP1, leu2/leu2::smc3(K652A)::LEU2*
K21143	*MATa/α, SMC1/smc1Δ::KanMX4, SMC3/smc3Δ::HphNT1, SCC4/scc4Δ::HIS3, trp1/trp1::smc1(D588H)::TRP1, leu2/leu2::smc3(K652V)::LEU2*
K21144	*MATa/α, SMC1/smc1Δ::KanMX4, SMC3/smc3Δ::HphNT1, SCC4/scc4Δ::HIS3, trp1/trp1::smc1(D588H)::TRP1, leu2/leu2::SMC3::LEU2*
K21418	*MATa/α, smc1(D588Y)::HphNT1/smc1(D588Y)::HphNT1*
K21419	*MATa/α, smc1(D588Y)::HphNT1/smc1(D588Y)::HphNT1, scc4Δ::HIS3/scc4Δ::HIS3*
K21468	*MATa, leu2::tetR-GFP:LEU2, ura3::3xURA3tetO112, MET3-CDC20::NatMX4, smc1Δ::KanMX4, trp1::SMC1::TRP1*
K21474	*MATa, leu2::tetR-GFP:LEU2, ura3::3xURA3tetO112, MET3-CDC20::NatMX4, smc1Δ::KanMX4, trp1::smc1(D588F)::TRP1*
K21476	*MATa, leu2::tetR-GFP:LEU2, ura3::3xURA3tetO112, MET3-CDC20::NatMX4, smc1Δ::KanMX4, trp1:: smc1(D588F)::TRP1*
K21478	*MATa, leu2::tetR-GFP:LEU2, ura3::3xURA3tetO112, MET3-CDC20::NatMX4, smc1Δ::KanMX4, trp1::smc1(D588Y)::TRP1*
K21480	*MATa, leu2::tetR-GFP:LEU2, ura3::3xURA3tetO112, MET3-CDC20::NatMX4, smc1Δ::KanMX4, trp1::smc1(D588Y)::TRP1, scc4Δ::HIS3*
K21483	*MATα, CFIII (CEN3.L.YPH278) URA3 SUP11, smc1Δ:KanMX4, trp1::SMC1::TRP1*
K21485	*MATα, CFIII (CEN3.L.YPH278) URA3 SUP11, smc1Δ:KanMX4, trp1::smc1(D588W)::TRP1*

K21487	*MATα, CFIII (CEN3.L.YPH278) URA3 SUP11, smc1Δ:KanMX4, trp1::smc1(D588W)::TRP1, scc4Δ:HIS3*
K21489	*MATα, CFIII (CEN3.L.YPH278) URA3 SUP11, smc1Δ:KanMX4, trp1::smc1(D588F)::TRP1*
K21491	*MATα, CFIII (CEN3.L.YPH278) URA3 SUP11, smc1Δ:KanMX4, trp1::smc1(D588F)::TRP1, scc4Δ:HIS3*
K21492	*MATα, CFIII (CEN3.L.YPH278) URA3 SUP11, smc1Δ:KanMX4, trp1::smc1(D588Y)::TRP1*
K21494	*MATα, CFIII (CEN3.L.YPH278) URA3 SUP11, smc1Δ:KanMX4, trp1::smc1(D588Y)::TRP1, scc4Δ:HIS3*
K21597	*MATa/α, scc4Δ::HIS3/scc4Δ::HIS3, smc1(D588Y)::HphNT1/ smc1(D588Y)::HphNT1, scc2(N77-T1493)::NatMX4/SCC2*
K21598	*MATa/α, scc2(N77-T1493)::NatMX4/SCC2*
K21599	*MATa/α, scc4Δ::HIS3/scc4Δ::HIS3, smc1(D588Y)::HphNT1/ smc1(D588Y)::HphNT1, SCC2::NatMX4/SCC2*
K21600	*MATa/α, SCC2::NatMX4/SCC2*
K21630	*MATa/α, scc4Δ::HIS3/scc4Δ::HIS3, smc1(D588Y)::HphNT1/ smc1(D588Y)::HphNT1, scc2(S750-T1493)::NatMX4/SCC2*
K21631	*MATa/α, scc2(S750-T1493)::NatMX4/SCC2*
K21632	*MATa/α, scc4Δ::HIS3/scc4Δ::HIS3, smc1(D588Y)::HphNT1/ smc1(D588Y)::HphNT1, scc2(L301-T1493)::NatMX4/SCC2*
K21633	*MATa/α, scc2(L301-T1493)::NatMX4/SCC2*
K21973	*MATa/α, SCC4/scc4Δ::HIS3, SMC1/smc1::KanMX4, trp1/trp1::SMC1::TRP1*
K21974	*MATa/α, SCC4/scc4Δ::HIS3, SMC1/smc1::KanMX4, trp1/trp1::smc1(D588Y)::TRP1*
K21988	*MATa, SMC3-myc$_{18}$::URA3, ADE+*
K21989	*MATa, scc4Δ::HIS3, leu2::scc4-4::LEU2, SMC3-myc$_{18}$::URA3, ADE+*
K21990	*MATa/α, SCC4/scc4Δ::HIS3, SMC1/smc1Δ::KanMX4, trp1/ trp1::smc1(D588F)::TRP1*
K22011	*MATα, smc1Δ::KanMX4, trp1::smc1(D588W)::TRP1*
K22012	*MATa/α, SCC4/scc4Δ::HIS3, SMC1/smc1Δ::KanMX4, trp1/ trp1::smc1(D588W)::TRP1*
K22021	*MATa, scc4Δ::HIS3, leu2::scc4-4::LEU2, SMC3-myc$_{18}$::URA3, smc1(D588Y)::HphNT1, ADE+*
K22055	*MATa/α, scc4Δ::HIS3, smc1(D588Y)::HphNT1, SCC2-GFP::KanMX4, MTW1-RFP::KanMX4, ADE+*
K22057	*MATa/α, smc1(D588Y)::HphNT1, SCC2-GFP::KanMX4, MTW1-RFP::KanMX4, ADE+*
K22133	*MATa. scc2::NatMX4, YCplac33 SCC2, YCplac111 SCC2*
K22134	*MATa, scc2::NatMX4, YCplac33 SCC2, YCplac111 SCC2*
K22135	*MATa, scc2::NatMX4, YCplac33 SCC2, YCplac111*
K22136	*MATa, scc2::NatMX4, YCplac33 SCC2, YCplac111*
K22137	*MATa, scc2::NatMX4, YCplac33 SCC2, YCplac111 scc2(D468A)*
K22138	*MATa, scc2::NatMX4, YCplac33 SCC2, YCplac111 scc2(D468A)*

References

Akiyoshi, B., Sarangapani, K.K., Powers, A.F., Nelson, C.R., Reichow, S.L., Arellano-Santoyo, H., Gonen, T., Ranish, J.A., Asbury, C.L., and Biggins, S. (2010). Tension directly stabilizes reconstituted kinetochore-microtubule attachments. Nature *468*, 576–579.

Alani, E., Subbiah, S., and Kleckner, N. (1989). The yeast RAD50 gene encodes a predicted 153-kD protein containing a purine nucleotide-binding domain and two large heptad-repeat regions. Genetics *122*, 47–57.

Almedawar, S., Colomina, N., Bermúdez-López, M., Pociño-Merino, I., and Torres-Rosell, J. (2012). A SUMO-dependent step during establishment of sister chromatid cohesion. Curr. Biol. *22*, 1576-1581.

Anderson, D.E., Losada, A., Erickson, H.P., and Hirano, T. (2002). Condensin and cohesin display different arm conformations with characteristic hinge angles. J. Cell Biol. *156*, 419–424.

Andrade, M.A., and Bork, P. (1995). HEAT repeats in the Huntington's disease protein. Nat. Genet. *11*, 115–116.

Aristotle (343BC). Book V: The History of Animals. Translated by D'Arcy Wentworth Thompson (Clarendon Press).

Arnold, K., Bordoli, L., Kopp, J., and Schwede, T. (2006). The SWISS-MODEL workspace: a web-based environment for protein structure homology modelling. Bioinformatics *22*, 195–201.

Arumugam, P., Gruber, S., Tanaka, K., Haering, C.H., Mechtler, K., and Nasmyth, K. (2003). ATP hydrolysis is required for cohesin's association with chromosomes. Curr. Biol. *13*, 1941–1953.

Arumugam, P., Nishino, T., Haering, C.H., Gruber, S., and Nasmyth, K. (2006). Cohesin's ATPase activity is stimulated by the C-terminal Winged-Helix domain of its kleisin subunit. Curr. Biol. *16*, 1998–2008.

Bailis, J.M., Bernard, P., Antonelli, R., Allshire, R.C., and Forsburg, S.L. (2003). Hsk1-Dfp1 is required for heterochromatin-mediated cohesion at centromeres. Nat. Cell Biol. *5*, 1111–1116.

Barlow, D.J., and Thornton, J.M. (1983). Ion-pairs in proteins. J. Mol. Biol. *168*, 867–885.

Beckouët, F., Hu, B., Roig, M.B., Sutani, T., Komata, M., Uluocak, P., Katis, V.L., Shirahige, K., and Nasmyth, K. (2010). An Smc3 acetylation cycle is essential for establishment of sister chromatid cohesion. Mol. Cell *39*, 689–699.

Bermudez, V.P., Farina, A., Higashi, T.L., Du, F., Tappin, I., Takahashi, T.S., and Hurwitz, J. (2012). In vitro loading of human cohesin on DNA by the human Scc2-Scc4 loader complex. Proc. Natl. Acad. Sci. U.S.A. *109*, 9366–9371.

Bernard, P., Drogat, J., Maure, J.-F., Dheur, S., Vaur, S., Genier, S., and Javerzat, J.-P. (2006). A screen for cohesion mutants uncovers Ssl3, the fission yeast counterpart of the cohesin loading factor Scc4. Curr. Biol. *16*, 875–881.

Bhat, M.A., Philp, A.V., Glover, D.M., and Bellen, H.J. (1996). Chromatid segregation at anaphase requires the barren product, a novel chromosome-associated protein that interacts with Topoisomerase II. Cell *80*, 1103-1114.

Birkenbihl, R.P., and Subramani, S. (1992). Cloning and characterization of rad21 an essential gene of Schizosaccharomyces pombe involved in DNA double-strand-break repair. Nucleic Acids Res. *20*, 6605–6611.

Blat, Y., and Kleckner, N. (1999). Cohesins bind to preferential sites along yeast chromosome III, with differential regulation along arms versus the centric region. Cell *98*, 249–259.

Blatch, G.L., and Lässle, M. (1999). The tetratricopeptide repeat: a structural motif mediating protein-protein interactions. Bioessays *21*, 932–939.

Boeke, J.D., Croute, F., and Fink, G.R. (1984). A positive selection for mutants lacking orotidine-5'-phosphate decarboxylase activity in yeast: 5-fluoro-orotic acid resistance. Mol. Gen. Genet. *197*, 345–346.

Borges, V., Lehane, C., Lopez-Serra, L., Flynn, H., Skehel, M., Rolef Ben-Shahar, T., and Uhlmann, F. (2010). Hos1 deacetylates Smc3 to close the cohesin acetylation cycle. Mol. Cell *39*, 677–688.

Bradford, M.M. (1976). A rapid and sensitive method for the quantitation of microgram quantities of protein utilizing the principle of protein-dye binding. Anal. Biochem. *72*, 248-254.

Braunholz, D., Hullings, M., Gil-Rodríguez, M.C., Fincher, C.T., Mallozzi, M.B., Loy, E., Albrecht, M., Kaur, M., Limon, J., Rampuria, A., Clark, D., Kline, A., Daiski, A., Eckhold, J., Tzschach, A., Hennekam, R., Gillessen-Kaesbach, G., Wierzba, J., Krantz, D., Deardorff, M.A., and Kaiser, F.J. (2012). Isolated NIBPL missense mutations that cause Cornelia de Lange syndrome alter MAU2 interaction. Eur. J. Hum. Genet. *20*, 271–276.

Buheitel, J., and Stemmann, O. (2013). Prophase pathway-dependent removal of cohesin from human chromosomes requires opening of the Smc3-Scc1 gate. EMBO J. *32*, 666–676.

Bücking-Throm, E., Duntze, W., Hartwell, L.H., and Manney, T.R. (1973). Reversible arrest of haploid yeast cells in the initiation of DNA synthesis by a diffusible sex factor. Exp. Cell Res. *76*, 99–110.

Bürmann, F., Shin, H.-C., Basquin, J., Soh, Y.-M., Giménez-Oya, V., Kim, Y.-G., Oh, B.-H., and Gruber, S. (2013). An asymmetric SMC-kleisin bridge in prokaryotic condensin. Nat. Struct. Mol. Biol. *20*, 371–379.

Carlson, R.D., Olins, A.L., and Olins, D.E. (1975). Urea denaturation of chromatin periodic structure. Biochemistry *14*, 3122-3125.

Chan, K.-L., Roig, M.B., Hu, B., Beckouët, F., Metson, J., and Nasmyth, K. (2012). Cohesin's DNA Exit Gate Is Distinct from Its Entrance Gate and Is Regulated by Acetylation. Cell *150*, 961–974.

Chen, H.-T., Warfield, L., and Hahn, S. (2007). The positions of TFIIF and TFIIE in the RNA polymerase II transcription preinitiation complex. Nat. Struct. Mol. Biol. *14*, 696–703.

Chin, J.W., Cropp, T.A., Anderson, J.C., Mukherji, M., Zhang, Z., and Schultz, P.G. (2003). An expanded eukaryotic genetic code. Science *301*, 964–967.

Chiu, A., Revenkova, E., and Jessberger, R. (2004). DNA interaction and dimerization of eukaryotic SMC hinge domains. J. Biol. Chem. *279*, 26233–26242.

Ciosk, R., Shirayama, M., Shevchenko, A., Tanaka, T., Tóth, A., Shevchenko, A., and Nasmyth, K. (2000). Cohesin's binding to chromosomes depends on a separate complex consisting of Scc2 and Scc4 proteins. Mol. Cell *5*, 243–254.

Cobbe, N., and Heck, M.M.S. (2006). The evolution of ATPase activity in SMC proteins. Proteins *63*, 685–696.

Cooper, G.M. (2000). The Cell: A Molecular Approach (Sunderland (MA): ASM Press).

Cromie, G.A., Connelly, J.C., and Leach, D.R. (2001). Recombination at double-strand breaks and DNA ends: conserved mechanisms from phage to humans. Mol. Cell *8*, 1163–1174.

Cuylen, S., Metz, J., and Haering, C.H. (2011). Condensin structures chromosomal DNA through topological links. Nat. Struct. Mol. Biol. *18*, 894–901.

D'Ambrosio, C., Schmidt, C.K., Katou, Y., Kelly, G., Itoh, T., Shirahige, K., and Uhlmann, F. (2008). Identification of cis-acting sites for condensin loading onto budding yeast chromosomes. Genes Dev. *22*, 2215–2227.

D'Andrea, L.D., and Regan, L. (2003). TPR proteins: the versatile helix. Trends Biochem. Sci. *28*, 655–662.

Das, A.K., Cohen, P.W., Barford, D. (1998). The structure of the tetratricopeptide repeats of protein phosphatase 5: implications for TPR-mediated protein-protein interactions. EMBO J. *17*, 1192–1199.

Deardorff, M.A., Kaur, M., Yaeger, D., Rampuria, A., Korolev, S., Pié, J., Gil-Rodríguez, C., Arnedo, M., Loeys, B., Kline, A.D., Wilson, M., Lillquist, K., Siu, V., Ramos, F.J., Musio, A., Jackson, L.S., Dorsett, D., and Krantz, I.D. (2007). Mutations in cohesin complex members SMC3 and SMC1A cause a mild variant of Cornelia de Lange Syndrome with predominant mental retardation. Am. J. Hum. Genet. *80*, 485–494.

DiNardo, S., Voelkel, K., and Sternglanz, R. (1984). DNA topoisomerase II mutant of Saccharomyces cerevisiae: topoisomerase II is required for segregation of daughter molecules at the termination of DNA replication. Proc. Natl. Acad. Sci. U.S.A. *81*, 2616–2620.

Dormán, G., and Prestwich, G.D. (1994). Benzophenone photophores in biochemistry. Biochemistry *33*, 5661–5673.

Dorsett, D., and Krantz, I.D. (2009). On the molecular etiology of Cornelia de Lange syndrome. Ann. N. Y. Acad. Sci. *1151*, 22–37.

Eckert, C.A., Gravdahl, D.J., and Megee, P.C. (2007). The enhancement of pericentromeric cohesin association by conserved kinetochore components promotes high-fidelity chromosome segregation and is sensitive to microtubule-based tension. Genes Dev. *21*, 278–291.

Eichinger, C.S., Kurze, A., Oliveira, R.A., and Nasmyth, K. (2013). Disengaging the Smc3/kleisin interface releases cohesin from Drosophila chromosomes during interphase and mitosis. EMBO J. *32*, 656–665.

Evans, T., Rosenthal, E.T., Youngblom, J., Distel, D., and Hunt, T. (1983). Cyclin: a protein specified by maternal mRNA in sea urchin eggs that is destroyed at each cleavage division. Cell *33*, 389–396.

Farcas, A.-M., Uluocak, P., Helmhart, W., and Nasmyth, K. (2011). Cohesin's concatenation of sister DNAs maintains their intertwining. Mol. Cell *44*, 97–107.

Fernius, J., and Marston, A.L. (2009). Establishment of cohesion at the pericentromere by the Ctf19 kinetochore subcomplex and the replication fork-associated factor, Csm3. PLoS Genet. *5*, e1000629.

Fernius, J., Nerusheva, O.O., Galander, S., Alves, F. de L., Rappsilber, J., and Marston, A.L. (2013). Cohesin-dependent association of Scc2/4 with the centromere initiates pericentromeric cohesion establishment. Curr. Biol. *23*, 599-606.

Feytout, A., Vaur, S., Genier, S., Vazquez, S., and Javerzat, J.-P. (2011). Psm3 acetylation on conserved lysine residues is dispensable for viability in fission yeast but contributes to Eso1-mediated sister chromatid cohesion by antagonizing Wpl1. Mol. Cell. Biol. *31*, 1771–1786.

Furuya, K., Takahashi, K., and Yanagida, M. (1998). Faithful anaphase is ensured by Mis4, a sister chromatid cohesion molecule required in S phase and not destroyed in G1 phase. Genes Dev. *12*, 3408–3418.

Gandhi, R., Gillespie, P.J., and Hirano, T. (2006). Human Wapl is a cohesin-binding protein that promotes sister-chromatid resolution in mitotic prophase. Curr. Biol. *16*, 2406–2417.

Gasteiger, E., Hoogland, C., Gattiker, A., Duvaud, S., Wilkins, M.R., Appel, R.D., and Bairoch, A. (2005). Protein Identification and Analysis Tools on the ExPASy Server. (Totowa, NJ: Humana Press), pp. 571–607.

Gaudet, R., and Wiley, D.C. (2001). Structure of the ABC ATPase domain of human TAP1, the transporter associated with antigen processing. EMBO J. *20*, 4964–4972.

Gerlich, D., Koch, B., Dupeux, F., Peters, J.-M., and Ellenberg, J. (2006). Live-cell imaging reveals a stable cohesin-chromatin interaction after but not before DNA replication. Curr. Biol. *16*, 1571–1578.

Gillespie, P.J., and Hirano, T. (2004). Scc2 couples replication licensing to sister chromatid cohesion in Xenopus egg extracts. Curr. Biol. *14*, 1598–1603.

Glynn, E.F., Megee, P.C., Yu, H.-G., Mistrot, C., Ünal, E., Koshland, D.E., DeRisi, J.L., and Gerton, J.L. (2004). Genome-wide mapping of the cohesin complex in the yeast Saccharomyces cerevisiae. PLoS Biol. *2*, E259.

Griese, J.J., Witte, G., and Hopfner, K.-P. (2010). Structure and DNA binding activity of the mouse condensin hinge domain highlight common and diverse features of SMC proteins. Nucleic Acids Res. *38*, 3454–3465.

Grigoryev, S.A., and Woodcock, C.L. (2012). Chromatin organization - the 30 nm fiber. Exp. Cell Res. *318*, 1448–1455.

Groves, M.R., Hanlon, N., Turowski, P., Hemmings, B.A., Barford, D. (1999). The structure of the protein phosphatase 2A PR65/A subunit reveals the conformation of its 15 tandemly repeated HEAT motifs. Cell *96*, 99–110.

Gruber, S., Arumugam, P., Katou, Y., Kuglitsch, D., Helmhart, W., Shirahige, K., and Nasmyth, K. (2006). Evidence that loading of cohesin onto chromosomes involves opening of its SMC hinge. Cell *127*, 523–537.

Gruber, S., Haering, C.H., and Nasmyth, K. (2003). Chromosomal cohesin forms a ring. Cell *112*, 765–777.

Guacci, V., Koshland, D., and Strunnikov, A. (1997). A direct link between sister chromatid cohesion and chromosome condensation revealed through the analysis of MCD1 in S. cerevisiae. Cell *91*, 47–57.

Haering, C.H., Farcas, A.-M., Arumugam, P., Metson, J., and Nasmyth, K. (2008). The cohesin ring concatenates sister DNA molecules. Nature *454*, 297–301.

Haering, C.H., Löwe, J., Hochwagen, A., and Nasmyth, K. (2002). Molecular architecture of SMC proteins and the yeast cohesin complex. Mol. Cell *9*, 773–788.

Haering, C.H., Schoffnegger, D., Nishino, T., Helmhart, W., Nasmyth, K., and Löwe, J. (2004). Structure and stability of cohesin's Smc1-kleisin interaction. Mol. Cell *15*, 951–964.

Hartwell, L.H., Mortimer, R.K., Culotti, J., and Culotti, M. (1973). Genetic control of the cell division cycle in yeast: V. Genetic analysis of cdc mutants. Genetics *74*, 267–286.

Hayashi, M.T., Takahashi, T.S., Nakagawa, T., Nakayama, J.-I., and Masukata, H. (2009). The heterochromatin protein Swi6/HP1 activates replication origins at the pericentromeric region and silent mating-type locus. Nat. Cell Biol. *11*, 357–362.

Hieter, P., Mann, C., Snyder, M., and Davis, R.W. (1985). Mitotic stability of yeast chromosomes: a colony color assay that measures nondisjunction and chromosome loss. Cell *40*, 381–392.

Hirano, M., and Hirano, T. (2002). Hinge-mediated dimerization of SMC protein is essential for its dynamic interaction with DNA. EMBO J. *21*, 5733–5744.

Hirano, M., and Hirano, T. (2006). Opening Closed Arms: Long-Distance Activation of SMC ATPase by Hinge-DNA Interactions. Mol. Cell *21*, 175-186.

Hirano, T. (2005). Condensins: Organizing and Segregating the Genome. Curr. Biol. *15*, R265–R275.

Hirano, T. (2006). At the heart of the chromosome: SMC proteins in action. Nat. Rev. Mol. Cell Biol. *7*, 311–322.

Hodges, C.A., Revenkova, E., Jessberger, R., Hassold, T.J., and Hunt, P.A. (2005). SMC1β-deficient female mice provide evidence that cohesins are a missing link in age-related nondisjunction. Nat Genet *37*, 1351–1355.

Hooke, R. (1665). Micrographia (London: J. Martyn and J. Allestry).

Hopfner, K.P., Karcher, A., Shin, D.S., Craig, L., Arthur, L.M., Carney, J.P., and Tainer, J.A. (2000). Structural biology of Rad50 ATPase: ATP-driven conformational control in DNA double-strand break repair and the ABC-ATPase superfamily. Cell *101*, 789–800.

Hopfner, K.-P., Craig, L., Moncalian, G., Zinkel, R.A., Usui, T., Owen, B.A.L., Karcher, A., Henderson, B., Bodmer, J.-L., McMurray, C.T., Carney, J.P., Petrini, J.H., and Tainer, J.A. (2002). The Rad50 zinc-hook is a structure joining Mre11 complexes in DNA recombination and repair. Nature *418*, 562–566.

Hu, B., Itoh, T., Mishra, A., Katoh, Y., Chan, K.-L., Upcher, W., Godlee, C., Roig, M.B., Shirahige, K., and Nasmyth, K. (2011). ATP hydrolysis is required for relocating cohesin from sites occupied by its Scc2/4 loading complex. Curr. Biol. *21*, 12–24.

Ivanov, D., and Nasmyth, K. (2005). A topological interaction between cohesin rings and a circular minichromosome. Cell *122*, 849–860.

Ivanov, D., Schleiffer, A., Eisenhaber, F., Mechtler, K., Haering, C.H., and Nasmyth, K. (2002). Eco1 is a novel acetyltransferase that can acetylate proteins involved in cohesion. Curr. Biol. *12*, 323–328.

Jessberger, R., Podust, V., Hübscher, U., and Berg, P. (1993). A mammalian protein complex that repairs double-strand breaks and deletions by recombination. J. Biol. Chem. *268*, 15070–15079.

Jessberger, R., Riwar, B., Baechtold, H., and Akhmedov, A.T. (1996). SMC proteins constitute two subunits of the mammalian recombination complex RC-1. EMBO J. *15*, 4061–4068.

Jessberger, R. (2002). The many functions of SMC proteins in chromosome dynamics. Nat. Rev. Mol. Cell Biol. *3*, 767–778.

Jones, P.M., and George, A.M. (2002). Mechanism of ABC transporters: a molecular dynamics simulation of a well characterized nucleotide-binding subunit. Proc. Natl. Acad. Sci. U.S.A. *99*, 12639–12644.

Jones, S., and Sgouros, J. (2001). The cohesin complex: sequence homologies, interaction networks and shared motifs. Genome Biol. *2*, RESEARCH0009.

Kiburz, B.M., Reynolds, D.B., Megee, P.C., Marston, A.L., Lee, B.H., Lee, T.I., Levine, S.S., Young, R.A., and Amon, A. (2005). The core centromere and Sgo1 establish a 50-kb cohesin-protected domain around centromeres during meiosis I. Genes Dev. *19*, 3017–3030.

Klein, F., Mahr, P., Galova, M., Buonomo, S.B., Michaelis, C., Nairz, K., and Nasmyth, K. (1999). A central role for cohesins in sister chromatid cohesion, formation of axial elements, and recombination during yeast meiosis. Cell *98*, 91–103.

Krantz, I.D., McCallum, J., DeScipio, C., Kaur, M., Gillis, L.A., Yaeger, D., Jukofsky, L., Wasserman, N., Bottani, A., Morris, C.A., Nowaczyk, M.J., Toriello, H., Bamshad, M.J., Carey, J.C., Rappaport, E., Kawauchi, S., Lander, A.D., Calof, A.L., Li, H.H., Devoto, M., and Jackson, L.G. (2004). Cornelia de Lange syndrome is caused by mutations in NIPBL, the human homolog of Drosophila melanogaster Nipped-B. Nat. Genet. *36*, 631–635.

Ku, B., Lim, J.-H., Shin, H.-C., Shin, S.-Y., and Oh, B.-H. (2010). Crystal structure of the MukB hinge domain with coiled-coil stretches and its functional implications. Proteins *78*, 1483–1490.

Kueng, S., Hegemann, B., Peters, B.H., Lipp, J.J., Schleiffer, A., Mechtler, K., and Peters, J.-M. (2006). Wapl controls the dynamic association of cohesin with chromatin. Cell *127*, 955–967.

Kurze, A., Michie, K.A., Dixon, S., Mishra, A., Itoh, T., Khalid, S., Strmecki, L., Shirahige, K., Haering, C.H., Löwe, J., and Nasmyth, K. (2011). A positively charged channel within the Smc1/Smc3 hinge required for sister chromatid cohesion. EMBO J. *30*, 364–378.

Laloraya, S., Guacci, V., and Koshland, D. (2000). Chromosomal addresses of the cohesin component Mcd1p. J. Cell Biol. *151*, 1047–1056.

Lengronne, A., Katou, Y., Mori, S., Yokobayashi, S., Kelly, G.P., Itoh, T., Watanabe, Y., Shirahige, K., and Uhlmann, F. (2004). Cohesin relocation from sites of chromosomal loading to places of convergent transcription. Nature *430*, 573–578.

Lengronne, A., McIntyre, J., Katou, Y., Kanoh, Y., Hopfner, K.-P., Shirahige, K., and Uhlmann, F. (2006). Establishment of sister chromatid cohesion at the S. cerevisiae replication fork. Molecular Cell *23*, 787–799.

Li, Y., Schoeffler, A.J., Berger, J.M., and Oakley, M.G. (2010). The crystal structure of the hinge domain of the Escherichia coli structural maintenance of chromosomes protein MukB. J. Mol. Biol. *395*, 11–19.

Lindroos, H.B., Ström, L., Itoh, T., Katou, Y., Shirahige, K., and Sjögren, C. (2006). Chromosomal association of the Smc5/6 complex reveals that it functions in differently regulated pathways. Mol. Cell *22*, 755–767.

Liu, D., Vader, G., Vromans, M.J.M., Lampson, M.A., and Lens, S.M.A. (2009). Sensing chromosome bi-orientation by spatial separation of aurora B kinase from kinetochore substrates. Science *323*, 1350–1353.

Losada, A., Hirano, M., and Hirano, T. (1998). Identification of Xenopus SMC protein complexes required for sister chromatid cohesion. Genes Dev. *12*, 1986–1997.

Maeshima, K., Hihara, S., and Eltsov, M. (2010). Chromatin structure: does the 30-nm fibre exist in vivo? Curr. Opin. Cell Biol.

Marsden, M.P., and Laemmli, U.K. (1979). Metaphase chromosome structure: evidence for a radial loop model. Cell *17*, 849–858.

Marston, A.L., Tham, W.-H., Shah, H., and Amon, A. (2004). A genome-wide screen identifies genes required for centromeric cohesion. Science *303*, 1367–1370.

Megee, P.C., and Koshland, D. (1999). A functional assay for centromere-associated sister chromatid cohesion. Science *285*, 254–257.

Megee, P.C., Mistrot, C., Guacci, V., and Koshland, D. (1999). The centromeric sister chromatid cohesion site directs Mcd1p binding to adjacent sequences. Mol. Cell *4*, 445–450.

Melby, T.E., Ciampaglio, C.N., Briscoe, G., and Erickson, H.P. (1998). The symmetrical structure of structural maintenance of chromosomes (SMC) and MukB proteins: long, antiparallel coiled coils, folded at a flexible hinge. J. Cell Biol. *142*, 1595–1604.

Michaelis, C., Ciosk, R., and Nasmyth, K. (1997). Cohesins: chromosomal proteins that prevent premature separation of sister chromatids. Cell *91*, 35–45.

Mishra, A., Hu, B., Kurze, A., Beckouët, F., Farcas, A.-M., Dixon, S., Katou, Y., Khalid, S., Shirahige, K., and Nasmyth, K. (2010). Both interaction surfaces within cohesin's hinge domain are essential for its stable chromosomal association. Curr. Biol. *20*, 279–289.

Misulovin, Z., Schwartz, Y.B., Li, X.-Y., Kahn, T.G., Gause, M., MacArthur, S., Fay, J.C., Eisen, M.B., Pirrotta, V., Biggin, M.D., and Dorsett, D. (2008). Association of cohesin and Nipped-B with transcriptionally active regions of the Drosophila melanogaster genome. Chromosoma *117*, 89–102.

Moldovan, G.-L., Pfander, B., and Jentsch, S. (2006). PCNA controls establishment of sister chromatid cohesion during S phase. Mol. Cell *23*, 723–732.

Morgan, D.O. (1997). Cyclin-dependent kinases: engines, clocks, and microprocessors. Annu. Rev. Cell Dev. Biol. *13*, 261–291.

Morgan, D. (2007). The Cell Cycle (New Science Press).

Musacchio, A., and Salmon, E.D. (2007). The spindle-assembly checkpoint in space and time. Nat. Rev. Mol. Cell Biol. *8*, 379–393.

Nasmyth, K., and Haering, C.H. (2009). Cohesin: its roles and mechanisms. Annu. Rev. Genet. *43*, 525–558.

Natsume, T., Müller, C.A., Katou, Y., Retkute, R., Gierliński, M., Araki, H., Blow, J.J., Shirahige, K., Nieduszynski, C.A., and Tanaka, T.U. (2013). Kinetochores coordinate pericentromeric cohesion and early DNA replication by Cdc7-Dbf4 kinase recruitment. Mol. Cell *50*, 661–674.

Neuwald, A.F., and Hirano, T. (2000). HEAT repeats associated with condensins, cohesins, and other complexes involved in chromosome-related functions. Genome Res. *10*, 1445–1452.

Ng, T.M., Waples, W.G., Lavoie, B.D., and Biggins, S. (2009). Pericentromeric sister chromatid cohesion promotes kinetochore biorientation. Mol. Biol. Cell *20*, 3818–3827.

Nigg, E.A. (2001). Mitotic kinases as regulators of cell division and its checkpoints. Nat. Rev. Mol. Cell Biol. *2*, 21–32.

Niki, H., Imamura, R., Kitaoka, M., Yamanaka, K., Ogura, T., and Hiraga, S. (1992). E.coli MukB protein involved in chromosome partition forms a homodimer with a rod-and-hinge structure having DNA binding and ATP/GTP binding activities. EMBO J. *11*, 5101–5109.

Nishino, Y., Eltsov, M., Joti, Y., Ito, K., and Takata, H. (2012). Human mitotic chromosomes consist predominantly of irregularly folded nucleosome fibres without a 30-nm chromatin structure. EMBO J. *31*, 1644-1653.

Nonaka, N., Kitajima, T., Yokobayashi, S., Xiao, G., Yamamoto, M., Grewal, S.I.S., and Watanabe, Y. (2002). Recruitment of cohesin to heterochromatic regions by Swi6/HP1 in fission yeast. Nature Cell Biology *4*, 89–93.

Novak, B., Tyson, J.J., Gyorffy, B., and Csikasz-Nagy, A. (2007). Irreversible cell-cycle transitions are due to systems-level feedback. Nat. Cell Biol. *9*, 724–728.

Nurse, P., Thuriaux, P., and Nasmyth, K. (1976). Genetic control of the cell division cycle in the fission yeast Schizosaccharomyces pombe. Mol. Gen. Genet. *146*, 167–178.

Ohsumi, K., Katagiri, C., and Kishimoto, T. (1993). Chromosome condensation in Xenopus mitotic extracts without histone H1. Science *262*, 2033–2035.

Olins, D.E., and Olins, A.L. (2003). Chromatin history: our view from the bridge. Nat. Rev. Mol. Cell Biol. *4*, 809–814.

Oliveira, R.A., Hamilton, R.S., Pauli, A., Davis, I., and Nasmyth, K. (2010). Cohesin cleavage and Cdk inhibition trigger formation of daughter nuclei. Nat. Cell Biol. *12*, 185–192.

Oudet, P., Gross-Bellard, M., and Chambon, P. (1975). Electron microscopic and biochemical evidence that chromatin structure is a repeating unit. Cell *4*, 281-300.

Panizza, S., Tanaka, T., Hochwagen, A., Eisenhaber, F., and Nasmyth, K. (2000). Pds5 cooperates with cohesin in maintaining sister chromatid cohesion. Curr. Biol. *10*, 1557–1564.

Parelho, V., Hadjur, S., Spivakov, M., Leleu, M., Sauer, S., Gregson, H.C., Jarmuz, A., Canzonetta, C., Webster, Z., Nesterova, T., Cobb, B.S., Yokomori, K., Dillon, N., Aragon, L., Fisher, A.G., and Merkenschlager, M. (2008). Cohesins functionally associate with CTCF on mammalian chromosome arms. Cell *132*, 422–433.

Peters, J.-M. (2002). The anaphase-promoting complex: proteolysis in mitosis and beyond. Mol. Cell *9*, 931–943.

Peters, J.-M., Tedeschi, A., and Schmitz, J. (2008). The cohesin complex and its roles in chromosome biology. Genes Dev. *22*, 3089–3114.

Revenkova, E., Herrmann, K., Adelfalk, C., and Jessberger, R. (2010). Oocyte cohesin expression restricted to predictyate stages provides full fertility and prevents aneuploidy. Curr. Biol. *20*, 1529–1533.

Rolef Ben-Shahar, T., Heeger, S., Lehane, C., East, P., Flynn, H., Skehel, M., and Uhlmann, F. (2008). Eco1-dependent cohesin acetylation during establishment of sister chromatid cohesion. Science *321*, 563–566.

Rowland, B.D., Roig, M.B., Nishino, T., Kurze, A., Uluocak, P., Mishra, A., Beckouët, F., Underwood, P., Metson, J., Imre, R., Mechtler, K., Katis, V.L., and Nasmyth, K. (2009). Building sister chromatid cohesion: smc3 acetylation counteracts an antiestablishment activity. Mol. Cell *33*, 763–774.

Rubio, E.D., Reiss, D.J., Welcsh, P.L., Disteche, C.M., Filippova, G.N., Baliga, N.S., Aebersold, R., Ranish, J.A., and Krumm, A. (2008). CTCF physically links cohesin to chromatin. Proc. Natl. Acad. Sci. U.S.A. *105*, 8309–8314.

Saka, Y., Sutani, T., Yamashita, Y., Saitoh, S., Takeuchi, M., Nakaseko, Y., and Yanagida, M. (1994). Fission yeast cut3 and cut14, members of a ubiquitous protein family, are required for chromosome condensation and segregation in mitosis. EMBO J. *13*, 4938–4952.

Schleiffer, A., Kaitna, S., Maurer-Stroh, S., Glotzer, M., Nasmyth, K., and Eisenhaber, F. (2003). Kleisins: a superfamily of bacterial and eukaryotic SMC protein partners. Mol. Cell *11*, 571–575.

Schueler, O., and Margalit, H. (1995). Conservation of salt bridges in protein families. J. Mol. Biol. *248*, 125–135.

Schwann, T., and Schleiden, M.J. (1847). Microscopical researches into the accordance in the structure and growth of animals and plants (London: Printed for the Sydenham Society).

Seitan, V.C., Banks, P., Laval, S., Majid, N.A., Dorsett, D., Rana, A., Smith, J., Bateman, A., Krpic, S., Hostert, A., Rollins, R.A., Erdjument-Bromage, H., Tempst, P., Bernard, C.Y., Hekimi, S., Newbury, S.F., and Strachan, T. (2006). Metazoan Scc4 homologs link sister chromatid cohesion to cell and axon migration guidance. PLoS Biol. *4*, e242.

Serebriiskii, I.G., and Golemis, E.A. (2001). Two-hybrid system and false positives: approahes to detection and elimination. In Two-Hybrid Systems, (New Jersey: Humana Press), pp. 123–134.

Sherratt, D.J. (2003). Bacterial chromosome dynamics. Science *301*, 780–785.

Sievers, F., Wilm, A., Dineen, D., Gibson, T.J., Karplus, K., Li, W., Lopez, R., McWilliam, H., Remmert, M., Söding, J., Thompson, J.D., and Higgins, D.G. (2011). Fast, scalable generation of high-quality protein multiple sequence alignments using Clustal Omega. Mol. Syst. Biol. *7*, 539.

Sigrist, C.J.A., Cerutti, L., Hulo, N., Gattiker, A., Falquet, L., Pagni, M., Bairoch, A., and Bucher, P. (2002). PROSITE: a documented database using patterns and profiles as motif descriptors. Brief. Bioinformatics *3*, 265–274.

Sjögren, C., and Nasmyth, K. (2001). Sister chromatid cohesion is required for postreplicative double-strand break repair in Saccharomyces cerevisiae. Curr. Biol. *11*, 991–995.

Smith, P.C., Karpowich, N., Millen, L., Moody, J.E., Rosen, J., Thomas, P.J., and Hunt, J.F. (2002). ATP binding to the motor domain from an ABC transporter drives formation of a nucleotide sandwich dimer. Mol. Cell *10*, 139–149.

Stedman, W., Kang, H., Lin, S., Kissil, J.L., Bartolomei, M.S., and Lieberman, P.M. (2008). Cohesins localize with CTCF at the KSHV latency control region and at cellular c-myc and H19/Igf2 insulators. EMBO J. *27*, 654–666.

Stemmann, O., Zou, H., Gerber, S.A., Gygi, S.P., and Kirschner, M.W. (2001). Dual inhibition of sister chromatid separation at metaphase. Cell *107*, 715–726.

Ström, L., and Sjögren, C. (2005). DNA damage-induced cohesion. Cell Cycle *4*, 536–539.

Ström, L., Lindroos, H.B., Shirahige, K., and Sjögren, C. (2004). Postreplicative recruitment of cohesin to double-strand breaks is required for DNA repair. Mol. Cell *16*, 1003–1015.

Strunnikov, A.V., Hogan, E., and Koshland, D. (1995). SMC2, a Saccharomyces cerevisiae gene essential for chromosome segregation and condensation, defines a subgroup within the SMC family. Genes Dev. *9*, 587–599.

Strunnikov, A.V., Larionov, V.L., and Koshland, D. (1993). SMC1: an essential yeast gene encoding a putative head-rod-tail protein is required for nuclear division and defines a new ubiquitous protein family. J. Cell Biol. *123*, 1635–1648.

Sudakin, V., Chan, G.K., and Yen, T.J. (2001). Checkpoint inhibition of the APC/C in HeLa cells is mediated by a complex of BUBR1, BUB3, CDC20, and MAD2. J. Cell Biol. *154*, 925–936.

Sumara, I., Vorlaufer, E., Gieffers, C., Peters, B.H., and Peters, J.M. (2000). Characterization of vertebrate cohesin complexes and their regulation in prophase. J. Cell Biol. *151*, 749–762.

Sumner, A.T. (1991). Scanning electron microscopy of mammalian chromosomes from prophase to telophase. Chromosoma *100*, 410–418.

Sundin, O., and Varshavsky, A. (1981). Arrest of segregation leads to accumulation of highly intertwined catenated dimers: dissection of the final stages of SV40 DNA replication. Cell *25*, 659–669.

Sutani, T., Kawaguchi, T., Kanno, R., Itoh, T., and Shirahige, K. (2009). Budding yeast Wpl1(Rad61)-Pds5 complex counteracts sister chromatid cohesion-establishing reaction. Curr. Biol. *19*, 492–497.

Tachibana-Konwalski, K., Godwin, J., van der Weyden, L., Champion, L., Kudo, N.R., Adams, D.J., and Nasmyth, K. (2010). Rec8-containing cohesin maintains bivalents without turnover during the growing phase of mouse oocytes. Genes Dev. *24*, 2505–2516.

Takahashi, T.S., Basu, A., Bermudez, V., Hurwitz, J., and Walter, J.C. (2008). Cdc7-Drf1 kinase links chromosome cohesion to the initiation of DNA replication in Xenopus egg extracts. Genes Dev. *22*, 1894–1905.

Takahashi, T.S., Yiu, P., Chou, M.F., Gygi, S., and Walter, J.C. (2004). Recruitment of Xenopus Scc2 and cohesin to chromatin requires the pre-replication complex. Nat. Cell Biol. *6*, 991–996.

Tanaka, T., Cosma, M.P., Wirth, K., and Nasmyth, K. (1999). Identification of cohesin association sites at centromeres and along chromosome arms. Cell *98*, 847–858.

Thoma, F., Koller, T., and Klug, A. (1979). Involvement of histone H1 in the organization of the nucleosome and of the salt-dependent superstructures of chromatin. J. Cell Biol. *83*, 403–427.

Tomonaga, T., Nagao, K., Kawasaki, Y., Furuya, K., Murakami, A., Morishita, J., Yuasa, T., Sutani, T., Kearsey, S.E., Uhlmann, F., Nasmyth, K., and Yanagida, M. (2000). Characterization of fission yeast cohesin: essential anaphase proteolysis of Rad21 phosphorylated in the S phase. Genes Dev. *14*, 2757–2770.

Tonkin, E.T., Wang, T.-J., Lisgo, S., Bamshad, M.J., and Strachan, T. (2004). NIPBL, encoding a homolog of fungal Scc2-type sister chromatid cohesion proteins and fly Nipped-B, is mutated in Cornelia de Lange syndrome. Nat. Genet. *36*, 636–641.

Tóth, A., Ciosk, R., Uhlmann, F., Galova, M., Schleiffer, A., and Nasmyth, K. (1999). Yeast cohesin complex requires a conserved protein, Eco1p(Ctf7), to establish cohesion between sister chromatids during DNA replication. Genes Dev. *13*, 320–333.

Uhlmann, F., and Nasmyth, K. (1998). Cohesion between sister chromatids must be established during DNA replication. Curr. Biol. *8*, 1095–1101.

Uhlmann, F., Lottspeich, F., and Nasmyth, K. (1999). Sister-chromatid separation at anaphase onset is promoted by cleavage of the cohesin subunit Scc1. Nature *400*, 37–42.

Uhlmann, F., Wernic, D., Poupart, M.A., Koonin, E.V., and Nasmyth, K. (2000). Cleavage of cohesin by the CD clan protease separin triggers anaphase in yeast. Cell *103*, 375–386.

Ünal, E., Heidinger-Pauli, J.M., Kim, W., Guacci, V., Onn, I., Gygi, S.P., and Koshland, D.E. (2008). A molecular determinant for the establishment of sister chromatid cohesion. Science *321*, 566–569.

Van Den Berg, D.J., and Francke, U. (1993). Roberts syndrome: a review of 100 cases and a new rating system for severity. Am. J. Med. Genet. *47*, 1104–1123.

Vega, H., Waisfisz, Q., Gordillo, M., Sakai, N., Yanagihara, I., Yamada, M., van Gosliga, D., Kayserili, H., Xu, C., Ozono, K., Jabs, E.W., Inui, K., and Joenje, H. (2005). Roberts syndrome is caused by mutations in ESCO2, a human homolog of yeast ECO1 that is essential for the establishment of sister chromatid cohesion. Nat. Genet. *37*, 468–470.

Verdon, G., Albers, S.V., Dijkstra, B.W., Driessen, A.J.M., and Thunnissen, A.M.W.H. (2003). Crystal structures of the ATPase subunit of the glucose ABC transporter from Sulfolobus solfataricus: nucleotide-free and nucleotide-bound conformations. J. Mol. Biol. *330*, 343–358.

Virchow, R. (1860). Cellular Pathology as Based Upon Physiological and Pathological Histology: 20 Lectures Delivered in the Pathological Institute of Berlin (New York: Robert M. De Witt).

Visintin, R., Prinz, S., and Amon, A. (1997). CDC20 and CDH1: a family of substrate-specific activators of APC-dependent proteolysis. Science *278*, 460–463.

Walker, J.E., Saraste, M., Runswick, M.J., and Gay, N.J. (1982). Distantly related sequences in the alpha- and beta-subunits of ATP synthase, myosin, kinases and other ATP-requiring enzymes and a common nucleotide binding fold. EMBO J. *1*, 945–951.

Waterhouse, A.M., Procter, J.B., Martin, D.M.A., Clamp, M., and Barton, G.J. (2009). Jalview Version 2--a multiple sequence alignment editor and analysis workbench. Bioinformatics *25*, 1189–1191.

Watrin, E., Schleiffer, A., Tanaka, K., Eisenhaber, F., Nasmyth, K., and Peters, J.-M. (2006). Human Scc4 is required for cohesin binding to chromatin, sister-chromatid cohesion, and mitotic progression. Curr. Biol. *16*, 863–874.

Weber, S.A., Gerton, J.L., Polancic, J.E., DeRisi, J.L., Koshland, D., and Megee, P.C. (2004). The kinetochore is an enhancer of pericentric cohesin binding. PLoS Biol. *2*, E260.

Weitzer, S., Lehane, C., and Uhlmann, F. (2003). A model for ATP hydrolysis-dependent binding of cohesin to DNA. Curr. Biol. *13*, 1930–1940.

Wendt, K.S., Yoshida, K., Itoh, T., Bando, M., Koch, B., Schirghuber, E., Tsutsumi, S., Nagae, G., Ishihara, K., Mishiro, T., Yahata, K., Imamoto, F., Aburatani, H., Nakao, M., Imamoto, N., Maeshima, K., Shirahige, K., and Peters, J.M. (2008). Cohesin mediates transcriptional insulation by CCCTC-binding factor. Nature *451*, 796–801.

Yeh, E., Haase, J., Paliulis, L.V., Joglekar, A., Bond, L., Bouck, D., Salmon, E.D., and Bloom, K.S. (2008). Pericentric chromatin is organized into an intramolecular loop in mitosis. Current Biology *18*, 81–90.

Yeong, F.M., Lim, H.H., Padmashree, C.G., and Surana, U. (2000). Exit from mitosis in budding yeast: biphasic inactivation of the Cdc28-Clb2 mitotic kinase and the role of Cdc20. Mol. Cell *5*, 501–511.

Zhang, J., Shi, X., Li, Y., Kim, B.-J., Jia, J., Huang, Z., Yang, T., Fu, X., Jung, S.Y., Wang, Y., Zhang, P., Kim, S.T., Pan, X., and Qin, J. (2008a). Acetylation of Smc3 by Eco1 is required for S phase sister chromatid cohesion in both human and yeast. Mol. Cell *31*, 143–151.

Zhang, N., Kuznetsov, S.G., Sharan, S.K., Li, K., Rao, P.H., and Pati, D. (2008b). A handcuff model for the cohesin complex. J. Cell Biol. *183*, 1019–1031.

APPENDIX I

ChIP-sequencing of SCC1-PK$_6$
Chromosome *II*
Experiment performed by Dr Yuki Katou

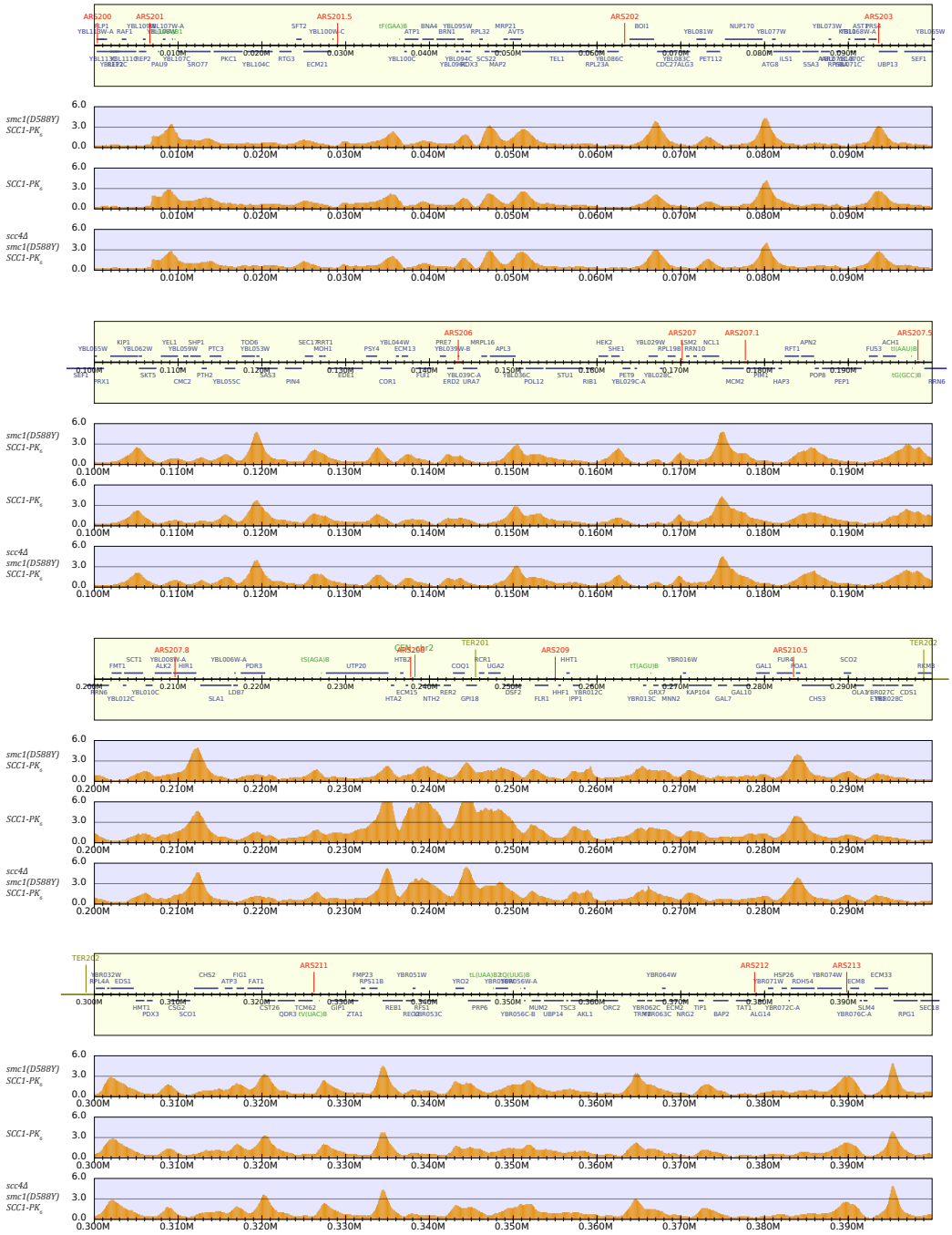

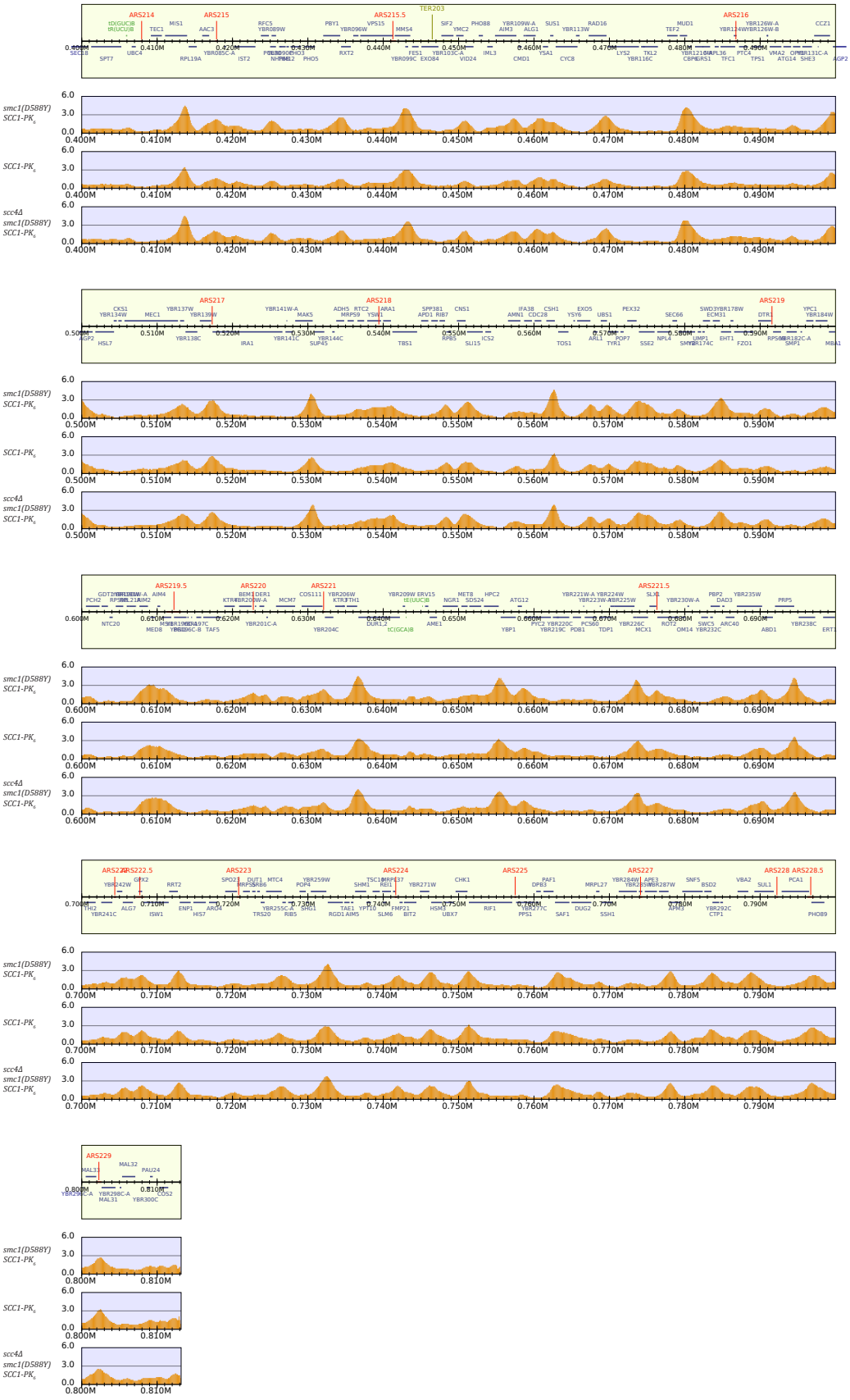
smc1(D588Y) SCC1-PK6
SCC1-PK6
scc4Δ smc1(D588Y) SCC1-PK6

APPENDIX II

ChIP-sequencing of SCC2-PK$_3$
Chromosome *II*
Experiment performed by Dr Yuki Katou

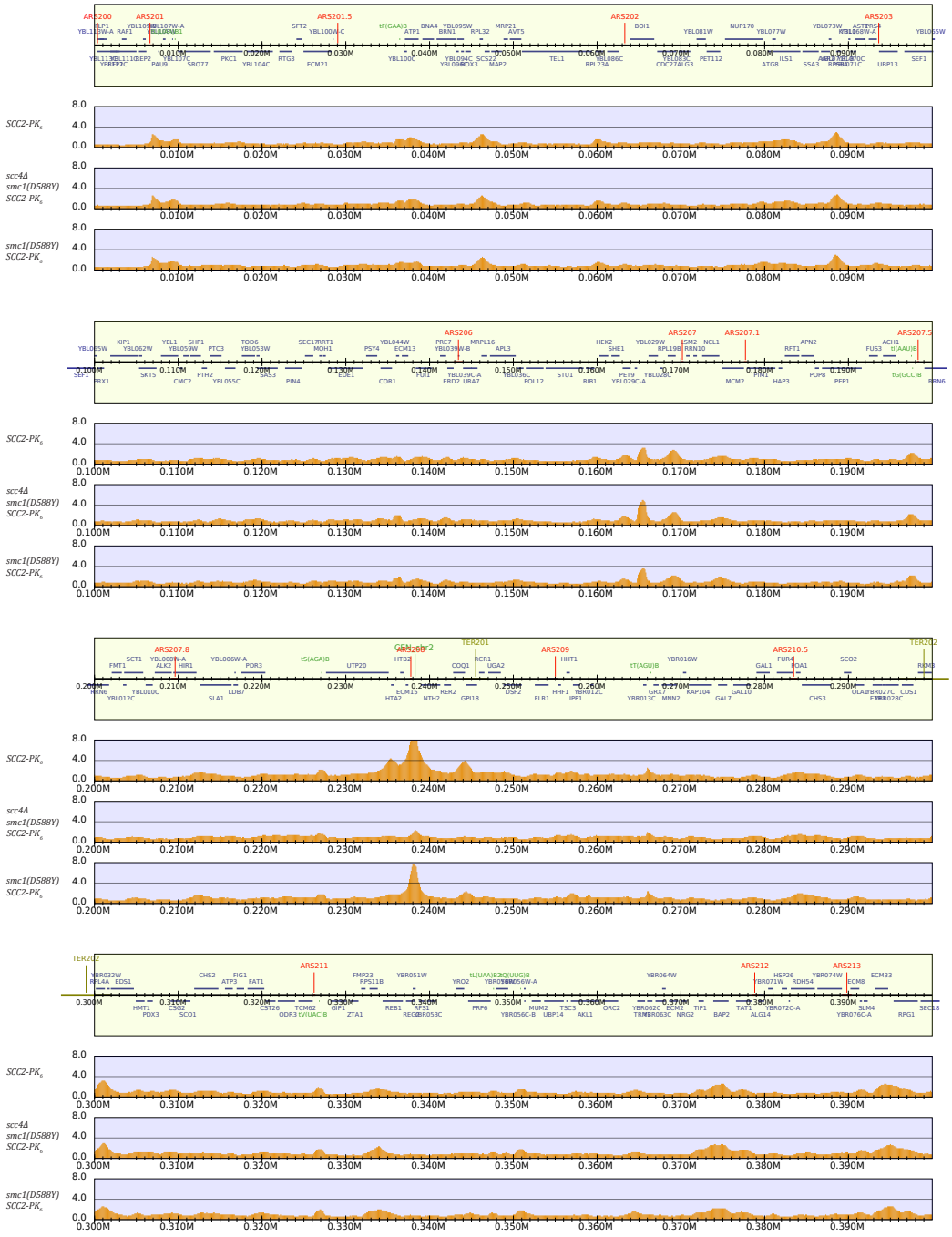

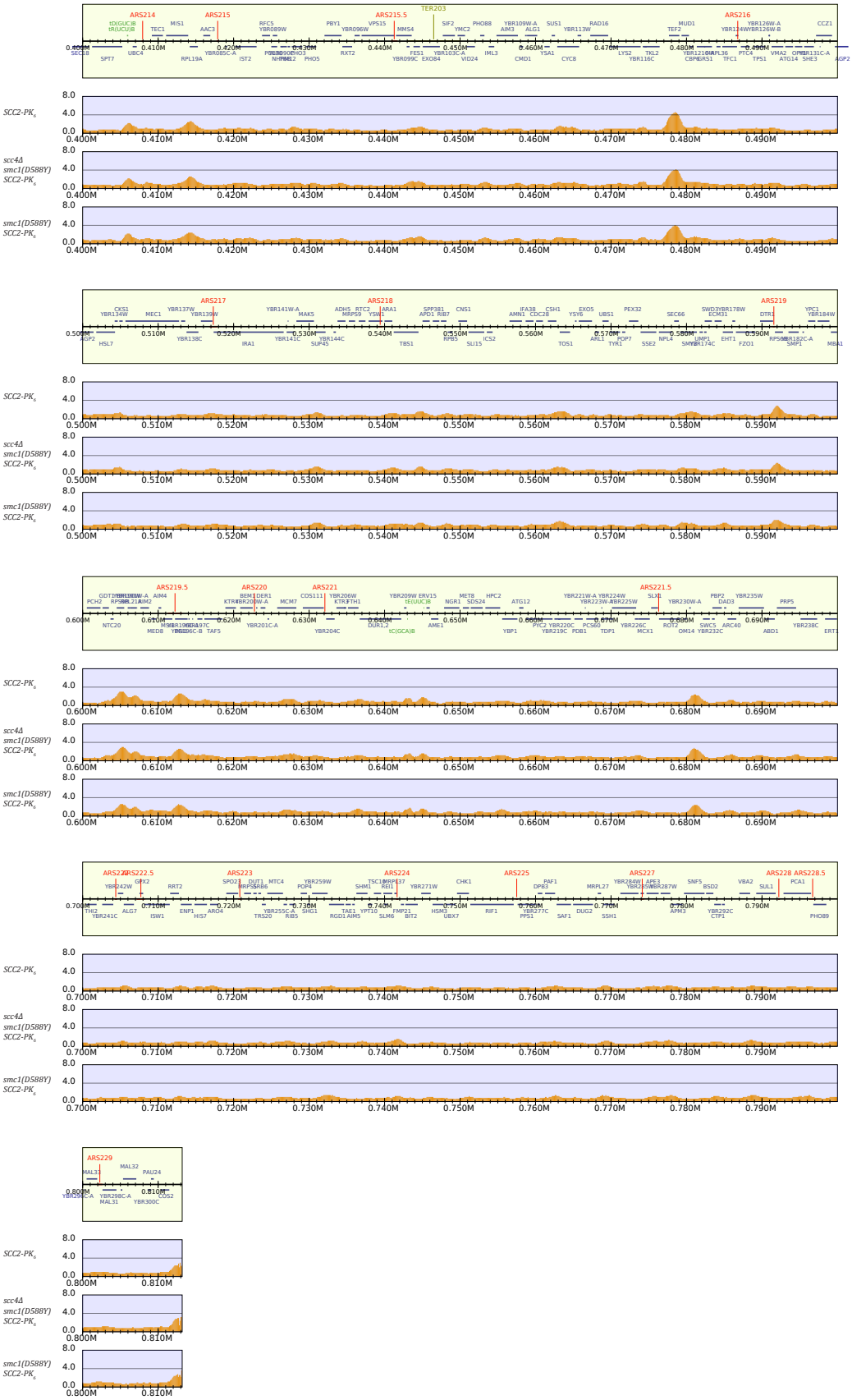
SCC2-PK6
scc4Δ smc1(D588Y) SCC2-PK6
smc1(D588Y) SCC2-PK6